THE DYNAMICS OF INJECTION HYDRAULICS IN THERMOPLASTICS INJECTION MOLDING

by

DIB ABU FARA

A Thesis Submitted to the Faculty of Graduate Studies
and Research in Partial Fulfilment of the
Requirements for the Degree of
Master of Engineering

Department of Chemical Engineering
McGill University
Montreal

 May, 1983

TO

MY DEAR PARENTS

AND

MY BELOVED WIFE

FACULTÉ DES ÉTUDES AVANCÉES ET DE LA RECHERCHE

Date: ____________________

NOM DE L'AUTEUR: ____________________

DEPARTEMENT: ____________________

TITRE DE LA THESE: ____________________

____

____

1.. Par la présente, l'auteur accorde à l'université McGill l'autorisation de mettre cette thèse à la disposition des lecteurs dans une bibliothèque de McGill ou une autre bibliothèque, soit sous sa forme actuelle, soit sous forme d'une réproduction. L'auteur détient cependant les autres droits de publications. Il est entendu, par ailleurs, que ni la thèse, ni les longs extraits de cette thèse ne pourront être imprimés ou reproduits par d'autres moyens sans l'autorisation écrite de l'auteur.

2.. La présente autorisation entre en vigueur à la date indiquée ci-dessus à moins que le Comité exécutif du conseil n'ait voté de différer cette date. Dans ce cas, la date différée sera le ____________________

____

Signature de l'auteur

Adresse permanente:

____

____

____

____

Signature du doyen si une date figure à l'alinéa 2.

(English on reverse)

ABSTRACT

Some aspects of injection molding dynamics were studied using a laboratory injection molding machine operated under the control of a microprocessor-based servocontrol system . Three types of experiments were performed :

(a) pseudo-static tests from which a linear relationship between hydraulic and nozzle pressures was found ;

(b) deterministic (step) tests which introduced step changes in the servovalve opening ;

(c) stochastic tests using pseudo-random binary sequence (PRBS) perturbations of the servovalve opening .

A simple relationship between nozzle and hydraulic pressures was derived from a force balance on the ram and was in good agreement with the experimental pseudo-static data. Deterministic models were developed for the hydraulic pressure, nozzle pressure and ram velocity. The model predictions were in good agreement with the experimental data. Stochastic transfer function-noise models were obtained for the nozzle pressure and ram velocity. The agreement between the stochastic models and the corresponding step test models was satisfactory .

RESUME

Certain aspects de la dynamique du moulage par injection ont été etudiés à l'aide d'un appareil (modèle de laboratoire) de moulage par injection commandé par servo-régulation à l'aid d'un microordinateur. Trois types d'essais ont été effectués :

(a) des essais pseudo-statiques à l'aide des quels une relation linéaire entre la pression hydraulique et la pression à la sortie a été observée ,

(b) des essais avec perturbations déterministes de type échelon affectées à l'ouverture de la servo-vanne ,

(c) des essais stochastiques suivant des séquences binaires pseudo-aléatoire aafectéis à l'ouverture de la servo-vanne.

Une relation simple entre la pression à la sortie et la pression hydraulique a été dérivé à partir du bilan des forces de la piston. Cette relation correspond bien aux valeurs experimentales obtenues des essais pseudo-statiques. Des modèles déterministes reliant la pression hydraulique , la pression à la sortie et la vitesse de la vis ont été décenés. Les valeurs obtenues de ces modèles correspondent de façon satisfaisante aux résultats experimentaux. Des modèles du type fonction de transfert stochastique reliant la pression à la sortie et la vitesse de la vis ont été dérivés. Les correspondances entre les modèles stochastiques et les modèles obtenus des perturbations de type échelon est satisfaisante.

ACKNOWLEDGEMENTS

I wish to express my sincere gratitude to all the people who contributed to the present study.

In particular, I am especially indebted to my Research Directors, Professor Musa R. Kamal and Professor W. Ian Patterson, for their guidance and encouragement throughout the duration of this work.

I would also like to thank:

- Mr A. Haber, Mr P. Lafleur and Mr Q. Samak, for their advice, comments and discussions throughout the course of this study.

- DuPont of Canada, for supplying the materials used in the study.

- The University of Jordan, for financial support in the form of a scholarship.

- Mrs D. Ross, for her perseverance and conscientious efforts in typing this manuscript.

TABLE OF CONTENTS

LIST OF TABLES

LIST OF FIGURES

CHAPTER 1

INTRODUCTION

The injection molding of thermoplastics is a multivariable process involving complex interactions between material characteristics, the molding conditions, and the desired properties of the molded article. It is necessary to understand the interactions between these variables to control the changes which occur during the injection molding cycle both in the process and the product.

Present injection molding models are generally based on the solution of the equations of continuity, momentum and energy in conjunction with suitable initial and boundary conditions. Although such models yield information regarding the relationships between the resin properties, molding conditions, the thermo-mechanical history of the resin and the ultimate properties of the molded article, they are too complicated for process control purposes which require simpler dynamic models.

The present work explores the feasibility of some simple phenomonological and empirical relationships between different important process variables in the form of dynamic models useful for controlling the injection molding process.

CHAPTER 2

GENERAL BACKGROUND

2.1 Injection Molding Simulation

The study of the injection molding of thermoplastics has received considerable attention in recent years. A number of studies has been concerned with the mathematical modelling of various phases of the injection molding process. Different models, of varying complexity, depending on the simplifying assumptions and the nature of the rheological constitutive equations and other relationships, have been proposed.

Harry and Parrott (1) presented a numerical model of the filling of a thin rectangular cavity. They assumed a power law viscosity model and solved both the momentum and energy equations, allowing for the temperature dependence of polymer properties. Berger and Gogos (2,3) and later Wu, Huang and Gogos (4) treated the filling of a circular disk cavity. Isothermal and non-isothermal one-dimensional models were analyzed in conjunction with a power law fluid. Kamal and Kenig (5,6,7) proposed a model to describe the molding behavior of thermoplastics in a semi-circular cavity. Their model presented an integrated mathematical treatment of the filling, packing and cooling phases of the injection molding cycle, and was derived from the equations of continuity, motion and energy for each phase of the cycle. Doan (8) extended Kenig's simulation to describe the behavior of commercial injection molding resins in thin rectangular cavities.

Kuo et al. (9) proposed an analytical expression for estimating the pressure distribution during the filling stage. This work also proposed an equation for the temperature distribution in the molten region during the cooling phase. Broyer, Gutfinger and Tadmor (10), as well as White (11), modelled the flow in a narrow gap mold by recognizing the similarities between this system and the classical Hele-Shaw flow. Their treatment neglected the time-dependent terms in the momentum equation. Kuo and Kamal (12) extended this analysis to unsteady, non-isothermal and non-Newtonian flows. They developed an analytical-numerical method for determining the shape of the progressing flow front and for computing the flow variables and temperature distributions during the filling stage. This analysis accounted for the general dependency of viscosity on both shear rate and temperature. Kuo and Kamal (13) also derived working equations to simulate the non-isothermal, compressible flow occurring during the packing stage, using the thin cavity approximations to simplify the governing equations. The model included the inertial effect and considered the compressibility of the polymer melt as the dominant feature in the packing stage.

Kamal and Tan (14) summarized the experimental studies which have been directed to the understanding of the complex interaction between moldability, material properties and process conditions. Lord (15) employed a model which incorporated the effect of pressure on viscosity. Kruger (16) presented experimental data for advancing melt profiles, pressures and temperatures during the filling of a rectangular cavity with variously shaped inserts. Their experimental data were in good agreement with the predictions of previously developed theoretical models. Ryan and Chung (17) developed a conformal mapping analysis of the mold filling behavior in rectangular cavities. The polymer melt was assumed to behave as a purely viscous Generalized Newtonian Fluid. This technique allowed the easy calculation of the position of the advancing flow front, the pressure distribution in the mold cavity, streamlines, constant temperature lines and the filling time.

Wang et al. (18) modelled the filling and cooling stages employing a viscoelastic constitutive equation. The model is one-dimensional, unsteady, non-isothermal pressure flow of polymer between two parallel plates. The model gives good predictions for the birefringence as a function of melt temperature, wall temperature, gap thickness and fill time. Recently, Lafleur and Kamal (19) proposed a computer simulation of the injection molding process which permits the prediction of some microstructural parameters in the molded articles, like the distributions of crystallinity and frozen stresses.

The above studies, without exception, require the numerical solution of the model equations, which is obtained only after considerable computation. Process control, however, demands simple empirical or theoretical models (relationships) which do not require long computational times or large computers. Such models should relate the time-varying distributions of process parameters like pressure, temperature and velocity to the relevant machine and material variables.

2.2 Dynamic Models and Injection Molding Control

The injection molding of thermoplastics involves complex interactions between the molding conditions, the processed material properties and the ultimate properties of the molded article. Menges et al. (20) and Hunkar (21) pointed out that the quality of the molded articles could be related to process variables, such as pressure and temperature in the mold, by utilization of the P-V-T diagram of the processed polymer. Mann(22) studied the effect of peak cavity pressure and cushion size on part shrinkage. The results showed that any variation in peak cavity pressure will cause a corresponding change in part dimensions.

Several workers have attempted to classify the injection process variables and to develop relationships between the variables.

Paulson (23) classified the injection molding process variables into machine variables and "plastic" variables or measurements. He suggested that molded part quality was related to both of these variables. Therefore, both machine and plastic variables should be considered in order to establish the proper setting for process controls. Typical machine variables are hydraulic pressure, screw displacement and barrel temperature. Plastic variables include polymer melt temperature at the nozzle and the melt pressure at the nozzle and in the cavity. Plant and Maher (24) presented a preliminary analysis of the injection molding process trying to describe the interactions between the process variables. They concluded that changes in injection pressure were accompanied with comparable changes in the nozzle melt pressure, and the increase in cushion caused a slight increase in nozzle pressure. Mold cavity pressure reacted to changes in most of the machine variables, like injection pressure, injection rate, back pressure and cushion. Therefore they strongly recommended the use of cavity pressure in controlling the injection process.

Ma (25) proposed qualitative functional relationships between the process variables during the three phases of the injection cycle, as follows:

Plastication phase:

$$T_{m\ell} = F1(N, P_{m\ell}, T_b, D1) \tag{2.1}$$

Injection phase:

$$P_{m\ell} = F2(V_j, T_{ml}, D2) \tag{2.2}$$

Packing phase:

$$P_{ml} = F3(P_k, T_{ml}, T_{md}, T_c, D3) \tag{2.3}$$

where:

$T_{m\ell}$ = melt temperature

N = rotational screw speed

$P_{m\ell}$ = melt pressure at the nozzle

T_b = barrel temperature

V_j = injection velocity

T_{m1} = runner melt temperature

P_{m1} = cavity pressure

P_k = hydraulic packing pressure

T_{md} = mold temperature

T_c = cooling time

D1,D2,D3 = external disturbances

Equation (2.1) does not include hydraulic back-pressure, which, as shown by Border (27), has a direct effect on the melt temperature during plastication. Also, the relationship for nozzle pressure, equation (2.2), does not include the effect of hydraulic pressure explicitly. Although the cooling time, T_c, included in equation (2.3), affects the properties of the molded part, it does not affect the peak cavity pressure.

Peter (26) conducted experiments to study the relationships between hydraulic pressure and the mold packing pressure, melt temperature and plastication time. On the basis of these studies, he proposed the following relationships:

$$P_{mold} = m\, P_{hyd_1} + b + \text{error} \tag{2.4}$$

$$T_{melt} = a(T_{barrel} + b) + m\, P_{hyd_2} + \text{error} \qquad (2.5)$$

$$t_{plast} = \frac{x}{N}\,(m\, P_{hyd_2} + b) + \text{error} \qquad (2.6)$$

where

P_{mold} = peak packing pressure in the mold

P_{hyd_1} = hydraulic pressure during packing

P_{hyd_2} = hydraulic back pressure during plastication

t_{plast} = plastication time

N = rotational screw speed

x = shot size

a, b, m = experimentally determined constants

Equation (2.4) shows that the mold pressure is linearly related to hydraulic packing pressure. Equation (2.5) shows the dependence of melt temperature on hydraulic back pressure which was not included in the relationship proposed by Ma (25).

Border and Suh (27) determined the theoretical aspect of the viscosity change of various thermoplastic materials and the possibility of controlling the viscosity change by varying the operating conditions. They proposed a model which relates the rate of change in viscosity to the change in temperature and the viscosity itself. The model was of the form:

$$\frac{\partial \eta}{\partial T} = - a \eta^{b} \qquad (2.7)$$

where a and b are constants. They also derived a linear relationship between the rate of change of melt temperature with respect to the change in back-pressure and the back-pressure itself, as:

$$\frac{\partial T}{\partial P_B} = K P_B \qquad (2.8)$$

where P_B = hydraulic back-pressure. This relationship is consistent with the relationship (2.5) proposed by Peter (26).

Besides these modelling efforts, several workers have discussed the different control strategies that can be employed with the injection molding process.

Patterson and Kamal (28) summarized and discussed the different control strategies that have been proposed for controlling the different phases of the injection molding cycle. Davis (29,30) and Davis and Thayer (31) discussed different closed loop controls. They concluded that servocontrolled injection ram velocity and hydraulic pressure provide a significant improvement in the repeatability of the mold cavity pressure. Takizawa et al. (32) obtained a similar conclusion, that with a programmed injection velocity, only small variations in cavity pressure were noticed.

The above review shows that, although the published studies are useful in examining the interactions between the process variables, the current knowledge of machine and process dynamics is still limited.

The present study represents an effort to generate some of the basic information required for the development of dependable control strategies for the injection molding process. It involves a study of the dynamics of the process with particular emphasis on the interactions between hydraulic pressure and important process variables.

CHAPTER 3

MODELLING TECHNIQUES

3.1 Introduction

The interactions and phenomena involving engineering variables in industrial processes may be described or modelled in two ways. The first method is based on solving the appropriate equations of continuity, momentum and energy in conjunction with suitable initial and boundary conditions. Examples of injection molding models obtained by this approach were presented in section 2.1. The use of these models is prohibitively complex when applied to a situation where the process variables are changing in response to time-variable forcing functions. In such situations, empirical models have proven to be a valuable tool for attaining rational and effective process control strategies.

Empirical models are often obtained in a transfer function form. The experimental method employed to obtain these models is based on introducing a controlled variation into a process input variable and measuring the corresponding response. The transfer function is then obtained from the ratio of the transformed input and output variations (33,34), as illustrated in Figure 3.1.

The transfer function approach suffers from two disadvantages:

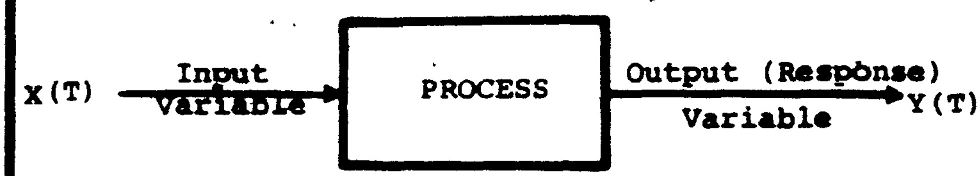

PROCESS TRANSFER FUNCTION, $G(T) = \frac{Y(T)}{X(T)}$

OR

TRANSFORMED TO LAPLACE DOMAIN, $G(s) = \frac{Y(s)}{X(s)}$

Figure 3.1 Transfer Function Representation of a Process

(a) the required data must be obtained from actual experimental runs carried out on the process;

(b) the method implicitly assumes that the process response is linear. Therefore, it is necessary to determine the limits of the validity of this assumption by experimentation.

A positive aspect of the transfer function approach is that it gives models which are significantly simpler than those of the transport phenomena approach, since, as pointed out earlier, the equations of change become partial differential equations and their solution is relatively complex. Thus transfer function models are better suited for process control applications.

3.2 Dynamic Models

3.2.1 Deterministic Models

Classically, the engineering methods for estimating transfer function models are based on deterministic perturbations of the input, such as step, pulse or sinusoidal changes (33,34,35,36). Typical responses to these inputs are shown in Figure 3.2. The step function is the most widely used, because it is physically difficult to use the pulse function and since the sinusoidal function requires long duration tests (34). The response of first and second order systems to step function inputs are given in Table 3.1. Figure 3.3

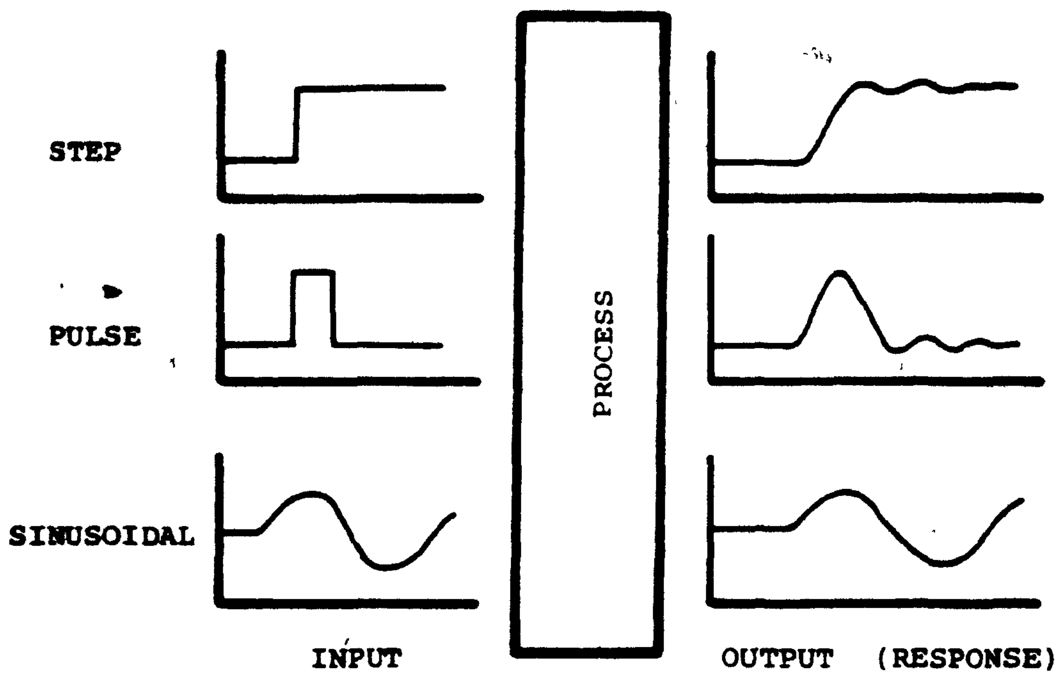

Figure 3.2 Deterministic Signals to Obtain the Transfer Function

TABLE 3.1 RESPONSES OF FIRST AND SECOND ORDER SYSTEMS TO A UNIT STEP FUNCTION

SYSTEM	RESPONSE	
First Order	$y(t) = 1 - e^{-t/\tau}$	(a)
Underdamped Second Order	$y(t) = 1 - \frac{1}{(1-\xi^2)^{1/2}} \sin\left[(1-\xi^2)^{1/2} \frac{t}{\tau} + \tan^{-1}\frac{(1-\xi^2)^{1/2}}{\xi}\right]$	(b)
Critically damped Second Order	$y(t) = 1 - (1 + \frac{t}{\tau})e^{-t/\tau}$	(c)
Overdamped Second Order	$y(t) = 1 - \frac{\tau_1\tau_2}{\tau_1-\tau_2} (\frac{1}{\tau_2} e^{-t/\tau_1} - \frac{1}{\tau_1} e^{-t/\tau_2})$	(d)

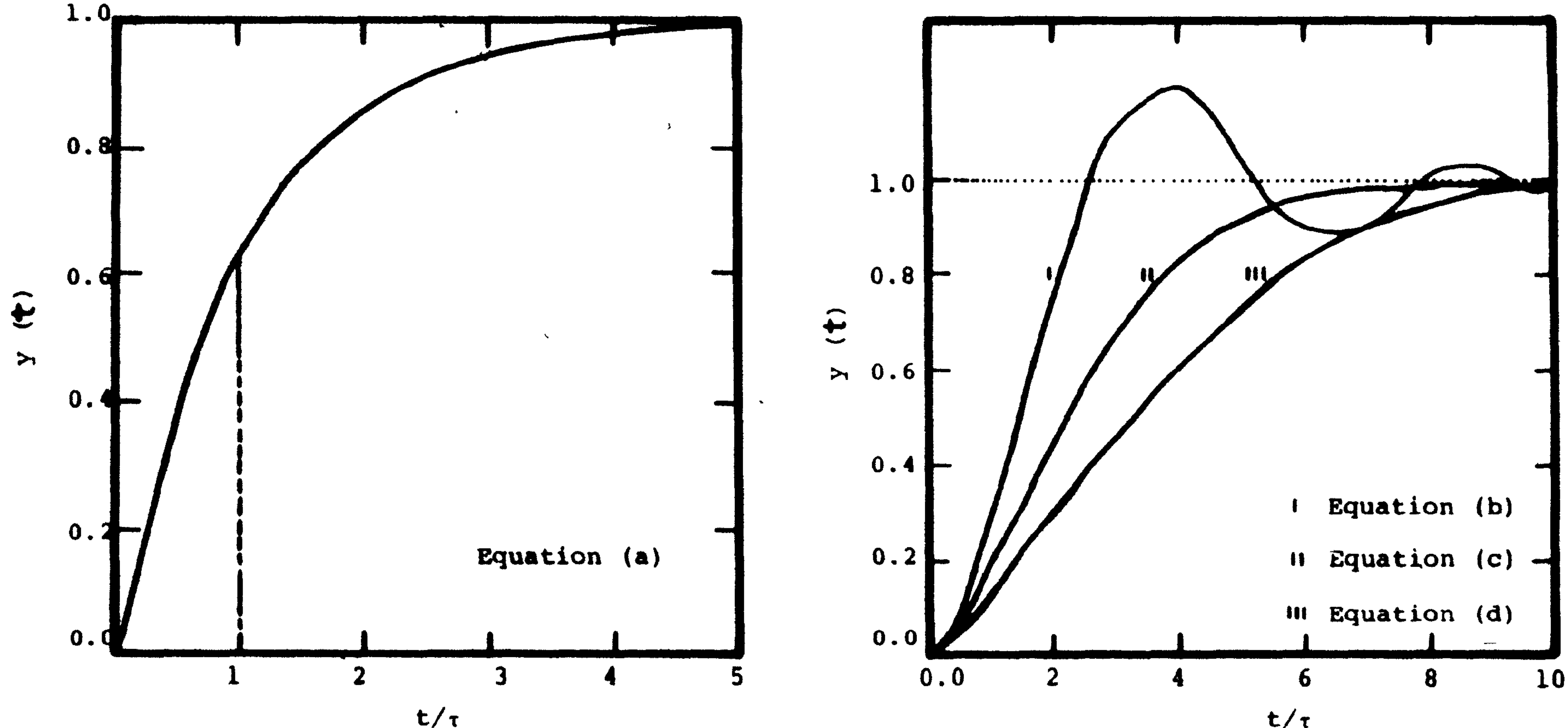

(a) First-Order System Response to a Unit Step Change

(b) Second-Order System Response to a Unit Step Change

Figure 3.3 Response to Step Function Input demonstrates a graphical method for estimating the model parameters (34). The errors introduced by graphical construction can be avoided by using a fitting program to estimate the parameters of the proposed models. In this study, the NONLINWOOD program (37) was employed.

The disadvantage of the deterministic models is that they are useful only when the system involves small amounts of noise (random disturbances). Moreover, it is difficult to distinguish between second and third or higher order systems.

3.2.2 Stochastic Models

The measured variables of most industrial processes include experimental errors. The process itself is also subject to random disturbances. Recently, statistical techniques have been developed (38,39) which, after treatment of the measured response, determine both the transfer function and a model of the noise associated with the process. This technique, using a pseudo-random binary sequence (PRBS) input (40,41), is illustrated in Figure 3.4. Ideally, the PRBS is generated by a computer which also measures the response at discrete time intervals.

The parametric models obtained by this approach are of the form (39):

$$y(k)(1-\delta_1 B-\delta_2 B^2- \text{-----} -\delta_r B^r) = (\omega_0-\omega_1 B-\omega_2 B^2- \text{-----}$$
$$-\omega_s B^s)x(k-b) + N(k) \qquad (3.1)$$

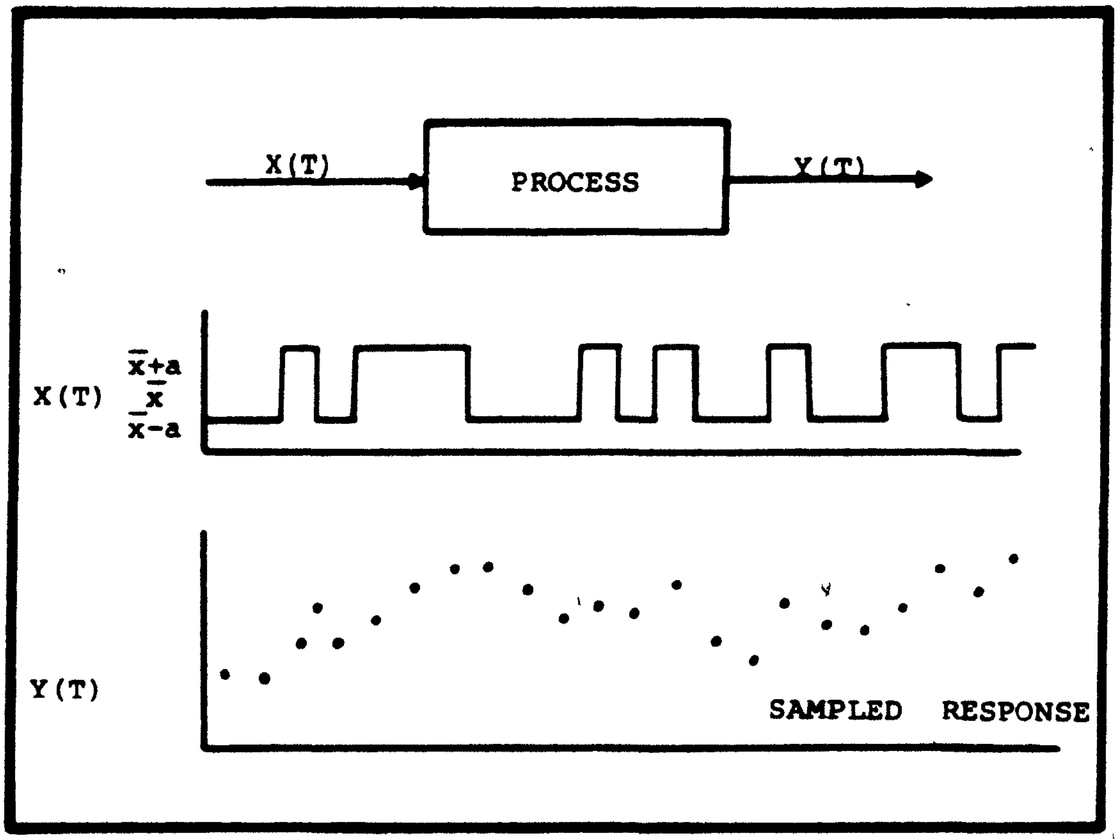

Figure 3.4 Stochastic Testing of a Process to Obtain the Transfer Function

or

$$y(k) = \frac{\omega_s(B)}{\delta_r(B)} \; x(k-b) + \frac{\theta_q(B)}{\phi_p(B)} \, a(k) \qquad (3.2)$$

where

$y(k)$ = the output at k^{th} measurement

$x(k-b)$ = the input at $(k-b)^{th}$ measurement

$N(k)$ = the noise at k^{th} measurement

B = the backwards operator; $B\,y(k) = y(k-1)$

b = number of lags

$\omega_s(B) = (\omega_0-\omega_1 B-\omega_2 B^2-\text{-----}-\omega_s B^s)$

$\delta_r(B) = (1-\delta_1 B-\delta_2 B^2-\text{-----}-\delta_r B^r)$

$\theta_q(B) = (1-\theta_1 B-\theta_2 B^2-\text{-----}-\theta_q B^q)$

$\phi_p(B) = (1-\phi_1 B-\phi_2 B^2-\text{-----}-\phi_p B^p)$

$a(k)$ = white (random) noise

δ_1, δ_2 -----, and $\omega_0, \omega_1, \omega_2$ ----- are parameters obtained from the analysis of the experimental data.

The deterministic process model of Figure 3.1 is modified to that of Figure 3.5, when the stochastic model is used.

3.3 Stochastic Models Identification

Box and Jenkins (39) have proposed a detailed procedure for identifying the stochastic model of a process. The iterative procedure, as shown in Figure 3.6, consists of three main steps:

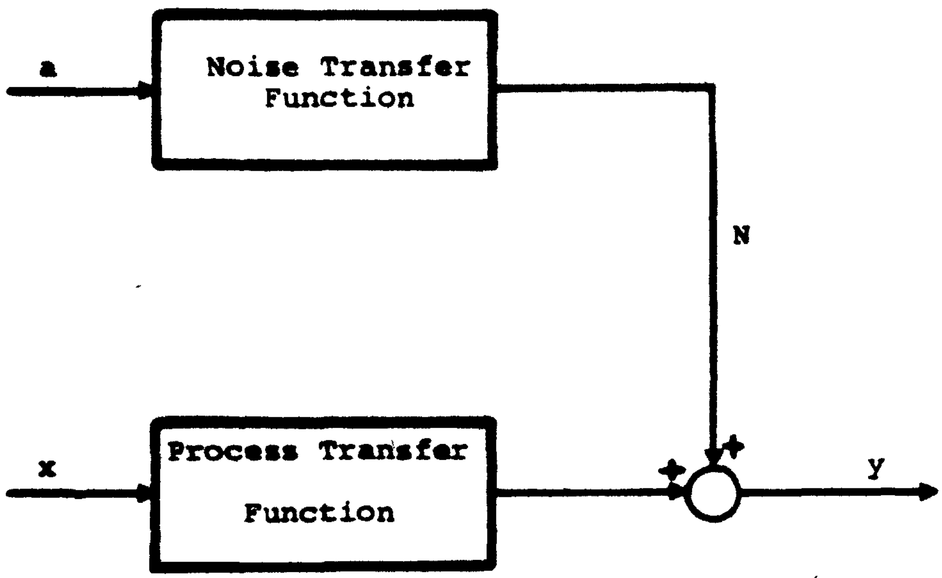

Figure 3.5 Representation of a Process with Added Noise

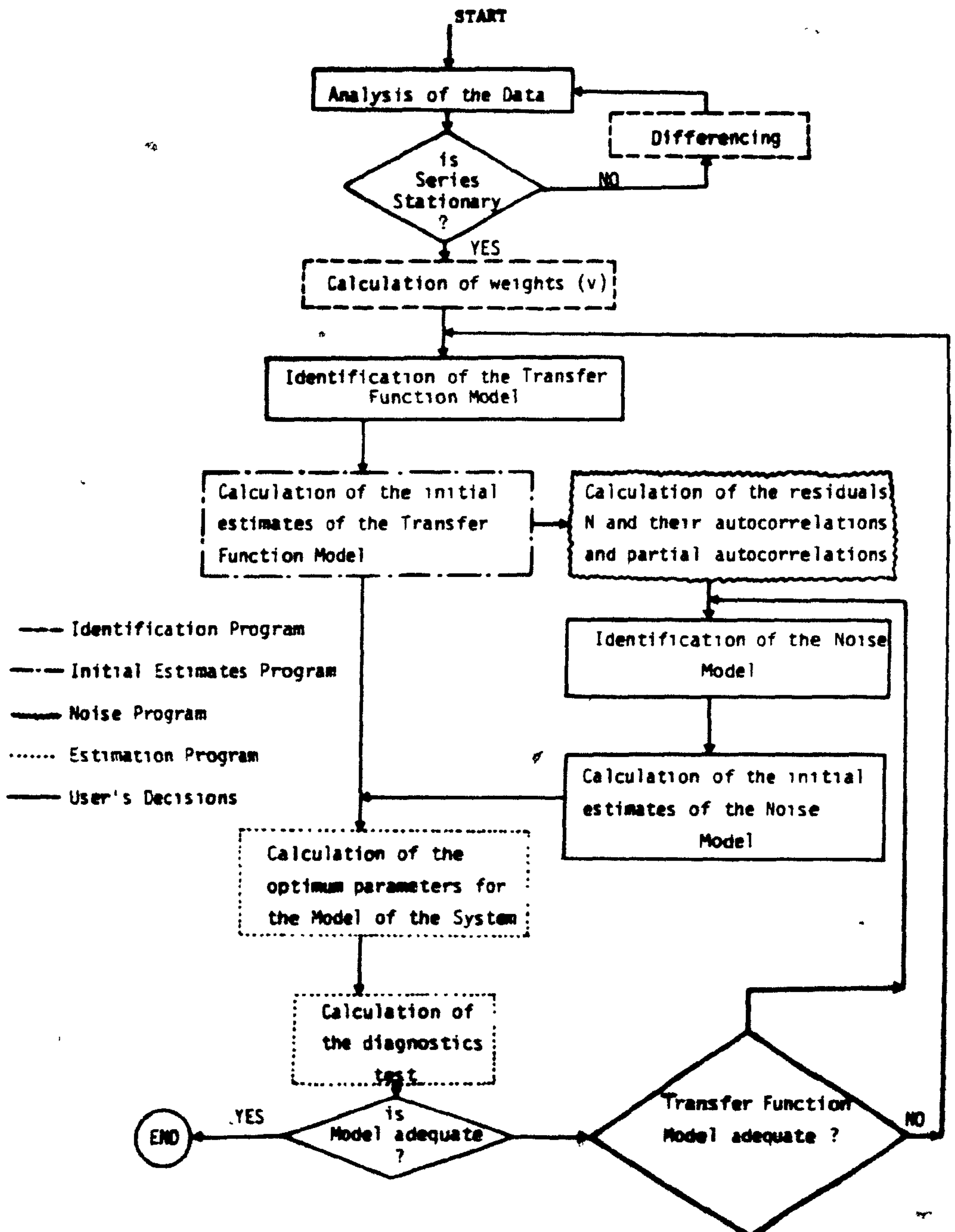

Figure 3.6 Block Diagram of Box and Jenkins Method

(a) identification of the order of the transfer function and noise models;

(b) estimation of the model parameters;

(c) diagnostic checking of the model.

3.3.1 Identification Step

The objective of the identification step is to indicate the order (or structure) of the transfer function and noise models, which are worthy of further investigation, and to estimate the initial values of the model parameters.

3.3.1.1 Identification of the Transfer Function Model

The basic tools employed in the process identification are the cross correlation of the input and output and the process impulse response. Equation (3.1) can be written as

$$y(k) = (v_0+v_1B+v_2B^2+ \text{---})\ x(k-b)+ N(k) \tag{3.3}$$

or

$$y(k) = v(B)\ x(k-b) + N(k) \tag{3.4}$$

where $v_0, v_1, v_2,$ --- v_n are the impulse response weights of the system at discrete time intervals, $t_0, t_1,$ ---, t_n.

The identification procedure then consists of the following steps:

(i) obtaining first estimates of the impulse response weights, v's, in equation (3.3);

(ii) using the observed pattern of the estimated impulse weights to choose a transfer function model, i.e. $\frac{\omega_s(B)}{\delta_r(B)}$, as illustrated by Box and Jenkins (39).

3.3.1.2 Identification of the Noise Model

The noise term N(k) in equation (3.1) can now be written in terms of the tentative transfer function model:

$$N(k) = y(k) - \frac{\omega_s(B)}{\delta_r(B)} x(k-b) \tag{3.5}$$

The autocorrelation and partial autocorrelation functions of the noise series can then be used to identify a noise model (39).

3.3.2 Estimation Step

The tentative model of equation (3.6):

$$y(k) = \frac{\omega_s(B)}{\delta_r(B)} x(k-b) + \frac{\theta_q(B)}{\phi_p(B)} a(k) \tag{3.6}$$

together with initial estimates of the model parameters $\underline{\omega}$, $\underline{\delta}$, $\underline{\theta}$ and $\underline{\phi}$ allow the a(k)'s to be calculated recursively as:

$$a(k) = \frac{\phi_p(B)}{\theta_q(B)} \{y(k) - \frac{\omega_s(B)}{\delta_r(B)} x(k-b)\}; \quad k = 1,2, ----- n \tag{3.7}$$

where n = number of observations.

The best estimates of the parameters $\underline{\omega}$, $\underline{\delta}$, $\underline{\theta}$ and $\underline{\phi}$ can be obtained by minimizing the sum of squares (39), using the maximum likelihood approach:

$$S(\delta,\omega,\theta,\phi) = \sum_{k=1}^{n} a_k^2(\delta,\omega,\theta,\phi) \tag{3.8}$$

3.3.3 Diagnostic Testing

This step is essential to check the statistical adequacy of the proposed model. A model is deemed adequate when the residuals are uncorrelated random deviates. This can be verified by comparing the autocorrelation function of the residuals and examining the cross-correlation between the input and the residuals (39). Two cases could arise:

(i) The transfer function model is correct, while the noise model is incorrect. In this case, the residuals are autocorrelated, but they are not cross-correlated with the input. The form of the autocorrelation function would indicate the appropriate modification of the noise model.

(ii) The transfer function model is incorrect. In this case, not only are the residuals cross-correlated with the input, but also they are autocorrelated even if the noise model is correct. The cross-correlation analysis indicates the required modifications to the transfer function model and the analysis is repeated (see Figure 3.6).

CHAPTER 4

SCOPE AND OBJECTIVES

The present work represents a part of a general research program in the field of injection molding, which has been in progress for the last decade in the Chemical Engineering Department at McGill University. The program covers a variety of aspects of injection molding, including resin characterization, mathematical modeling of the molding process and the analysis of microstructure and ultimate properties of injection molded articles. A substantial amount of work has involved the injection molding of thermoplastics (6,8,42,43,44). This work has led to the development of models and computer simulations, of varying degrees of complexity, to describe the injection molding process and the behavior of injection molded articles (5-9,12-14,19).

Recently, as part of the above effort, a laboratory injection molding machine was modified for operation using a microprocessor-based servocontrol system (45). The modified machine is used in this work to study some aspects of injection molding dynamics and to develop simple models suitable for the control of the injection molding process.

The specific objectives of the present work are:

(1) To develop models, suitable for control purposes, showing the relationships between the hydraulic pressure-time profile during the injection phase and the following:

(i) the nozzle pressure-time profile

(ii) the screw (ram) position-time profile

(iii) the screw (ram) velocity-time profile.

The models are based on both a simplified theoretical analysis and an empirical correlation of experimental data. The theoretical and empirical models are compared with regard to their agreement with experimental data.

(2) To study the dynamics of the injection molding process and to obtain dynamic models (transfer functions) useful for control purposes. The dynamic models are based on both deterministic (step) and stochastic (PRBS) tests, which have been carried out to relate changes of process variables (i.e. nozzle pressure, screw position, screw speed, and hydraulic pressure) to changes in the opening of the servovalve controlling the flow of oil in the hydraulic system.

CHAPTER 5

EXPERIMENTAL

5.1 Equipment

5.1.1 Injection Molding Machine

This work was performed on a Danson Metalmec 2 1/3 OZ, reciprocating screw injection molding machine, model 60-SR, Figure 5.1. The machine is equipped for operation in the automatic, semi-automatic, and manual modes. Injection, holding, and back pressures are set by adjusting the appropriate manual valve. The screw rotational speed is adjusted by means of a handwheel located on the screw speed valve which controls the rate of plastication. Injection and holding times are set on their respective timers. The barrel is divided into two heating zones. Each zone is independently heated by an electrical heating band. The two zone temperatures are controlled to within 3°C of the set temperatures by an on-off control action. Figure 5.2 shows a sketch of the barrel and screw. A rectangular mold with cavity dimensions 0.1 x 0.06 x 0.003m was employed.

The hydraulic system of the machine was redesigned and refitted to include a microprocessor-controlled servovalve (45). An electro-hydraulic servovalve (Moog type A076-103), with a capacity for passing 10 gallons (U.S.) per minute at a rated

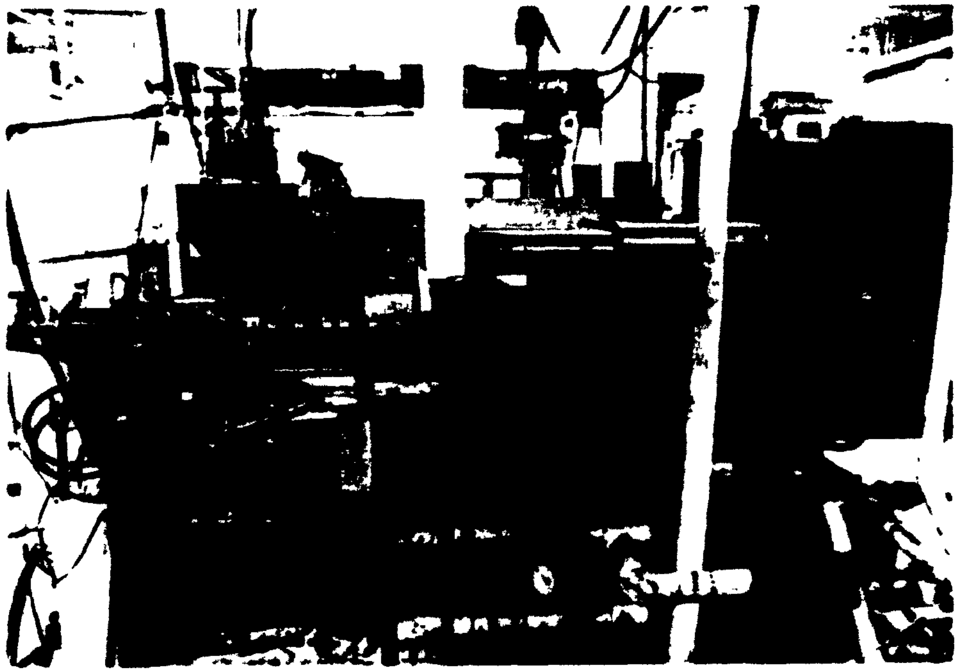

Figure 5.1 Danson Metalmec Injection Molding Machine and the Microprocessor System.

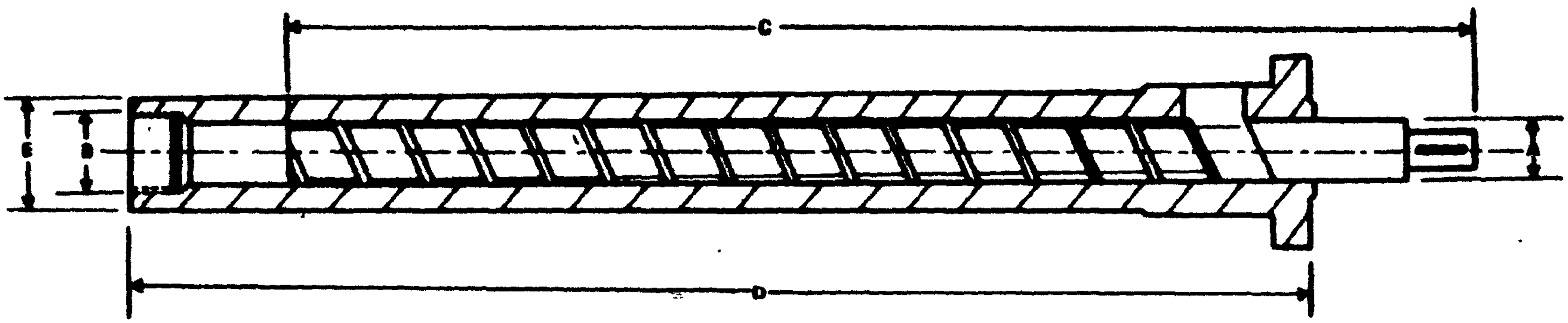

Dim.	mm.	in.
A	35	1.38
B	44	1.73
C	659	25.94
D	655	25.8
E	70	2.76

Figure 5.2

Barrel and Screw Dimensions (49)

pressure drop of 1000 psi (6.89×10^6 N/m^2), was installed. The full amplitude rise time was about eight milliseconds (Appendix A). A constant line pressure was assured by an accumulator installed before the servovalve to deliver additional oil to the system during pressure fluctuation. Figure 5.3 depicts the hydraulic system of the machine.

5.1.2 Microprocessor System

The microprocessor control system is based on a Cromenco Single Card Computer (SCC). The facilities include 13 K (K = 1024) bytes of random access memory (RAM) and 12 K bytes of read only memory (ROM). There are seven 8-bit parallel input and output ports, and four serial (RS232) ports. The ROM software provides a monitor and an integer BASIC. The peripherals available are: a Hazeltine CRT terminal (model 1400), digital input and output modules (Opto 22), a Burr Brown 12-bit, 8 channel, analog to digital converter (SDM-856), and an 8-bit digital to analog converter. The system was programmed using subroutines for the machine sequencing, control algorithms, and data acquisition programs for examining the process variables during the injection phase of the molding cycle. The subroutines were written in assembler language. A block diagram of the microprocessor is shown in Figure 5.4 .

Figure 5.3 The Hydraulic System of the Machine

Key

1. Injection cylinder
2. Carriage cylinder
3. Hydraulic motor
4. Servovalve
5. Clamp cylinder
6. Mold position valve
7. Check valve
8. Carriage position valve
9. Main relief valve
10. Screw speed valve
11. Heat exchanger
12. Low pressure filter
13. High pressure filter
14. Reservoir
15. Sump filter
16. 2-vane pump
17. Electric motor
18. Accumulator

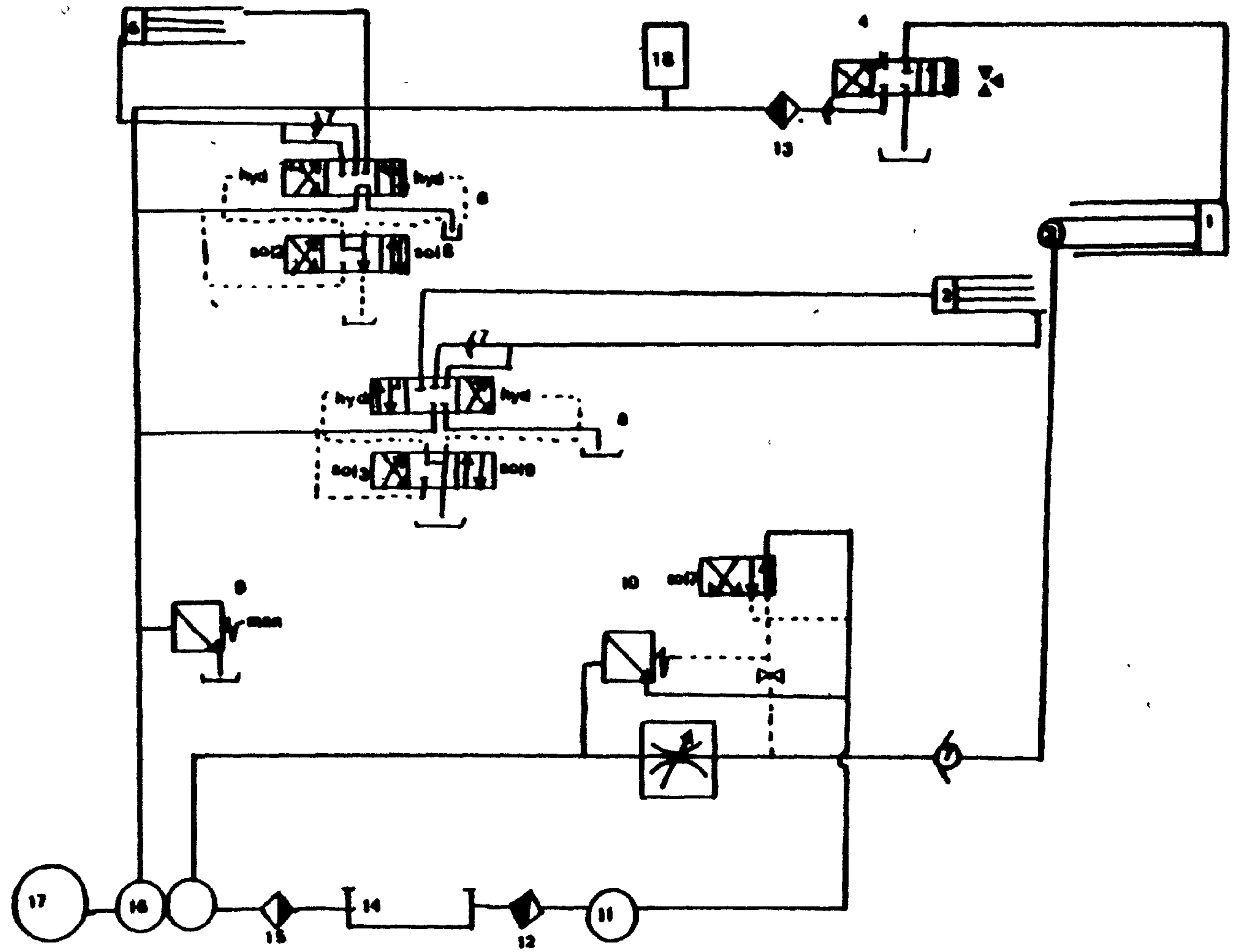

Figure 5.3 The Hydraulic System of the Machine (45)

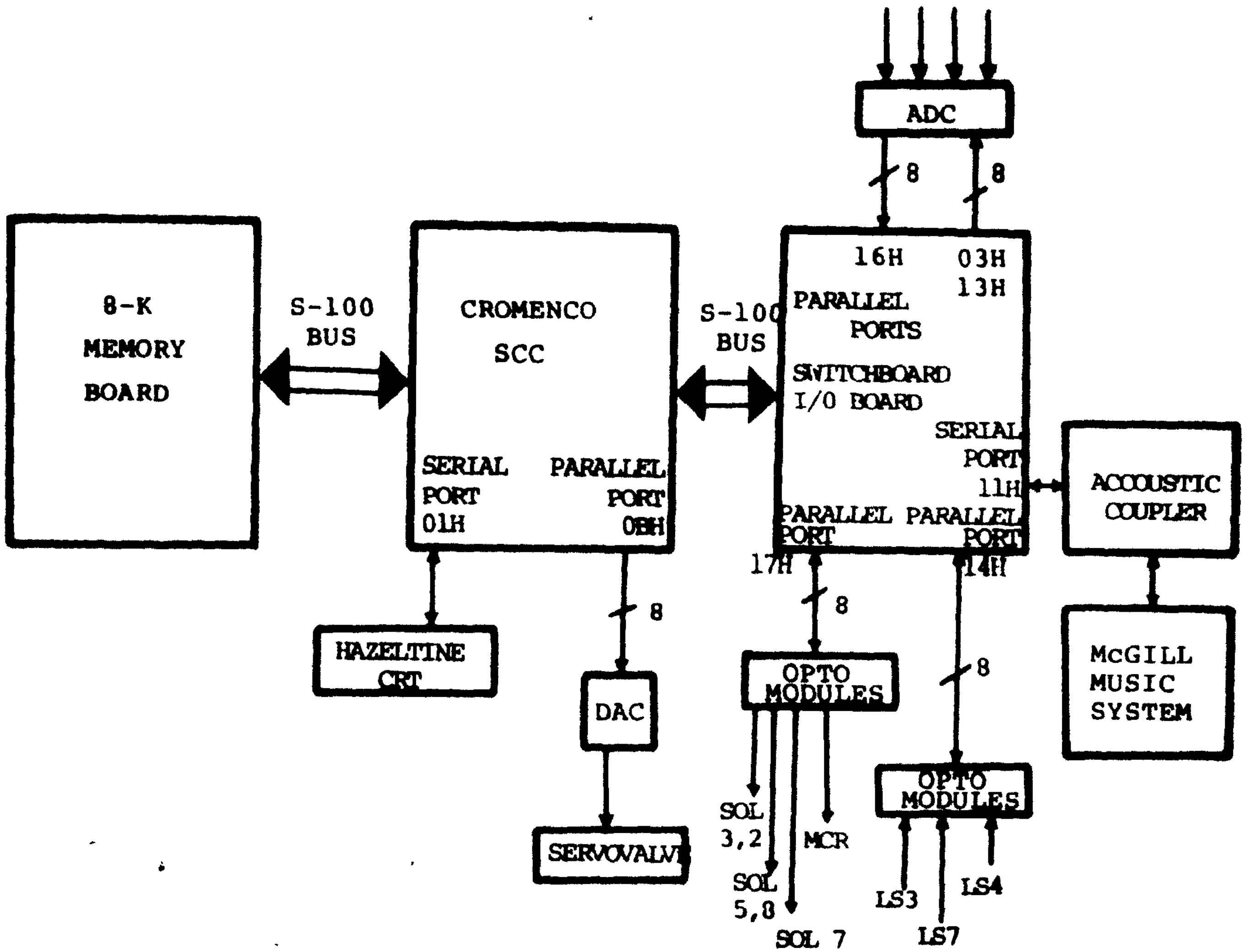

Figure 5.4 Block Diagram of the Microprocessor System (45)

5.2 Instrumentation

Two pressure transducers manufactured by Dynisco (model PT 435A) were used for pressure measurements. One pressure transducer (0-1000 psi) was located in the line between the servovalve and the injection cylinder to measure the hydraulic pressure. The second pressure transducer (0-10,000 psi) was mounted in the nozzle to measure the nozzle pressure.

A linear displacement transducer, manufactured by Markite (Model 4709) was used to monitor the displacement of the screw during the injection molding cycle. A linear velocity transducer, TRANS-TEK (model 112-001), measured the injection velocity. Figure 5.5 shows a sketch of the instrumented injection molding machine.

All the transducers were calibrated prior to installation to verify their gauge factors and linearity. A typical calibration curve is shown in Figure 5.6. The calibration data were fitted by the regression equations given in Table 5.1. The calibration data and a description of the calibration procedure are given in Appendix B.

5.3 Materials

Two injection molding grade polyethylene resins, designated as EX1 and EX2 and supplied by DuPont of Canada, were used in this study. These resins have been employed in a large number of injection molding studies carried out in the Department of Chemical Engineering, McGill University (43,44).

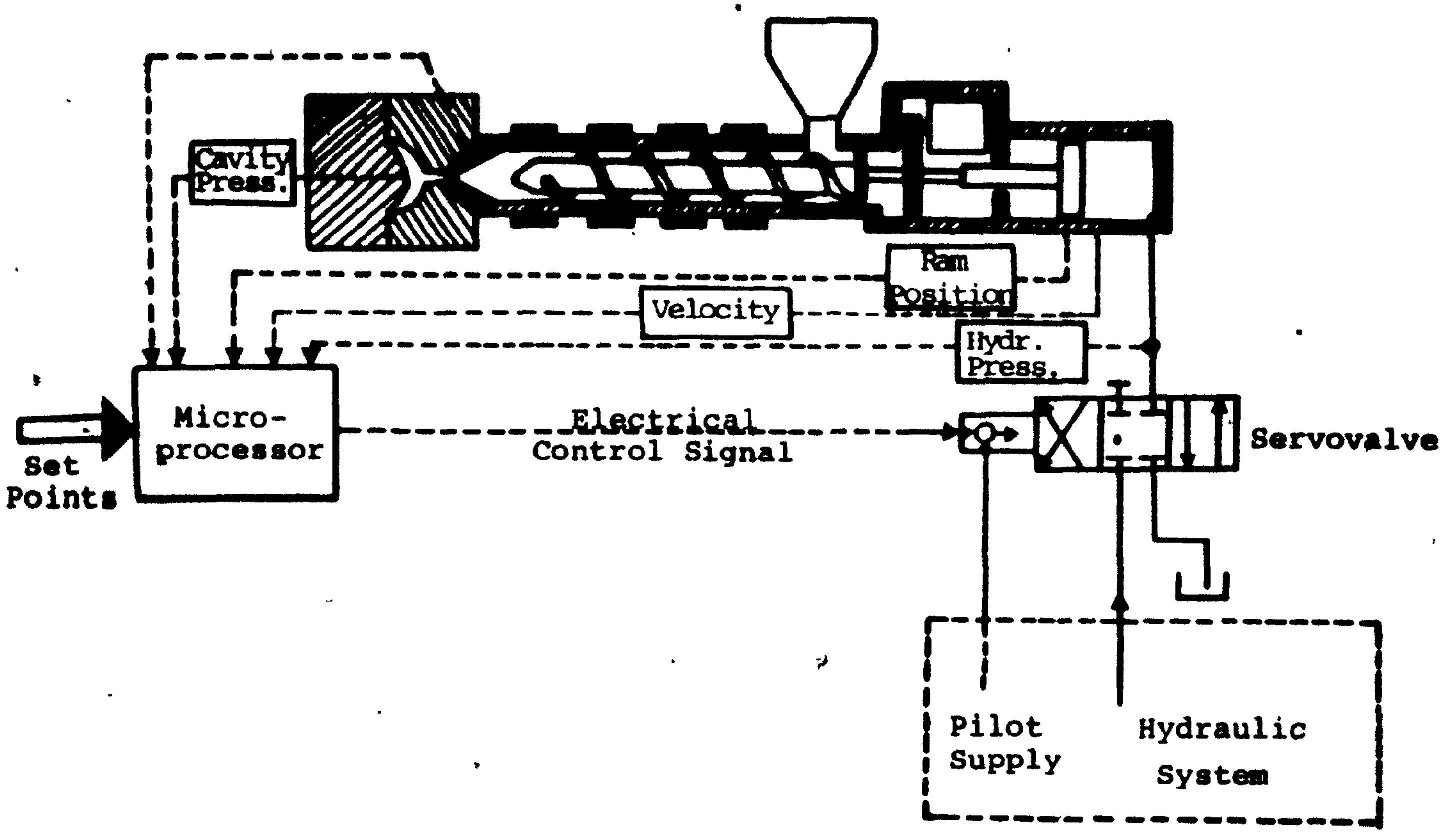

Figure 5.5 Diagram of the Instrumented Injection Molding Machine

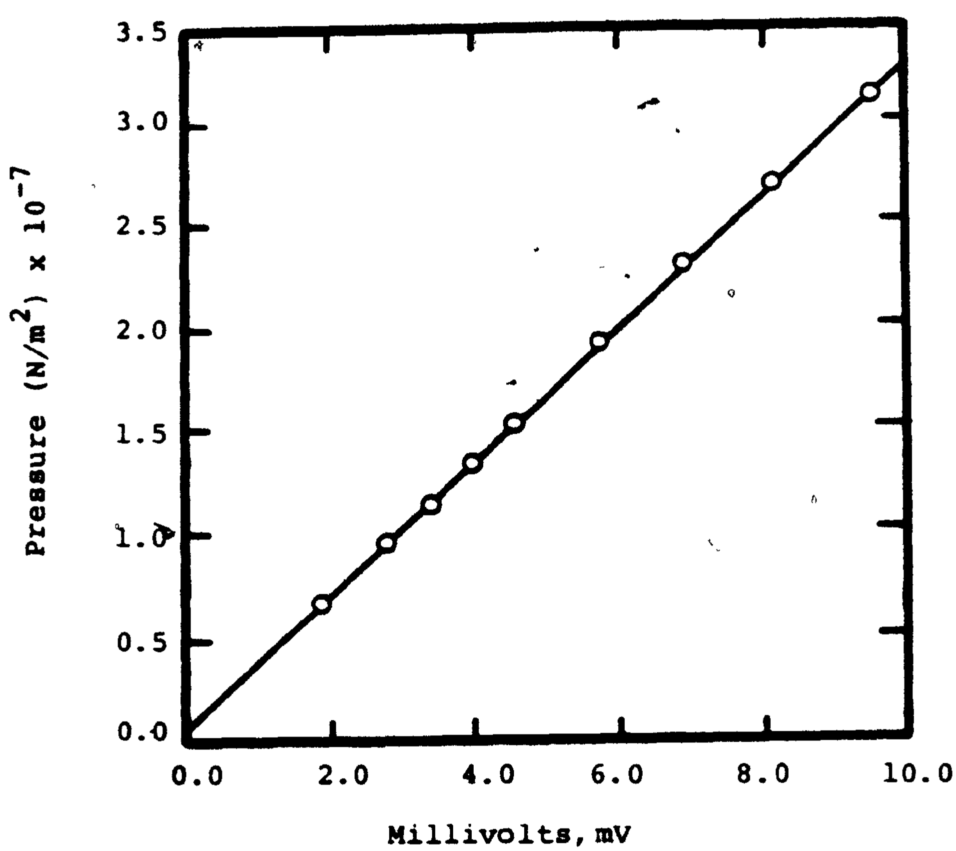

Figure 5.6 A Typical Pressure Transducer Calibration Curve

TABLE 5.1

Regression Coefficients for Transducer Calibration Equations

Transducer	Equation
Hydraulic pressure	P = 59.7 x (mV) + 66.2 psi
Nozzle pressure	P = 463. x (mV) + 51.2 psi
Linear displacement	L = 3.11 x (volts) cm
Linear velocity	V = 0.209 x (mV) - 0.004 mm/sec.

Note: 1 psi = 6.895×10^3 N/m^2

A substantial amount of data is available regarding the fundamental properties and molding characteristics of these resins. Some of these properties are given in Table 5.2.

5.4 Experimental Procedure

5.4.1 Start-Up and Operation of the Equipment

In order to insure reproducibility and smooth operation, the following sequence was employed in starting up and operating the injection molding machine and associated auxiliary equipment and instrumentation.

(a) Each set of experiments was begun by setting the barrel temperatures on the controllers and allowing one hour for the thermal stabilization of the injection unit.

(b) At this time, cold water at the desired temperature and flow rate was circulated in the mold cooling channels so as to achieve a uniform mold temperature. Cold water circulated around the hopper assembly to prevent premature melting and bridging of the resin pellets.

(c) The screw rotational speed control valve and the cam determining the shot size were set at predetermined positions, and these positions were maintained throughout the experiment.

TABLE 5.2

Physical Properties of Materials (44)

Physical Properties	Resin Material	
	EX1	EX2
$\bar{M}_W$ (Kg/Kmole)	8.92×10^4	7.45×10^4
$\bar{M}_N$	1.75×10^4	2.23×10^4
$\bar{M}_W/\bar{M}_N$	5.09	3.33
Density (Kg/m^3)	959	962
Melt Index (g/10 min)	8.07	7.40
Melting Range ($^{\circ}K$)	386-419	386-419
Average Specific Heat:		
c_p solid ($J/Kg/^{\circ}K$)	2.38×10^3	2.54×10^3
c_p melt ($J/Kg/^{\circ}K$)	2.46×10^3	2.45×10^3
Average Thermal Conductivity:		
K_s solid ($J/m/^{\circ}K/s$)	3.62×10^7	3.45×10^7
K_m melt ($J/m/^{\circ}K/s$)	2.61×10^7	2.61×10^7
Power Law Index, n	0.800	0.822
$\Delta E/R$ ($1/^{\circ}K$)	2338	2167.4
A ($Kg\ s^{n-2}/m$)	9.276	13.99

Note: $\eta_T = A \exp(E/RT) \dot{\gamma}_T^{\,n-1}$

(d) When all the components of the system were ready, the material was injected several times into the air, with the barrel retracted, to purge the barrel. This was done in the manual control mode using the by-pass valves and switches.

(e) The hydraulic and electric systems were switched over to the servo-controlled system.

(f) Under the control of the open loop injection computer program, run in conjunction with a predetermined combination of settings for servovalve opening, injection time and holding time, the polymer melt was injected into the mold cavity, and continuous readings were taken of hydraulic pressure, nozzle pressure, linear displacement of the ram and ram velocity.

(g) The output voltage responses of the transducers were converted into actual pressure, linear displacement and velocity through the calibration equations tabulated in Table 5.1.

5.4.2 Pseudo-Steady State Experiments

Runs were performed with different servovalve openings to determine the system constraints. Two resins, EX1 and EX2, and different barrel temperatures were used. Tests with barrel front zone temperatures of 466 K, 488 K and 505 K were performed with each resin to examine the effect of temperature on the relationships between the process variables under study.

After 10 runs were completed with a given resin, the hopper was emptied and the barrel was purged thoroughly. Then 20-25 purge shots were made with the new resin to ensure that all remaining previous resin had been eliminated, before data were collected with the new resin.

5.4.3 Deterministic (Step) and Stochastic Tests

When the start-up was complete, the machine was run under steady state operation for 30 minutes before beginning the step or stochastic experiments.

The step tests were performed by rapidly changing the servovalve opening. This was done under the control of the microprocessor either 0.880 or 1.528 seconds after the commencement of injection, depending on the experimental conditions. The responses of the hydraulic pressure, nozzle pressure, linear displacement and linear velocity were measured and recorded for later analysis.

The stochastic experiments were performed using a pseudo-random binary sequence (PRBS) (see Appendix C) to position the servovalve opening at one of two predetermined values which were symmetric about the mean value. The PRBS was begun 0.320 seconds after the commencement of injection.

The process variables (hydraulic pressure, nozzle pressure, and linear velocity) were measured and recorded.

The barrel temperatures were maintained at 472 ±3 K and 433 ±3 K for the front and rear zones, respectively, for all tests. The data sampling intervals were 0.005 seconds for the step tests and 0.01 seconds for the PRBS tests.

CHAPTER 6

PSEUDO-STATIC ANALYSIS OF THE INJECTION PHASE

The relationship between nozzle pressure (P_N) and hydraulic pressure (P_H) is examined in this chapter, using two approaches. The first approach is an empirical analysis of experimental data. The second is based on a simplified theoretical analysis of the interactions between the hydraulic pressure and the injection molding variables. The effects of the temperature and resin properties on the P_N-P_H relationship are included in both cases.

6.1 Empirical Approach

Figure 6.1 shows typical hydraulic pressure and nozzle pressure profiles for a 62% servovalve opening. It is obvious that the nozzle pressure-time profile closely follows the hydraulic pressure-time profile throughout the injection phase.

Experiments were performed for valve openings of 7.5, 12.5, 25, 37, 50, 62 and 75 percent to derive an empirical relationship between nozzle pressure and hydraulic pressure and to determine the linear range of the relationship. Three runs were made for each opening to verify the reproducibility of the data.

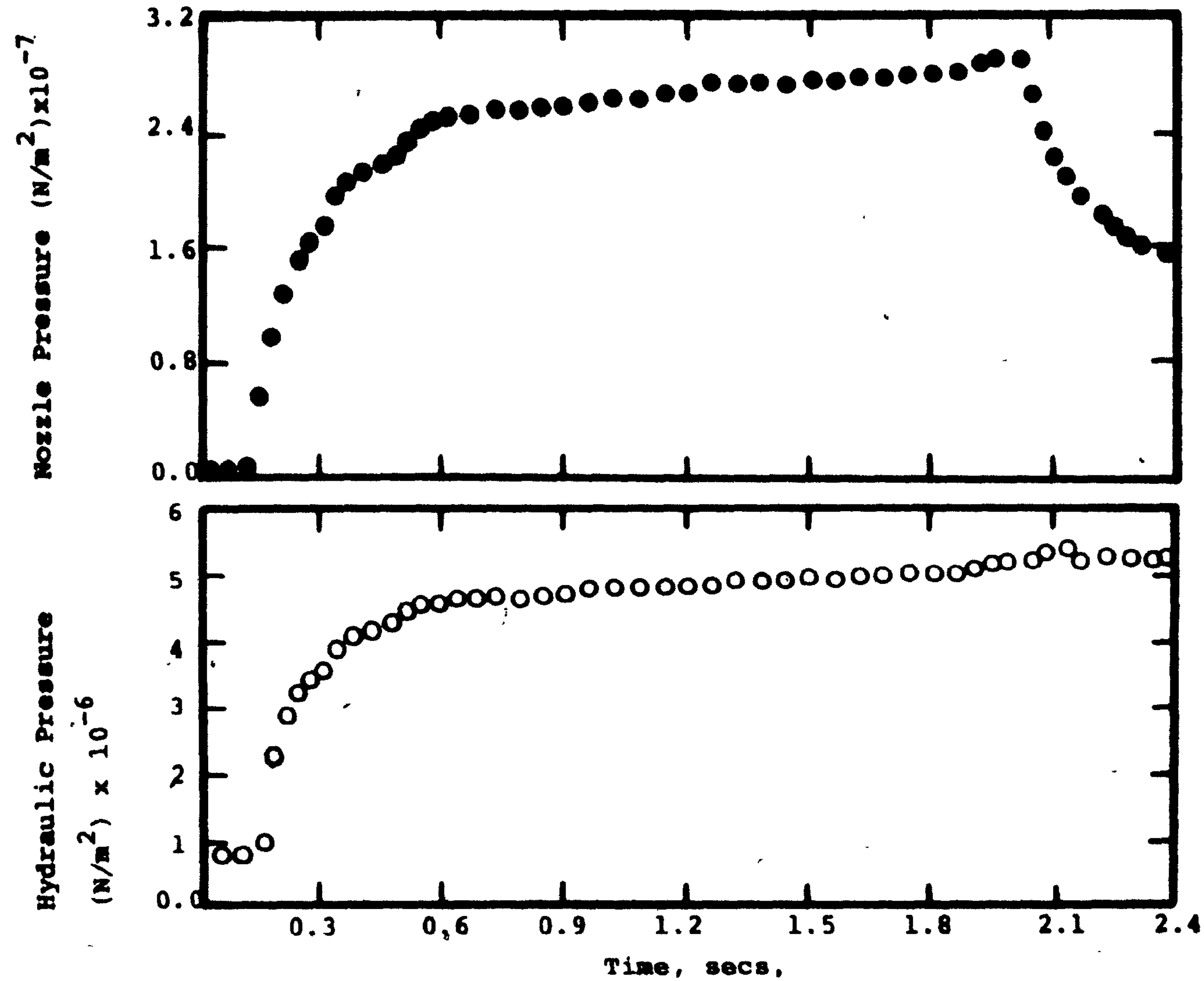

Figure 6.1 Typical Hydraulic and Nozzle Pressure Profiles for 62% Servovalve Opening

Figures 6.2 to 6.8 show the nozzle pressure as a function of hydraulic pressure. These results show that the relationship between nozzle pressure and hydraulic pressure is reasonably linear. The data were correlated, using linear regression, by the following equation:

$$P_N = K1 \times P_H + K2 \tag{6.1}$$

where

P_N = nozzle pressure, N/m^2

P_H = hydraulic pressure, N/m^2

K1 = slope of regression line, dimensionless

K2 = intercept with the ordinate, N/m^2

The values for K1 and K2 are given in Table 6.1, which also shows that the coefficients of correlation are greater than 0.98.

6.1.1 Effect of Resin Properties and Temperature on the P_N-P_H Relationship

Figure 6.9 shows the relationship between the nozzle and hydraulic pressures for resins EX1 and EX2 at a barrel temperature of 466 K. The nozzle pressure is higher for the EX2 resin, which is consistent with the experimental viscosity data published by Kalyon (43). His data showed that, for all

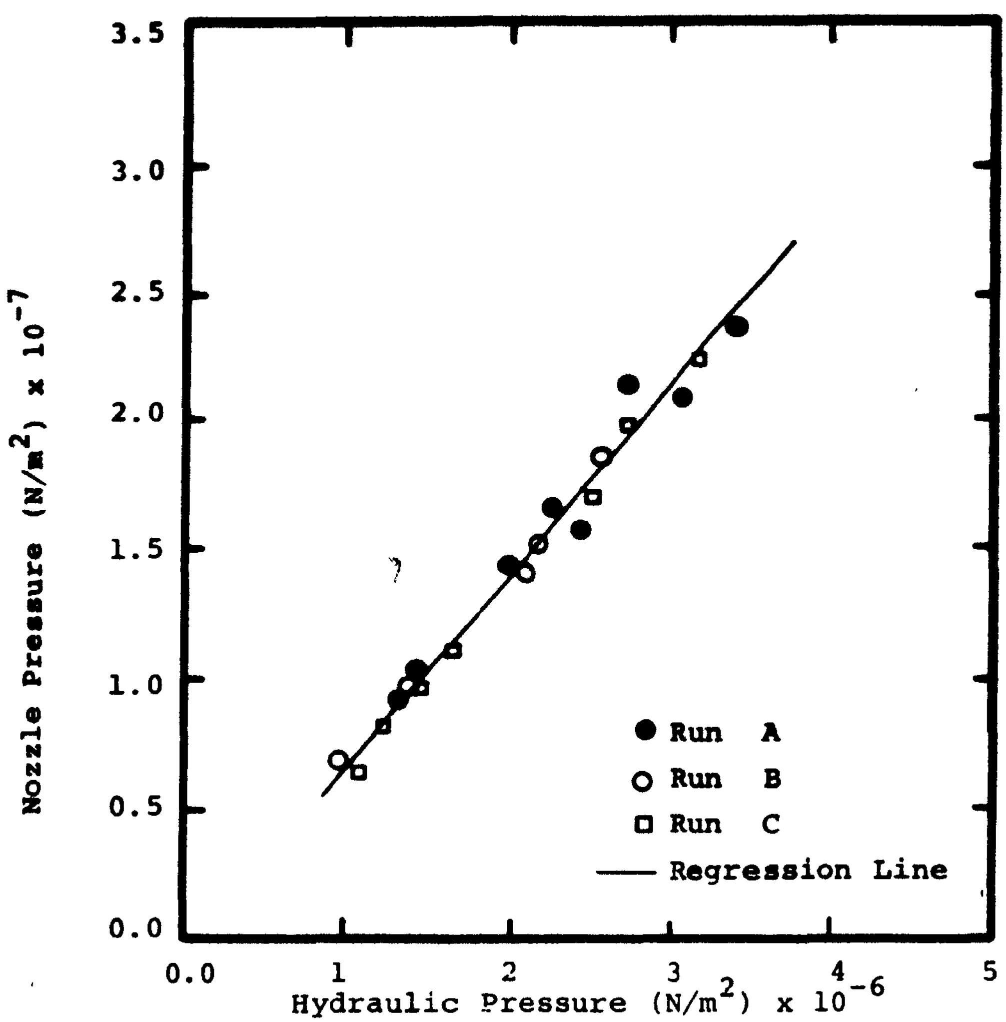

<u>Figure 6.2</u> Relation Between Nozzle Pressure and Hydraulic Pressure for 7.5% Valve Opening

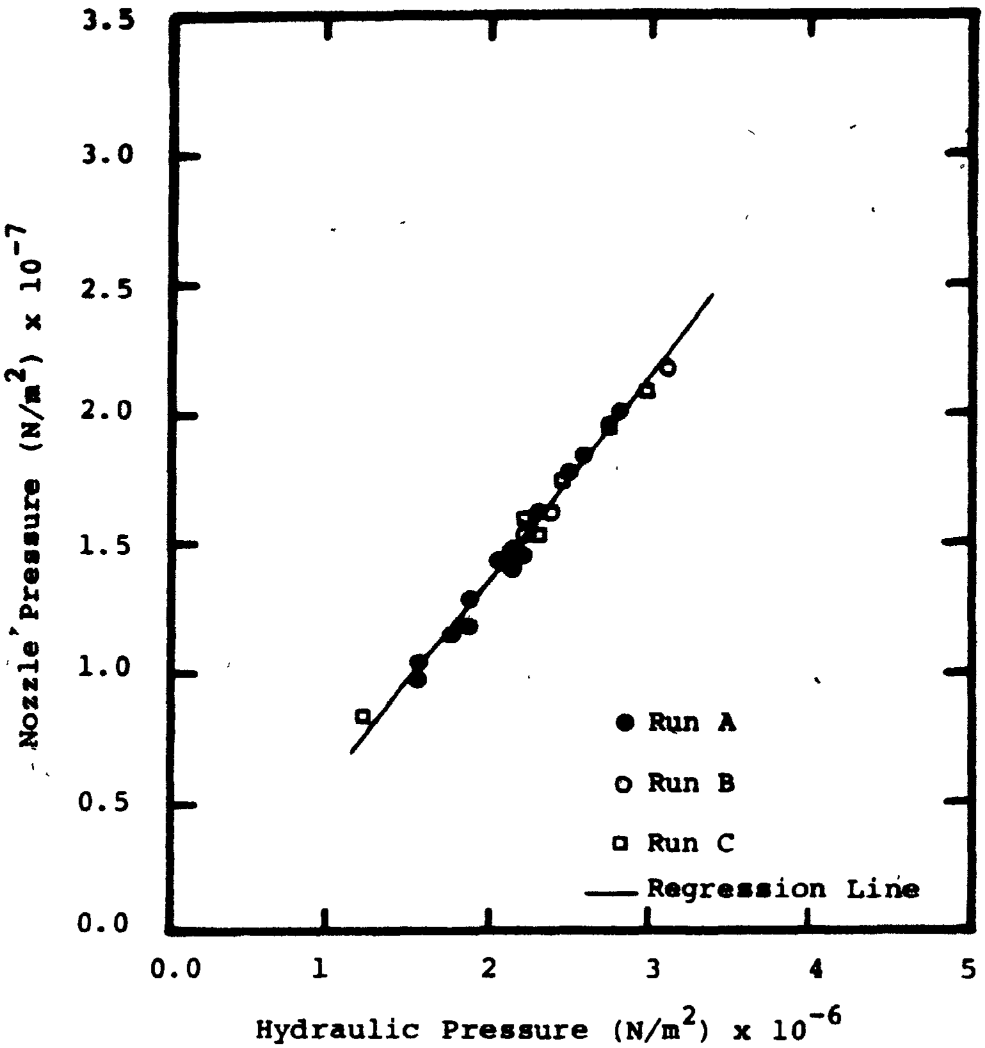

Figure 6.3 Relation Between Nozzle Pressure and Hydraulic Pressure for 12.5% Valve Opening

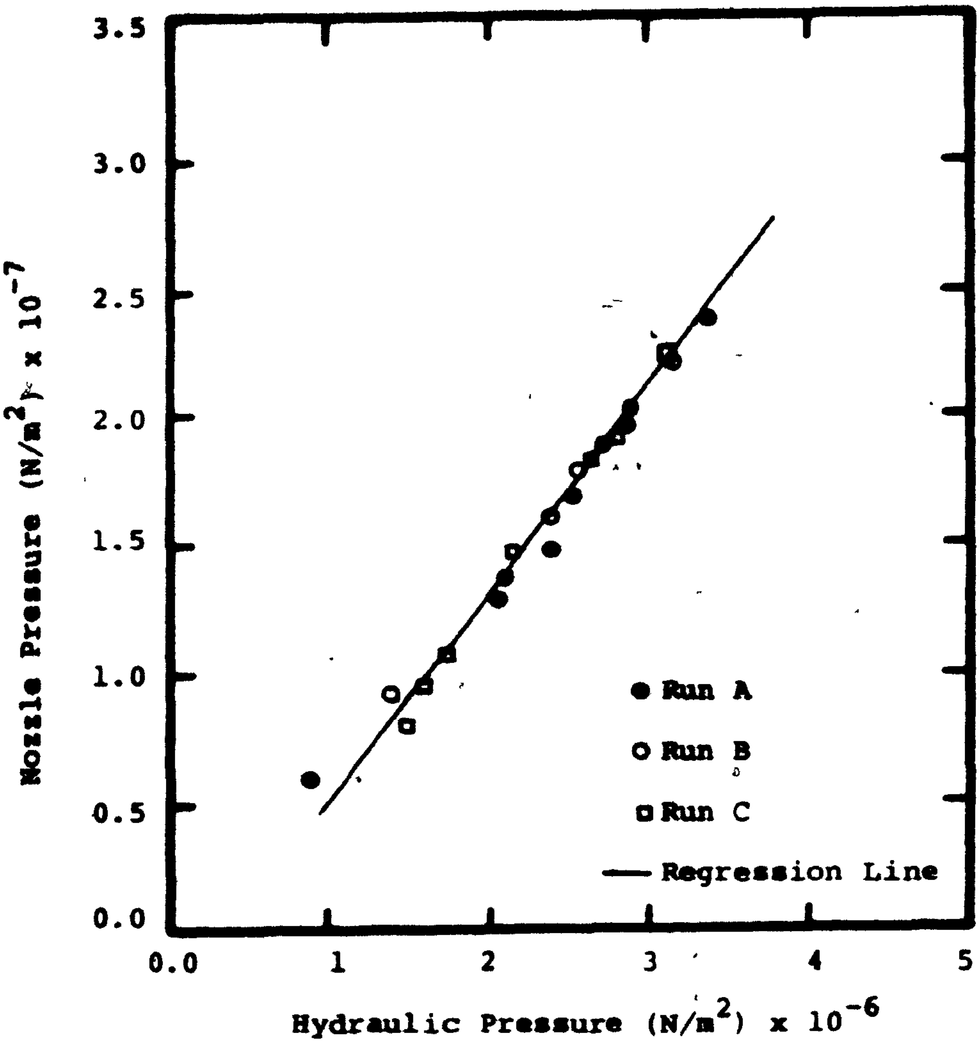

<u>Figure 6.4</u> Relation Between Nozzle Pressure and Hydraulic Pressure for 25% Valve Opening

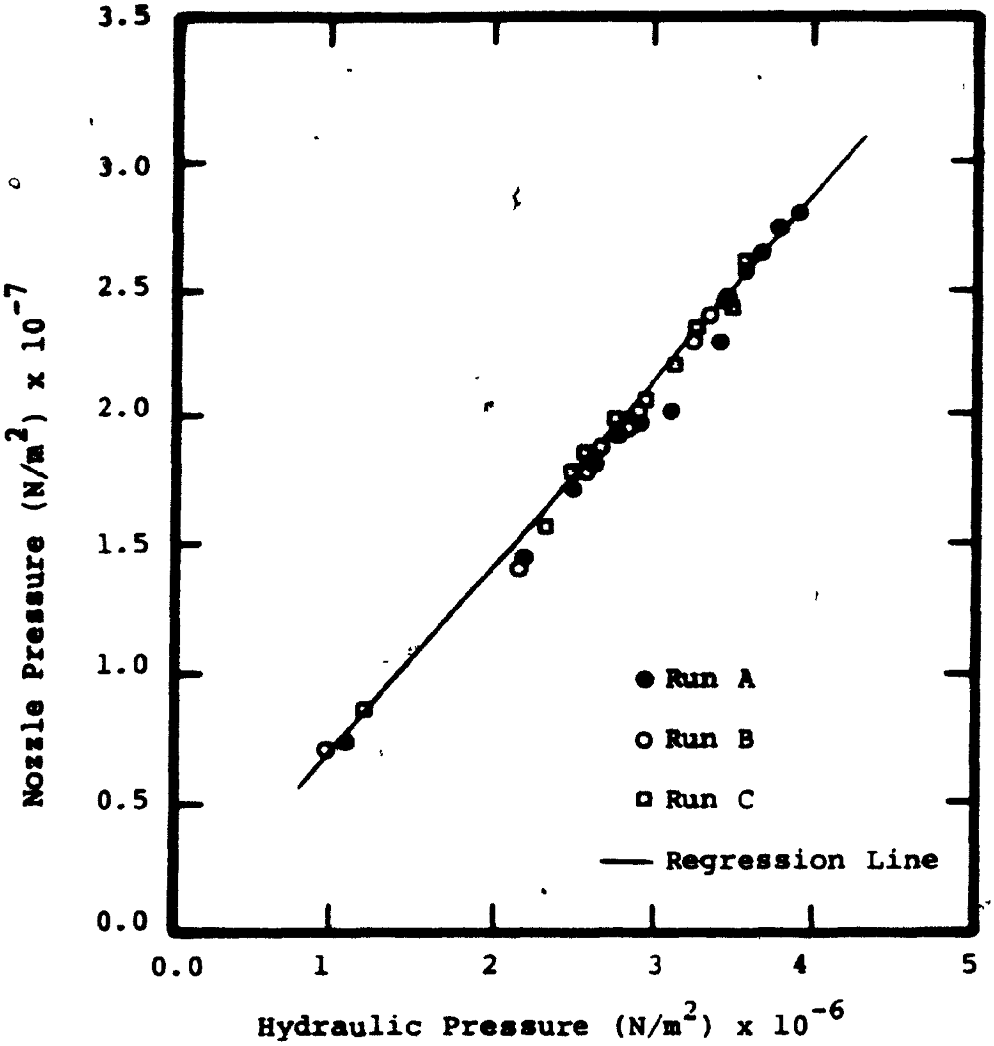

<u>Figure 6.5</u> Relation Between Nozzle Pressure and Hydraulic Pressure for 37% Valve Opening

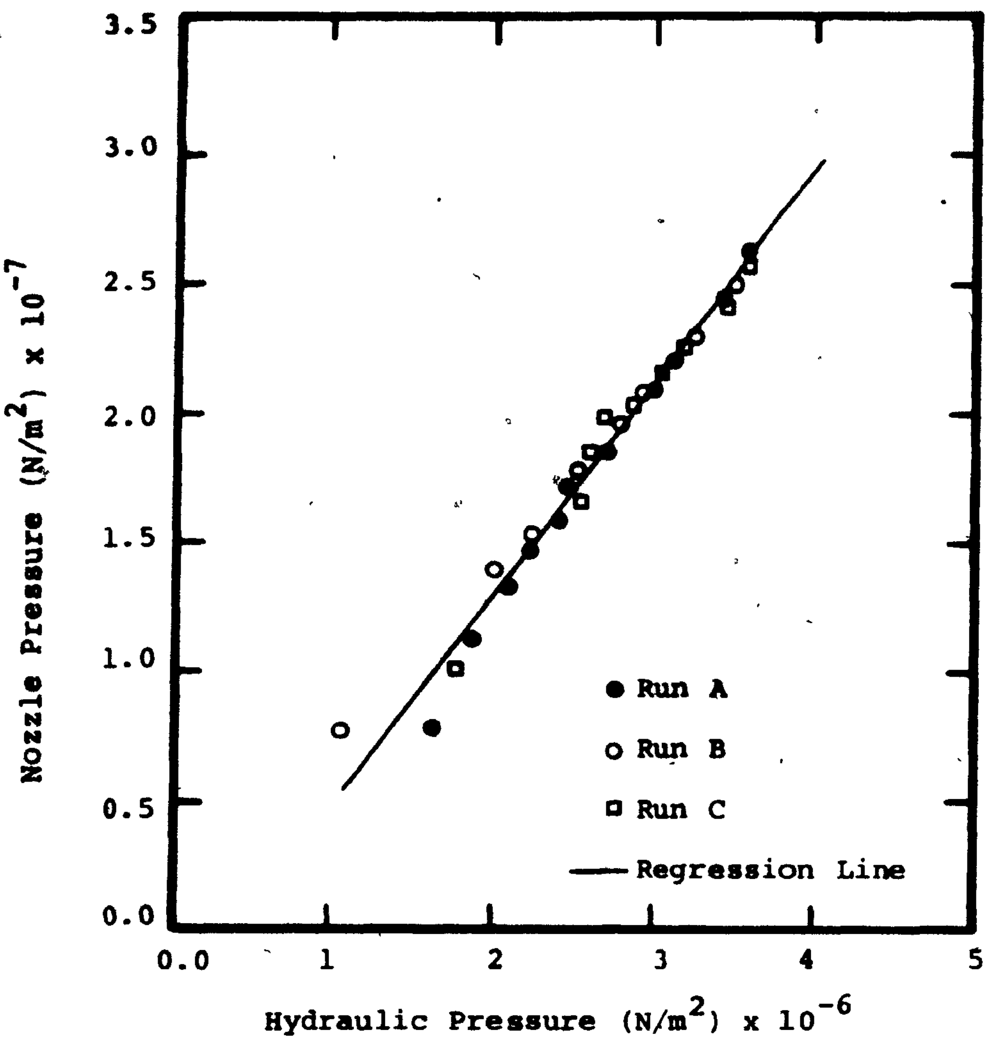

__Figure 6.6__ Relation Between Nozzle Pressure and Hydraulic Pressure for 50% Valve Opening

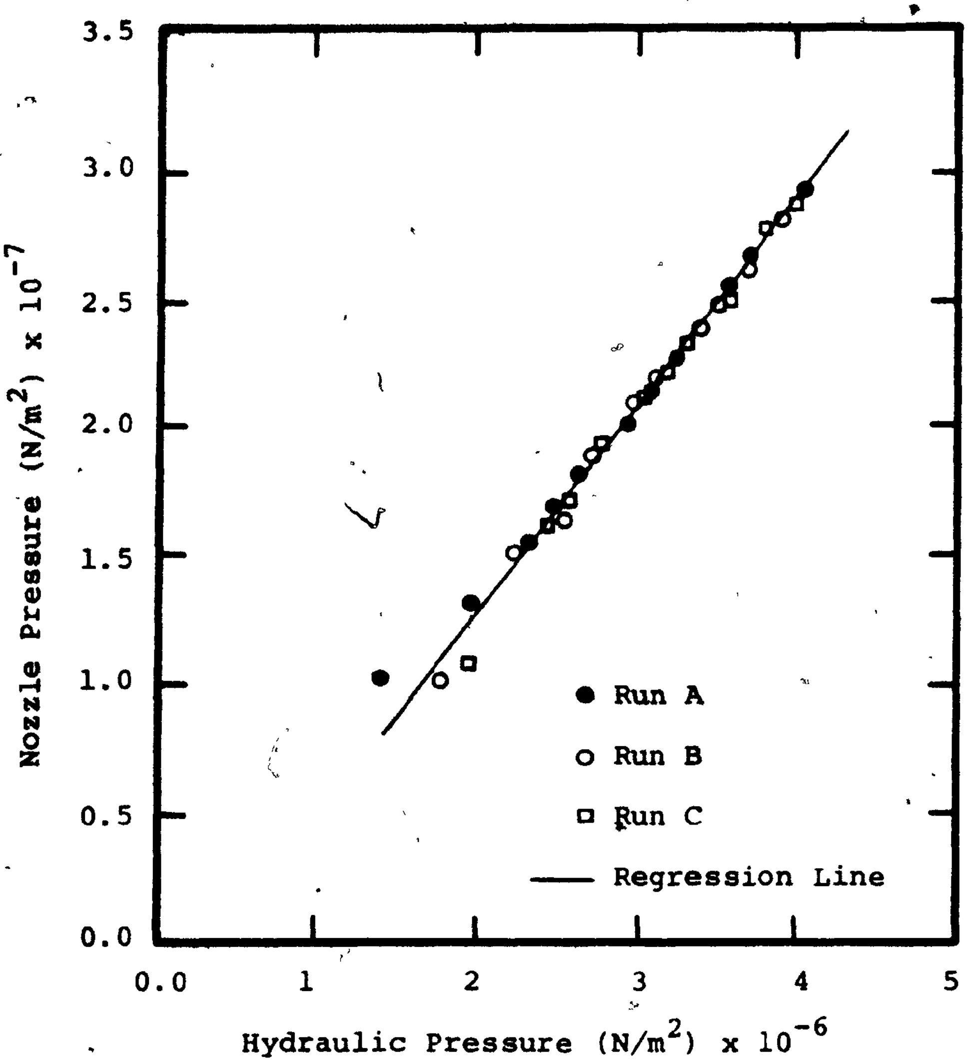

Figure 6.7. Relation Between Nozzle Pressure and Hydraulic Pressure for 62% Valve Opening

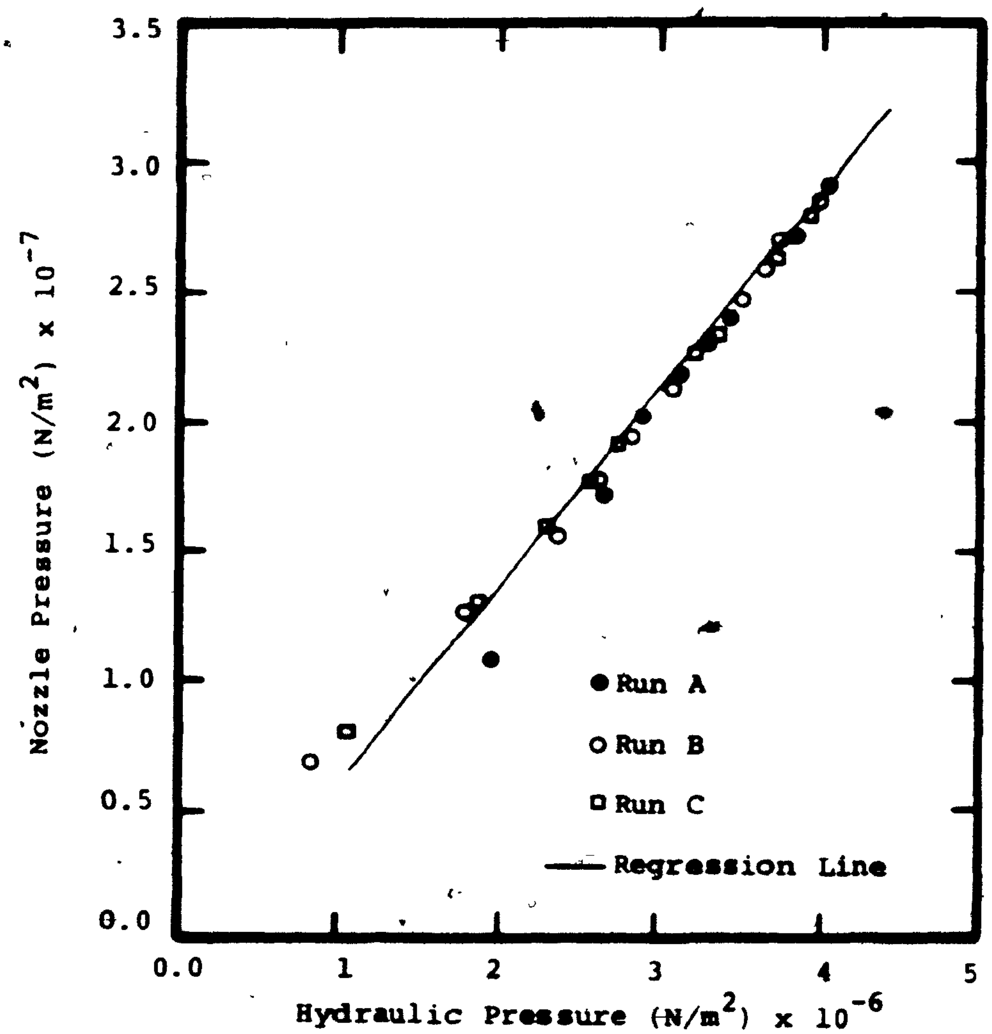

Figure 6.8 Relation Between Nozzle Pressure and Hydraulic Pressure for 75% Valve Opening

TABLE 6.1

Regression Coefficients for P_N - P_H Relationship, Equation (6.1)

Valve Opening %	K1	K2 $(N/m^2) \times 10^{-6}$	Coefficient of Correlation
25	7.05	-0.53	0.98
37	7.26	-1.55	0.99
50	7.76	-2.73	0.99
62	7.94	-3.37	0.99

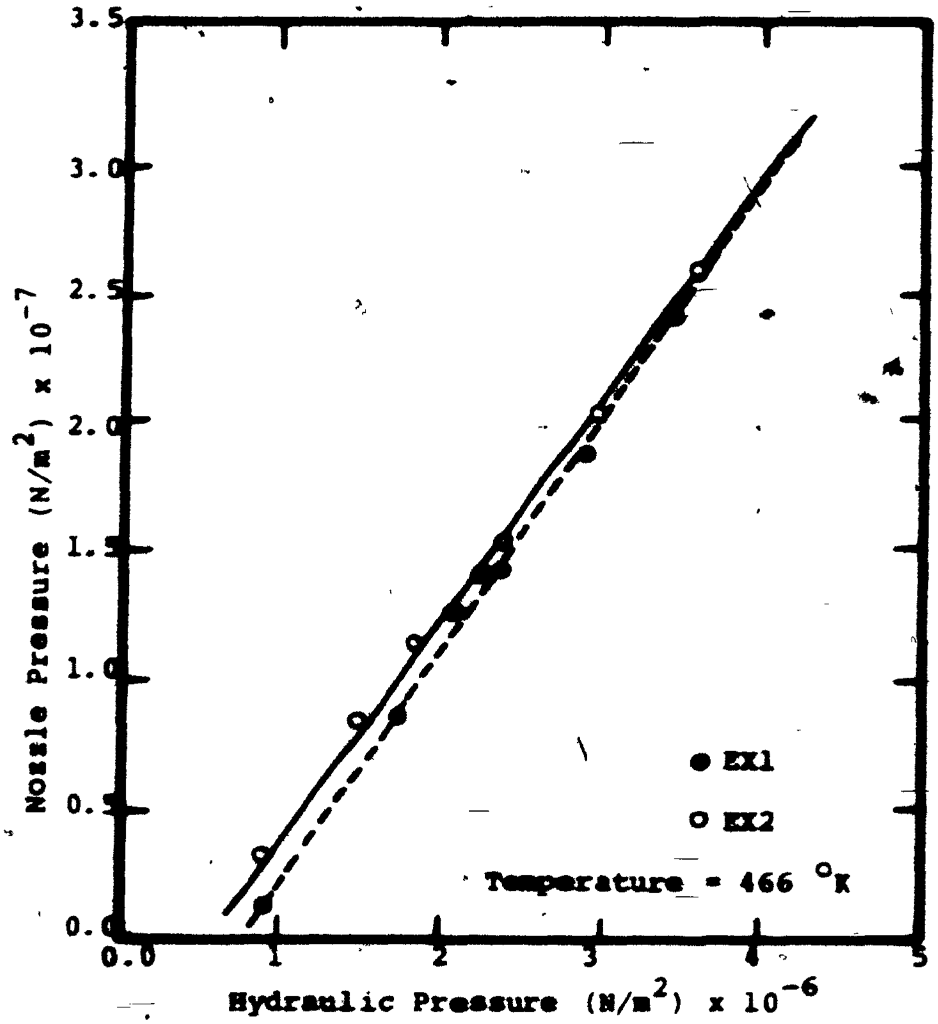

Figure 6.9 Relation Between Nozzle and Hydraulic Pressures for Resins EX1 and EX2 at Barrel Temperature of 466°K

temperatures and shear rates ($1 - 10^4$ sec^{-1}), EX2 has a higher viscosity than EX1.

Figure 6.10 shows the effect of temperature on the P_N-P_H relationship. A higher nozzle pressure is obtained at the lower temperature for the same hydraulic pressure. This effect may be attributed to the effect of temperature on viscosity.

Figures 6.9 and 6.10 show that, for hydraulic pressures > 550 psi (3.8×10^6 N/m^2), the effect of the difference in viscosity is negligible. This may be because, at high hydraulic pressure, the effect of the resistance of the shear force to the flow is negligible compared to the pushing hydraulic force.

6.2 Simplified Theoretical Treatment

This section presents relationships useful for control purposes, reflecting the interactions between process variables during the injection stage. The relationships are based on the following force balance applied to the screw shown in Figure 6.11.

$$P_H \times A_p = P_N \times A_f + F_s \qquad (6.2)$$

or

$$P_N = \frac{A_p}{A_f} \times P_H - \frac{F_s}{A_f} \qquad (6.3)$$

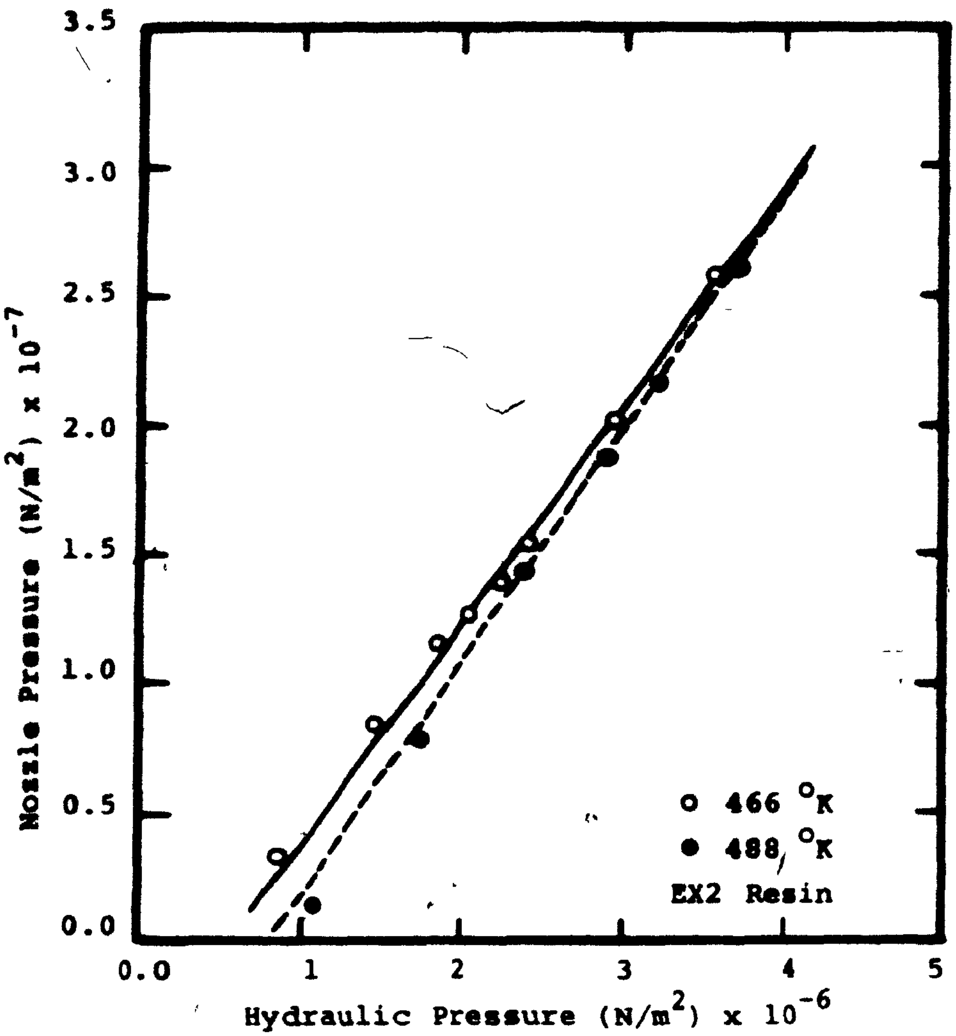

<u>Figure 6.10</u> Relation Between Nozzle and Hydraulic Pressures for Resin EX2 and Barrel Temperatures of 466°K and 488°K

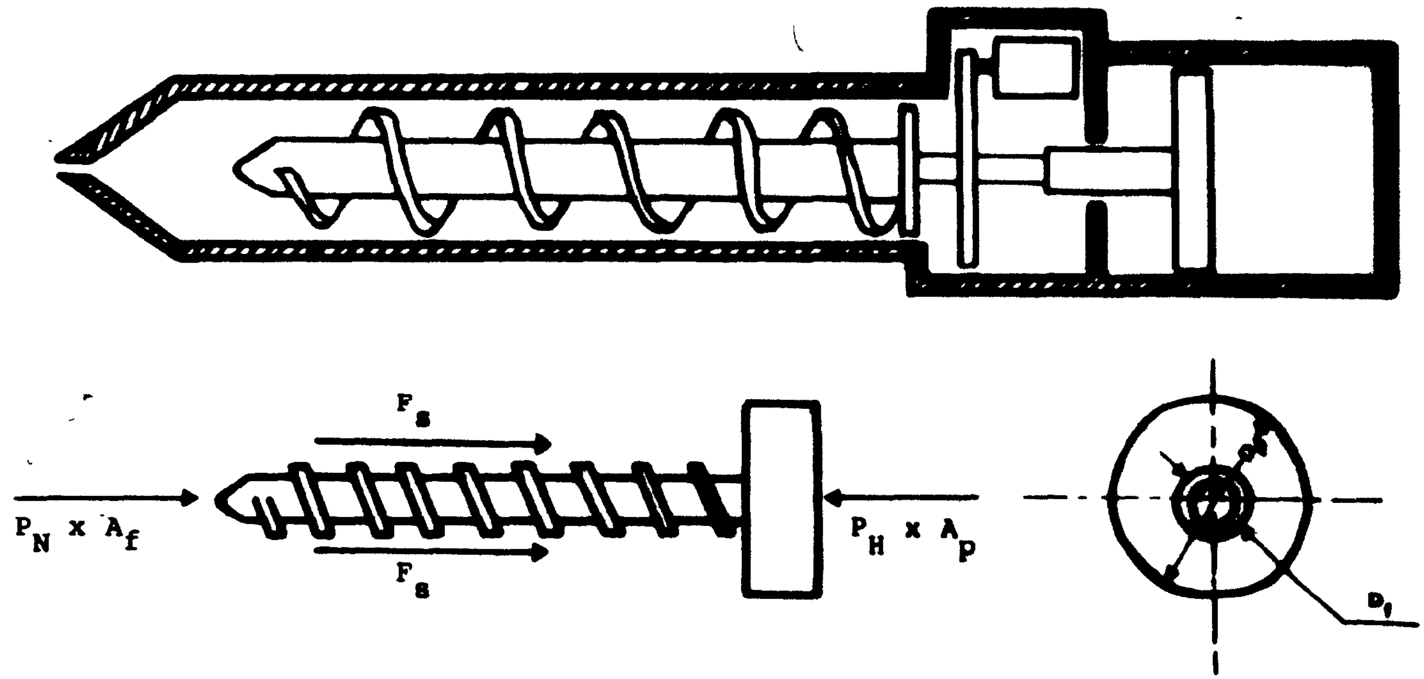

Figure 6.11 Injection Cylinder and Screw Representation

where

P_N = nozzle pressure, N/m^2

P_H = hydraulic pressure, N/m^2

A_p = cross-sectioned area of ram piston, m^2

A_f = cross-sectioned area of screw flight, m^2

F_s = shear force exerted by the polymer on the screw, N

The shear force can be estimated from the equation of change (46) using either of the following approximations:

(1) plane couette flow,

(2) axial annular couette flow.

6.2.1 Plane Couette Flow (PCF)

The polymer surrounding the screw during the injection phase may be represented as a fluid confined to the space between two horizontal planes, Figure 6.12. The upper plane is moving in the positive z-direction with a constant speed, v, the injection velocity.

Assuming the only non-zero velocity component is in the direction of the screw movement, v_z, the equations of change, in rectangular coordinates, are the following:

Continuity:

$$\frac{\partial}{\partial z} (\rho v_z) = 0 \qquad (6.4)$$

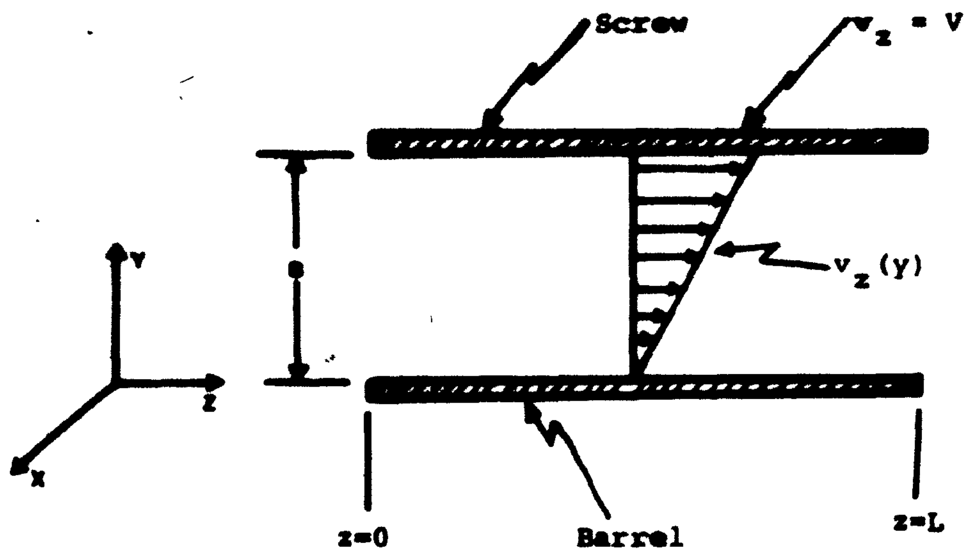

Figure 6.12 Flow Between Two Horizontal Planes with the Upper Plane Moving with a Constant Speed, V

Momentum:

$$\left(\frac{\partial v_z}{\partial t} + v_z \frac{\partial v_z}{\partial z}\right) = -\left(\frac{\partial \tau_{xz}}{\partial x} + \frac{\partial \tau_{yz}}{\partial y} + \frac{\partial \tau_{zz}}{\partial z}\right) \tag{6.5}$$

The assumptions made to obtain a simple solution of the problem were:

(a) The unsteady state terms in the continuity and momentum equations are negligible.

(b) The gradients of v_z in the x- and z-directions are negligible; thus

$$\frac{\partial v_z}{\partial x} = 0; \quad \tau_{xz} = 0 \text{ and } \frac{\partial v_z}{\partial z} = 0; \quad \tau_{zz} = 0.$$

(c) The polymer melt in the channels between the screw flights is considered to act as a solid, i.e. that the screw is a cylinder with a diameter equal to the diameter of the flight.

(d) Isothermal conditions (i.e. no viscous heat generation).

(e) The polymer melt is assumed to be incompressible and to obey the Power Law.

(f) The no-slip condition applies; i.e. $v_z = 0$ at $y = 0$, and $v_z = V$ at $y = B$.

The z-component of the equation of motion thus reduces to:

$$0 = - \frac{d\tau_{yz}}{dy} \tag{6.6}$$

The integration of equation (6.6) combined with a Power Law viscosity relationship and the boundary conditions of assumption (f) gives the velocity distribution as a function of y:

$$v_z = [\frac{V}{B}]y \tag{6.7}$$

and for the shear stress at any point in the gap, τ_{yz}:

$$\tau_{yz} = - M(\frac{V}{B})^n \tag{6.8}$$

where m and n are the parameters of the Power Law as defined by:

$$\tau_{yz} = - M(\frac{dv_z}{dy})^n \tag{6.9}$$

The shear force exerted by the polymer on the screw is:

$$F_s = \tau_{yz} \times \pi D_f L \tag{6.10}$$

where

F_s = shear force, N

D_f = flight diameter, m

L = screw length, m

The combination of (6.9) and (6.10) yields:

$$F_s = - \pi M \left(\frac{V}{B}\right)^n D_f L \tag{6.11}$$

6.2.2 Axial Annular Couette Flow (ACF)

This model considers the polymer melt to be sheared in the annular space between two co-axial cylinders. The inner cylinder (the screw) is moving at a constant velocity, V, in the z-direction, while the outer cylinder (the barrel) is stationary (Figure 6.13). The equation of motion for this case, with the assumptions of section 6.2.1, becomes:

$$0 = - \frac{1}{r} \frac{\partial}{\partial r} (r \; \tau_{rz}) \tag{6.12}$$

or

$$\frac{d}{dr} (r \; \tau_{rz}) = 0 \tag{6.13}$$

with the boundary conditions:

$$\text{at } r = KR, \; v_z = V \qquad K < 1 \tag{6.14}$$

$$r = R \; , \; v_z = 0 \tag{6.15}$$

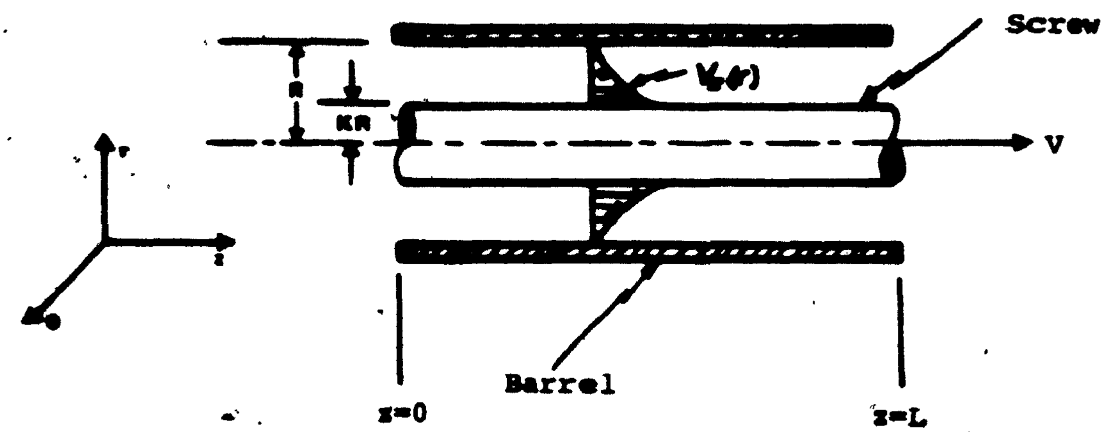

Figure 6.13 Geometry for Axial Annular Couette Flow

The integration of equation (6.13) using the Power Law relationship (equation (6.9)) yields the following velocity profile:

$$\frac{v_z(r)}{V} = \frac{(r/R)^{1-s} - 1}{K^{1-s} - 1} \qquad (6.16)$$

where

$$s = 1/n$$

The shear stress at the screw surface is given by:

$$\tau_{rz}\Big|_{r=KR} = \frac{M}{K} \cdot \frac{1}{R^n} \left[\frac{V}{\left(\frac{n}{1-n}\right)\left(K^{\frac{n-1}{n}} - 1\right)} \right]^n \qquad (6.17)$$

The shear force exerted by the polymer melt on the screw is obtained by:

$$F_s = \tau_{rz}\Big|_{r=KR} \cdot 2\pi KR\,L \qquad (6.18)$$

where

F_s = shear force, N

KR = flight radius, m

L = screw length, m

Equations (6.17) and (6.18) together give:

$$F_s = \frac{2\pi LM}{R^{n-1}} \left[\frac{V}{\left(\frac{n}{n-1}\right)\left(K^{\frac{n-1}{n}} - 1\right)} \right]^n \tag{6.19}$$

6.3 Results and Discussion

The nozzle pressure was calculated using equation (6.3) in conjunction with equations (6.11) and (6.19) reflecting plane couette and axial annular flows, respectively. The injection velocities for each combination of resin and barrel temperature were determined experimentally and are given in Table 6.2.

The resin characteristics were evaluated at an average temperature of the polymer melt film between the screw and the inside surface of the barrel. The average temperature was estimated using an expression developed by Tadmor and Klein (47):

$$T_{AV} = T_m + (T_b - T_m) \frac{\frac{A4}{2} + e^{-A4}\left(1 + \frac{1}{A4}\right) \frac{1}{A4}}{A4 + e^{-A4} - 1} \tag{6.20}$$

where

T_{AV} = average temperature of the polymer film

T_m = the melting point of the polymer, taken as the peak temperature in the specific heat vs. temperature curve obtained from a differential scanning calorimeter experiment (43)

TABLE 6.2

Experimental Values of

Injection Velocity

Resin	Barrel Temp., °K	Injection Velocity (m/sec) x 10^3
EX2	466	1.85
EX2	488	1.90
EX2	505	2.00
EX1	466	2.00
EX1	488	2.50

T_b = barrel temperature

$$A4 = \frac{a(T_b - T_m)}{n}$$

$$a = \frac{\Delta E}{R \, x T_m (T_b - T_m)}$$

n = Power Law index

The experimental nozzle and hydraulic pressure data collected during the filling phase, as typified by Figure 6.1, were replotted and used to test the models. The results for different constant injection velocities and different barrel temperatures for both resins are shown in Figures 6.14 to 6.18.

Although the ACF model is a more realistic representation of the physical situation, the PCF model yields almost identical results. This is explained by the small gap ($K \simeq 1$) between the flights and the barrel which allows the parallel plate model to be a valid approximation.

The model predictions were in good agreement with the experimental data and, generally, yield better agreement at lower hydraulic and nozzle pressures. Apparently, at higher pressures, the assumptions of isothermal flow and incompressibility lead to the observed deviations.

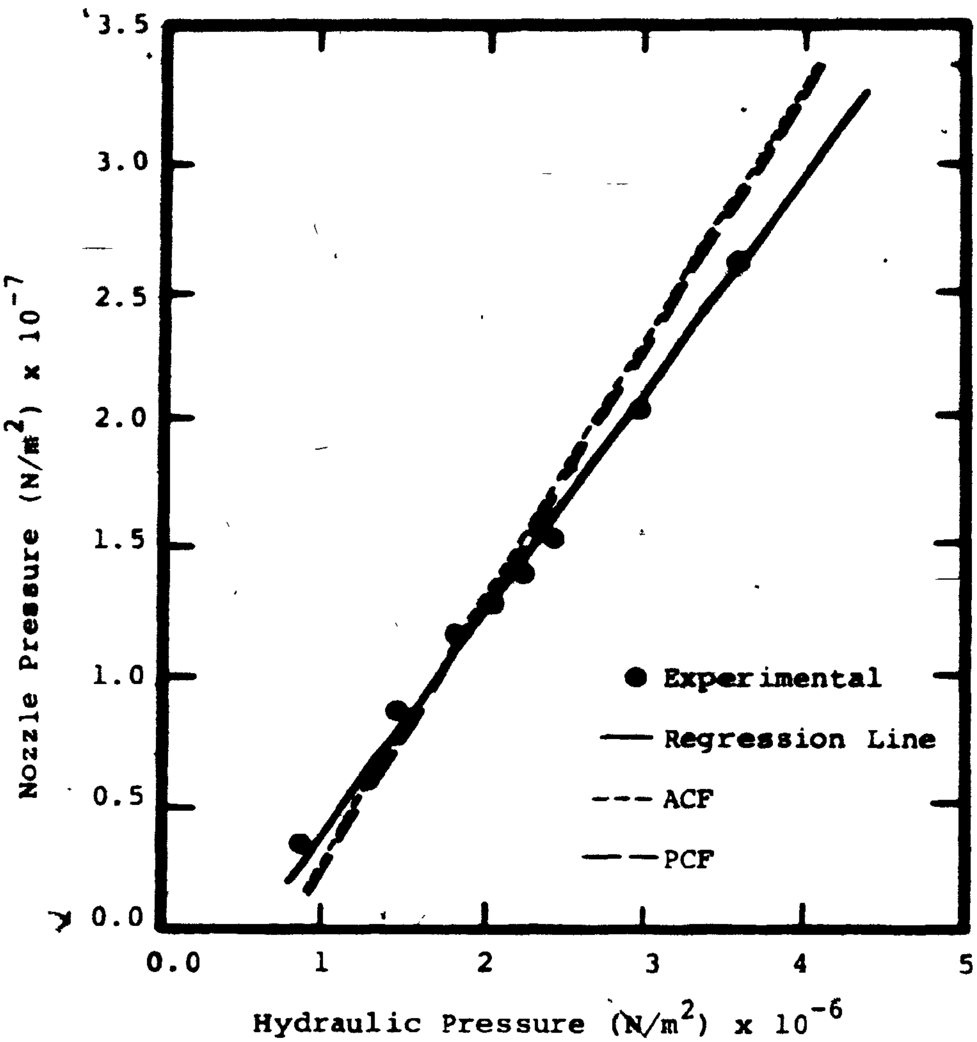

<u>Figure 6.14</u> Experimental and Calculated Nozzle Pressure as a Function of Hydraulic Pressure for Resin EX2; Barrel Temperature = 466 K; Injection Velocity = 1.85×10^{-2} M/sec

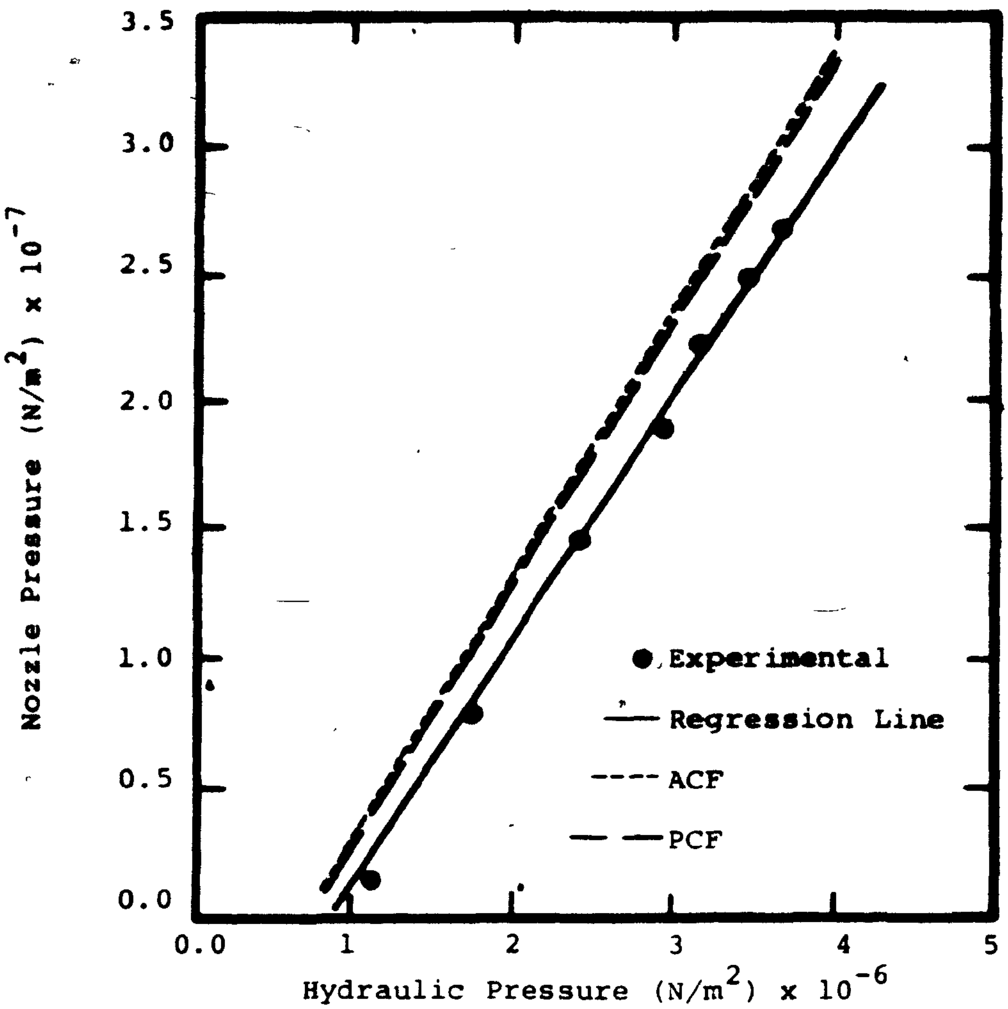

<u>Figure 6.15</u> Experimental and Calculated Nozzle Pressure as a Function of Hydraulic Pressure for Resin EX2; Barrel Temperature = 408 K; Injection Velocity = 1.9×10^{-2} M/sec

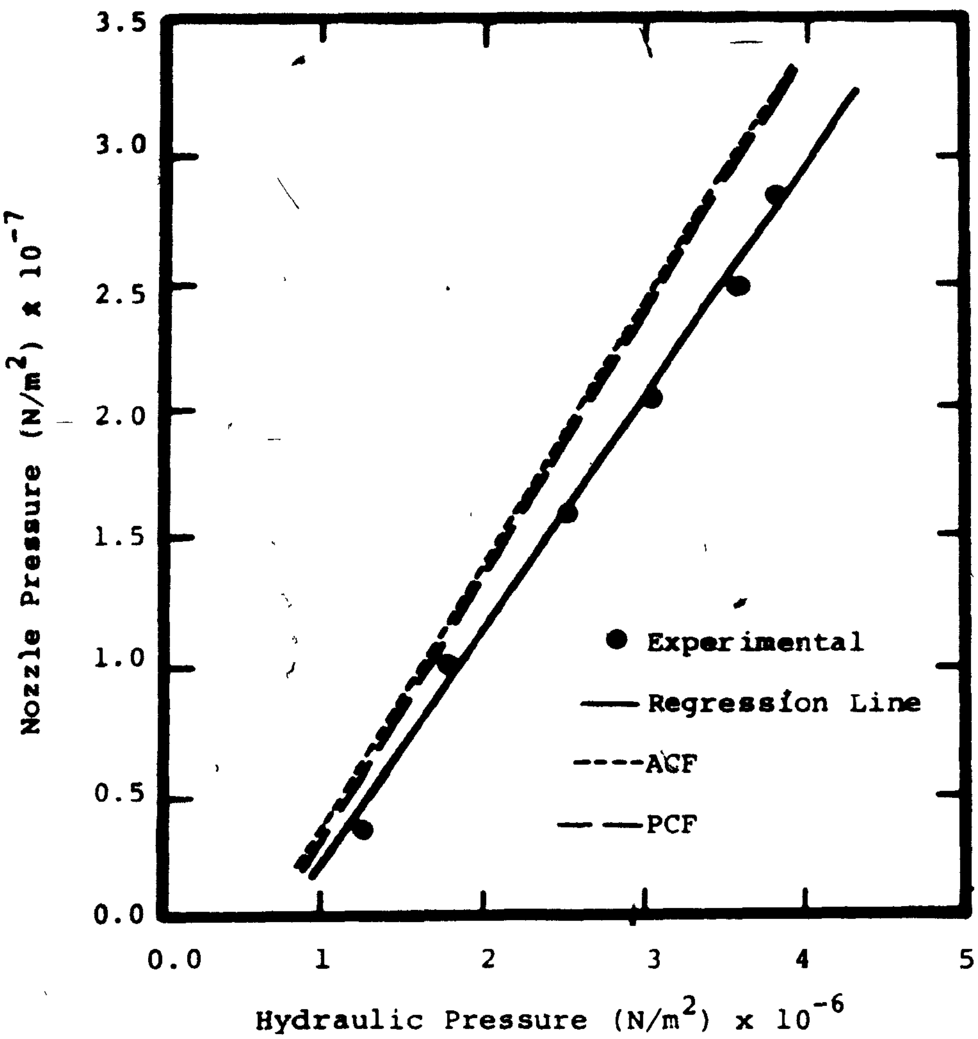

Figure 6.16 Experimental and Calculated Nozzle Pressure as a Function of Hydraulic Pressure for Resin EX2; Barrel Temperature = 505 K; Injection Velocity = 2 x 10^{-2} M/sec

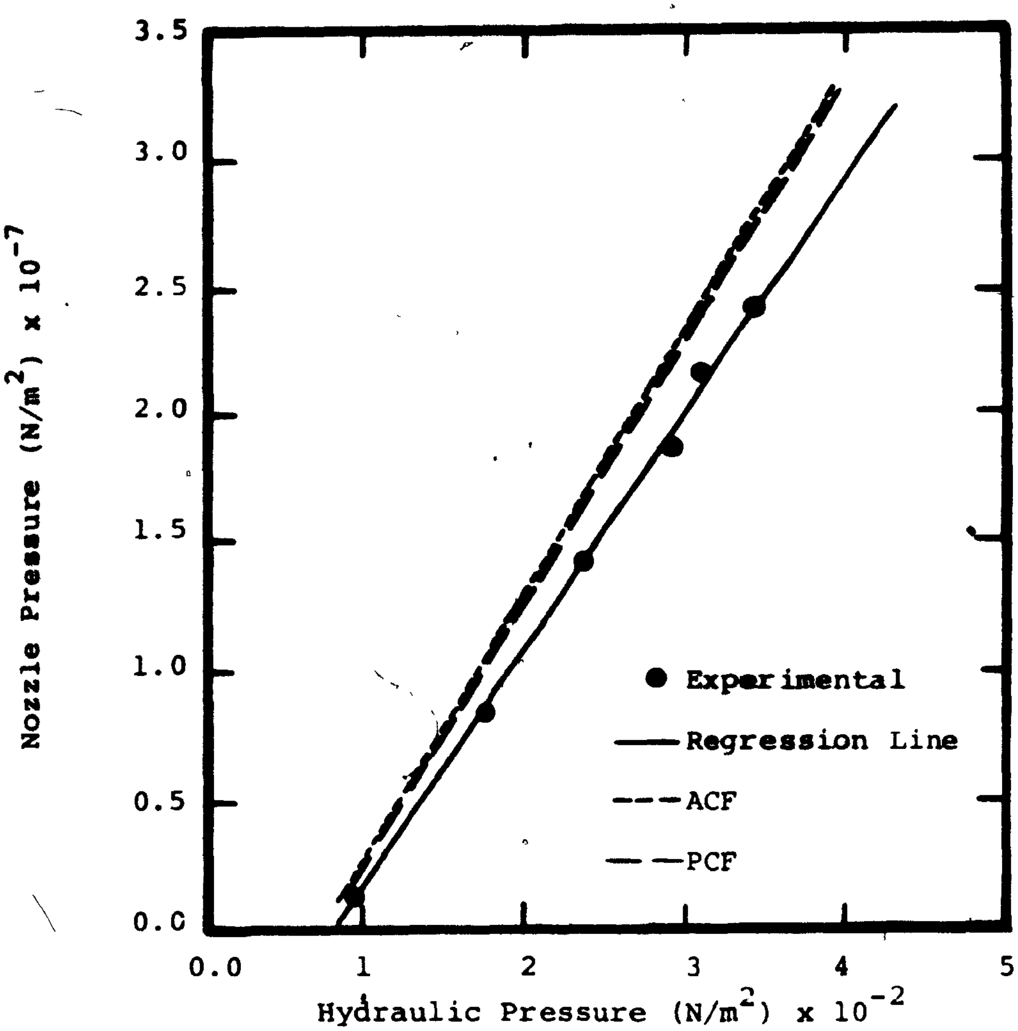

Figure 6.17 Experimental and Calculated Nozzle Pressure as a Function of Hydraulic Pressure for Resin EX1; Barrel Temperature = 466 K; Injection Velocity = 2.0 x 10^{-2} M/sec

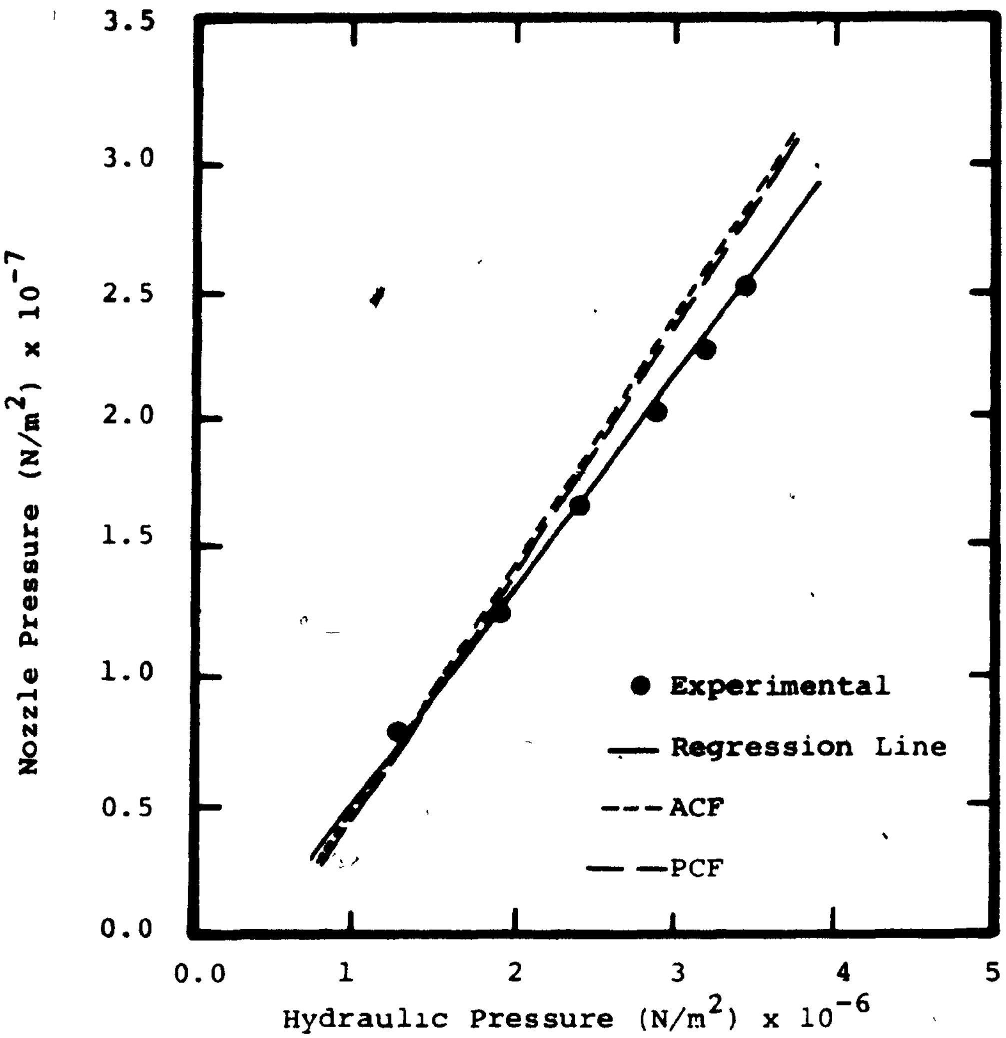

Figure 6.18 Experimental and Calculated Nozzle Pressure as a Function of Hydraulic Pressure for Resin EX1; Barrel Temperature = 488 K; Injection Velocity = 2.5 x 10^{-2} M/sec

CHAPTER 7

DYNAMIC MODELLING

7.1 Deterministic (Step) Tests

The deterministic (step) tests were performed by rapidly opening or closing the servovalve during the injection phase. The hydraulic pressure, nozzle pressure, linear displacement of the injection ram, and the injection velocity were measured throughout the injection phase. Steps of ±5, ±10, ±15, ±20 percent in the servovalve opening were used to estimate the dynamic parameters of the process and to examine the system linearity. Several runs were performed for each step change to verify the reproducibility of the data. The dynamic parameters of the process were obtained by fitting different models to the experimental data using the NONLINWOOD program (37).

7.1.1 Hydraulic Pressure

Figure 7.1 shows the response of the hydraulic pressure to the ±10, ±15, ±20 percent step changes in the servovalve opening. These responses indicate a noisy, over-damped second-order response superimposed on a constantly increasing (ramp) pressure component. This constantly increasing pressure occurs at constant valve opening and, for the purposes of dynamic behavior analysis, can be ignored.

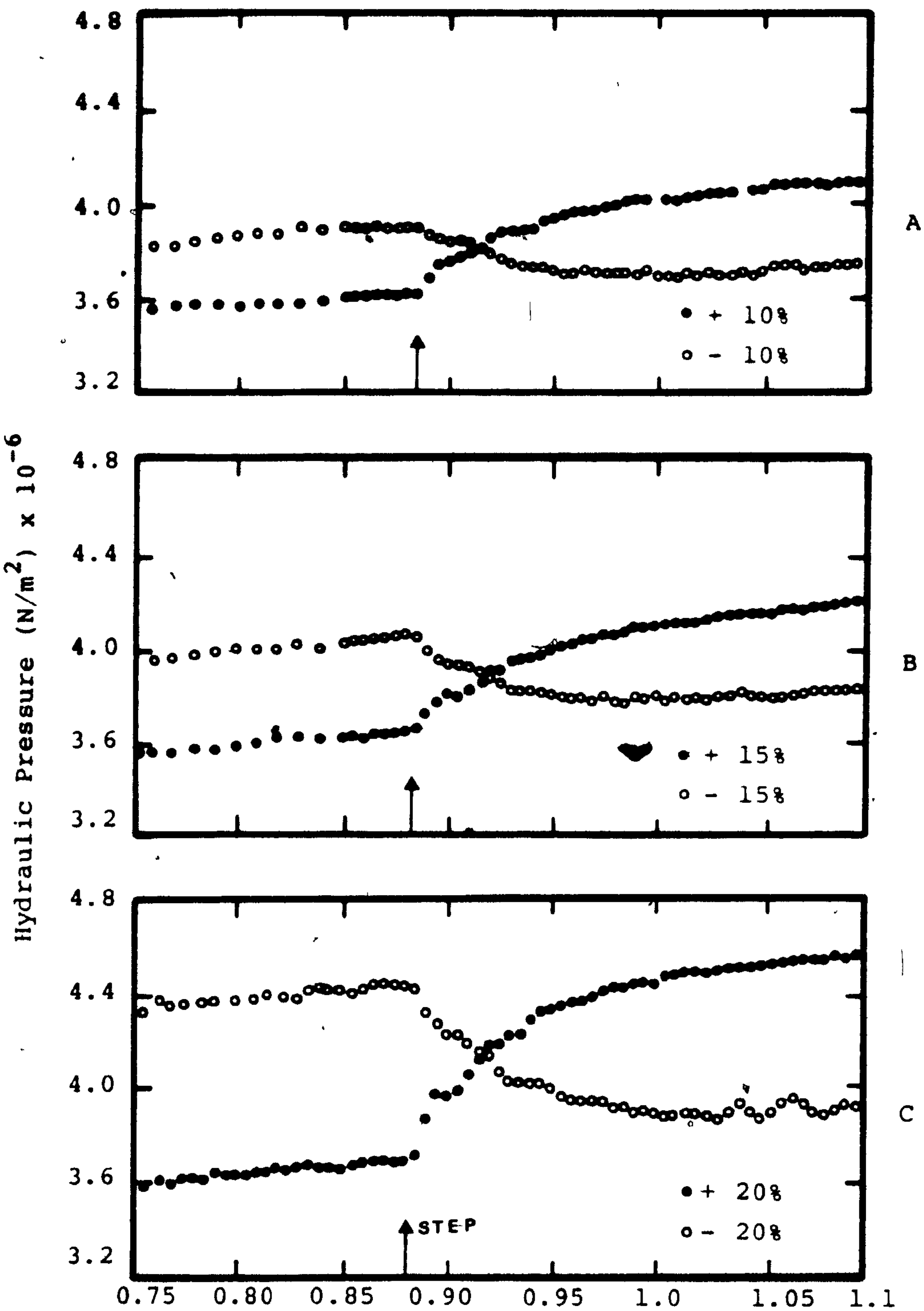

<u>Figure 7.1</u> Hydraulic Pressure Response to (a) ±10, (b) ±15, (c) ±20% Valve Opening Changes

A careful examination of Figure 7.1 reveals that the apparent noise, or random deviation from a second-order response, actually has a damped oscillatory nature. This is probably due to the servovalve overshoot and resonance (see Appendix A). The combined response can be modelled as (34):

$$P_H = G\left[1 - \frac{\tau_1\tau_2}{\tau_1-\tau_2}\left(\frac{1}{\tau_2} e^{-t/\tau_1} - \frac{1}{\tau_1} e^{-t/\tau_2}\right)\right] +$$

$$G_1\left[\frac{1}{(1-\xi^2)^{\frac{1}{2}}\tau_3} e^{-\xi t/\tau_3} \sin\{(1-\xi^2)^{\frac{1}{2}} \frac{t}{\tau_3}\}\right] \qquad (7.1)$$

where

P_H = hydraulic pressure, N/m^2

G_1, G_2 = process gains, $(N/m^2)/\%$ change in valve opening

τ_1, τ_2, τ_3 = time constants, seconds

ξ = damping factor

The first term on the right-hand side of equation (7.1) accounts for the basic second- order nature of the response, while the second term is the oscillatory, valve-induced, component. Although physical considerations support the use of equation (7.1), better fits to the data were obtained from a delayed first-order plus oscillatory response as given by equation (7.2):

$$P_H = G(1-e^{-(t-D)/\tau}) + G_1\left[\frac{1}{(1-\xi^2)^{1/2}\tau_1} e^{-\xi t/\tau_1} \sin\{(1-\xi^2)^{1/2}\frac{t}{\tau_1}\}\right] \quad (7.2)$$

where

D = time delay, seconds

The average values of the parameters of equation (7.2), as obtained with the NONLINWOOD program, (37), are given in Table 7.1.

A comparison between the predictions of equation (7.2) and the experimental data obtained using different step changes in the valve opening is shown in Figure 7.2. The model predictions are in good agreement with the experimental data.

Figure 7.3 shows the linearity of the response of hydraulic pressure to changes in the valve opening in the range of ±20%. This result indicates that the hydraulic pressure response gain is not a function of the magnitudes of changes in the valve opening in the range of ±20%.

7.1.2 Nozzle Pressure

The nozzle pressure response shown in Figure 7.4 has the appearance of an overdamped second-order response. There is, again, the constantly increasing component that is ignored in

TABLE 7.1

Values of the Parameters for the Hydraulic

Pressure Model, Equation (7.2)

First Order Model Parameters			Oscillatory Component		
Change in Valve Opening, %	Gain, G, $(N/m^2.\%)X10^{-4}$	Time Constant, τ (sec.)$X10^2$	Gain, G1, $(N/m^2.\%)X10^{-1}$	Time Constant, τ_1 secs.	Damping Factor, ξ
+ 10	2.96 ±0.19	4.0 ±0.30	2.62	0.005	0.16
- 10	3.22 ±0.21	4.9 ±0.48	2.06	0.005	0.20
+ 15	2.76 ±0.20	4.8 ±0.46	1.93	0.005	0.16
- 15	2.76 ±0.19	4.8 ±0.44	1.90	0.005	0.18
+ 20	3.45 ±0.15	4.1 ±0.33	2.48	0.005	0.13
- 20	3.31 ±0.16	4.6 ±0.39	2.34	0.005	0.18

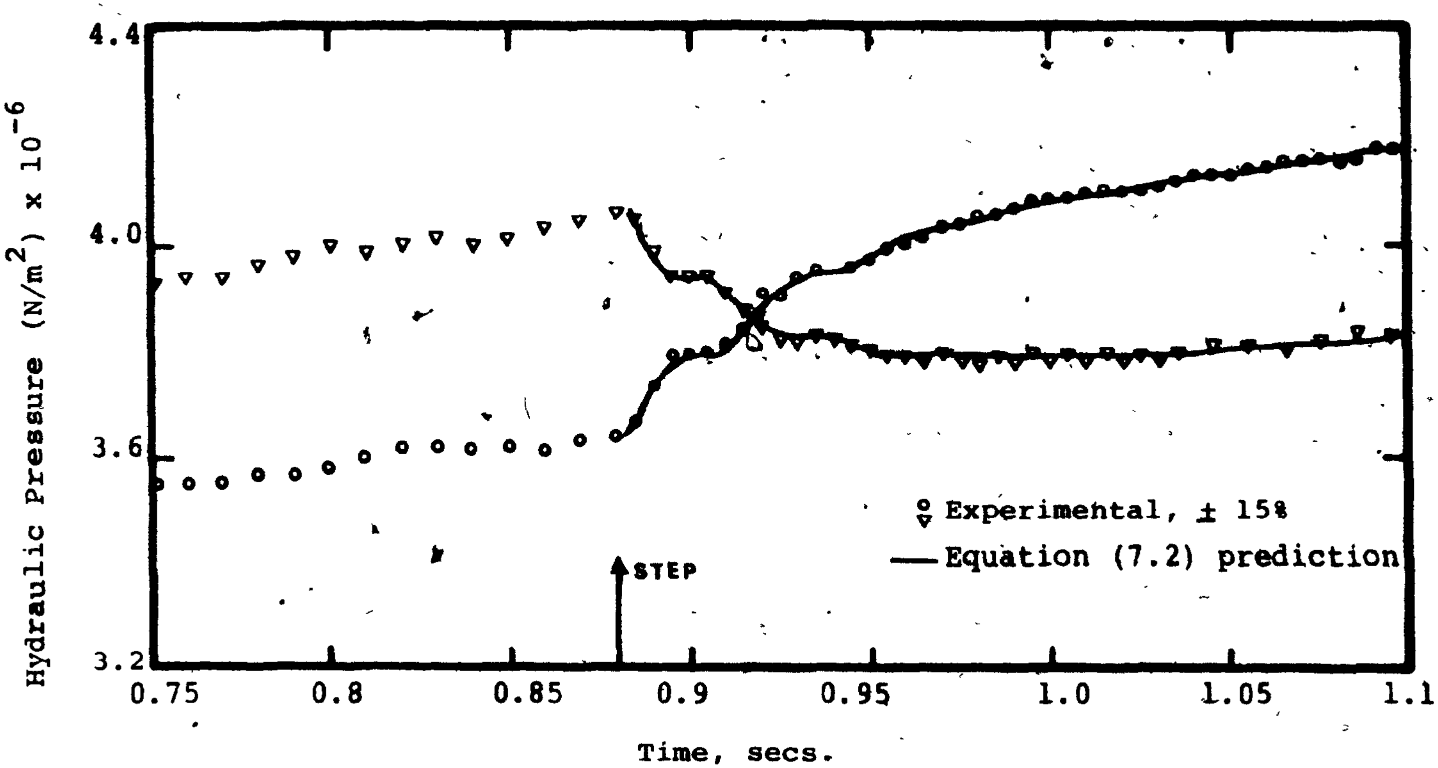

Figure 7.2 Comparison of Experimental Hydraulic Pressure Response to Fitted Model (Equation 7.2)

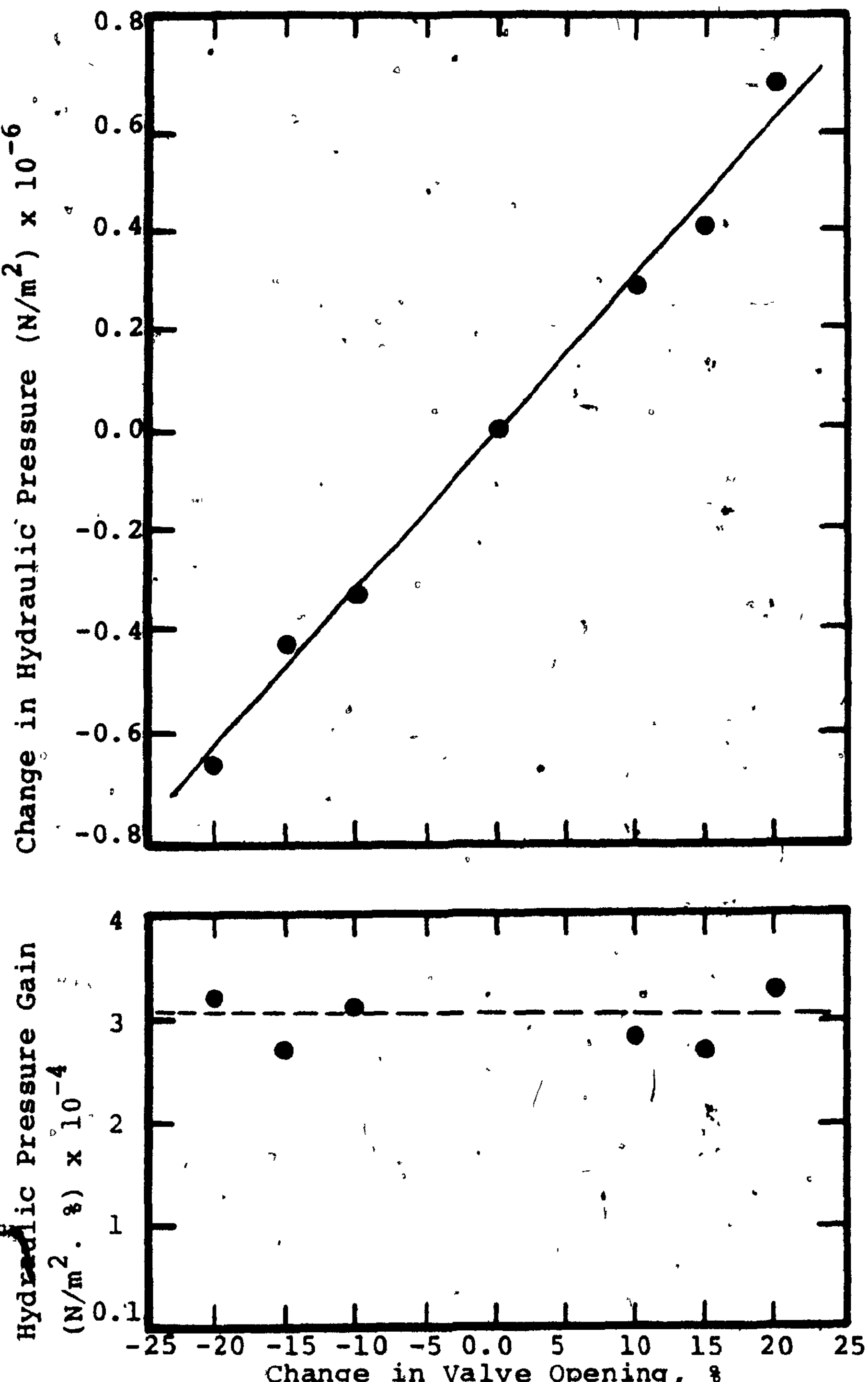

Figure 7.3 Linearity of Hydraulic Pressure Gain for Step Changes in Valve Opening

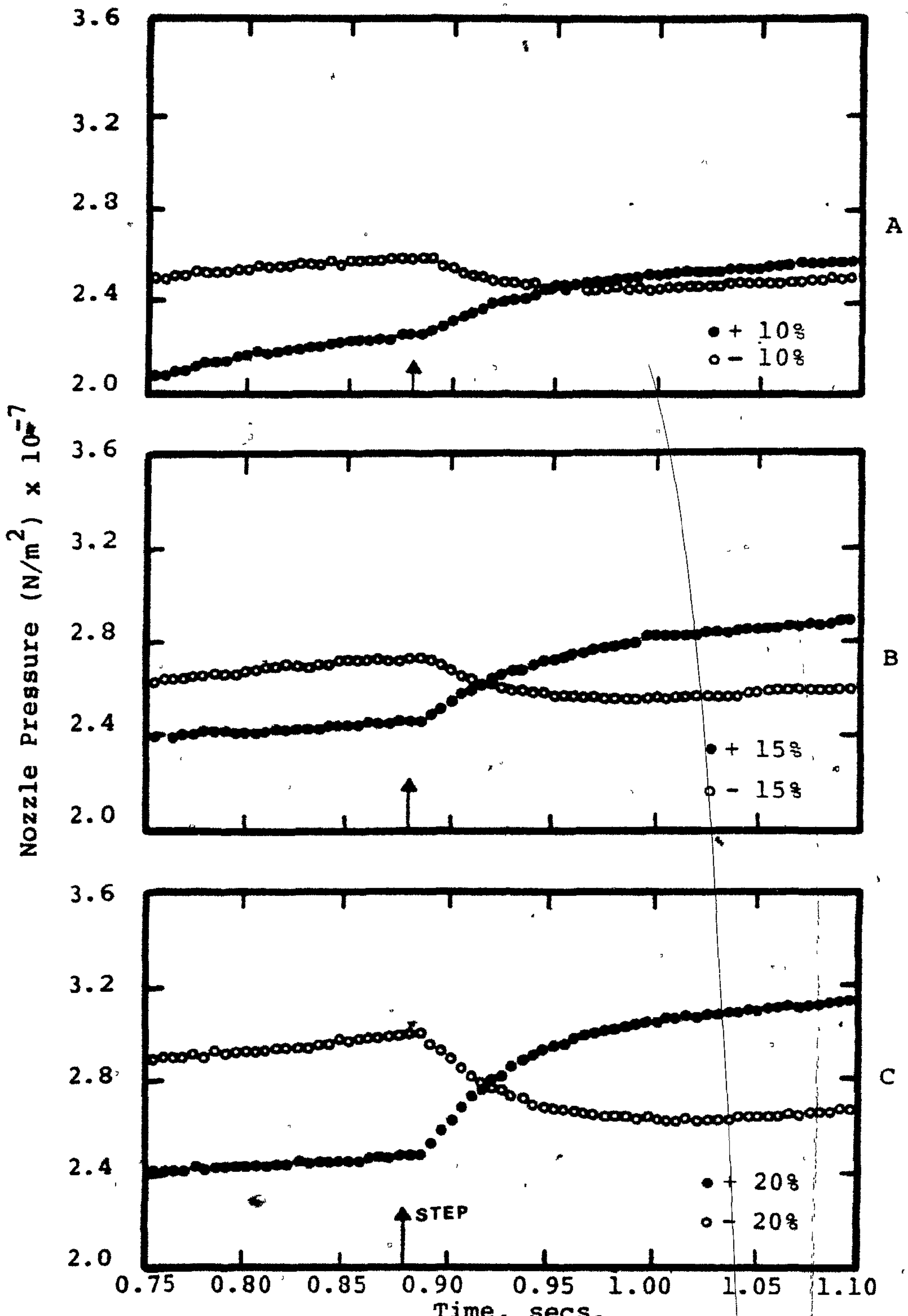

<u>Figure 7.4</u> Nozzle Pressure Response to (a) ±10, (b) ±15, (c) ±20% Valve Opening Changes

the present analysis. However, the small oscillatory component observed in the hydraulic pressure does not appear in the nozzle pressure. This is probably due to its attenuation by the hydraulic piston and ram system.

The nozzle pressure response was modelled as an overdamped second-order process:

$$P_N = G\left[1 - \frac{\tau_1\tau_2}{\tau_1-\tau_2}\left(\frac{1}{\tau_2} e^{-t/\tau_1} - \frac{1}{\tau_1} e^{-t/\tau_2}\right)\right] \qquad (7.3)$$

where P_N = nozzle pressure.

A first-order model with time delay was also fitted to the nozzle pressure data using equation (7.4):

$$P_N = G(1 - e^{-(t-D)/\tau}) \qquad (7.4)$$

The parameters for the fitted models, equations (7.3) and (7.4), are given in Tables 7.2 and 7.3, respectively. Figures 7.5 A and B compare the two models for the nozzle pressure to the experimental data. The fits for both models appear to be equally good, but a comparison of the two models using the sum of squares of the residuals indicates that equation (7.3) yields a better fit. The second-order model also is a more realistic representation of the physical situation of the process, in which the hydraulic system

TABLE 7.2

Values of the Parameters for

the Nozzle Pressure

Model: Second-Order, Equation (7.3)

Change in Valve Opening, %	Gain $(N/m^2)X10^{-5}$	Time Constants, (sec)X10^2	
		τ_1	τ_2
+ 10	2.06 ± 0.24	3.6 ± 1.26	1.14 ± 0.40
- 10	1.91 ± 0.19	3.5 ± 1.04	1.00 ± 0.35
+ 15	2.10 ± 0.23	4.0 ± 1.00	1.00 ± 0.20
- 15	1.94 ± 0.12	3.9 ± 0.70	0.99 ± 0.26
+ 20	2.23 ± 0.13	3.5 ± 0.53	1.03 ± 0.25
- 20	2.18 ± 0.11	4.1 ± 0.42	0.90 ± 0.20

TABLE 7.3

Values of the Parameters for the Nozzle Pressure Model: First-Order Plus Time Delay, Equation (7.4)

Change in Valve Opening, %	Gain, G, $(N/m^2 \cdot \%) X10^{-5}$	Time Constant τ, (sec) $X10^2$	Time Delay D, sec.
+ 10	2.08 ± 0.11	4.50 ± 0.51	0.0046
- 10	2.10 ± 0.09	4.80 ± 0.45	0.0043
+ 15	2.07 ± 0.10	5.20 ± 0.45	0.0046
- 15	1.95 ± 0.09	5.30 ± 0.40	0.0042
+ 20	2.29 ± 0.09	4.70 ± 0.33	0.0043
- 20	2.20 ± 0.08	5.00 ± 0.28	0.0034

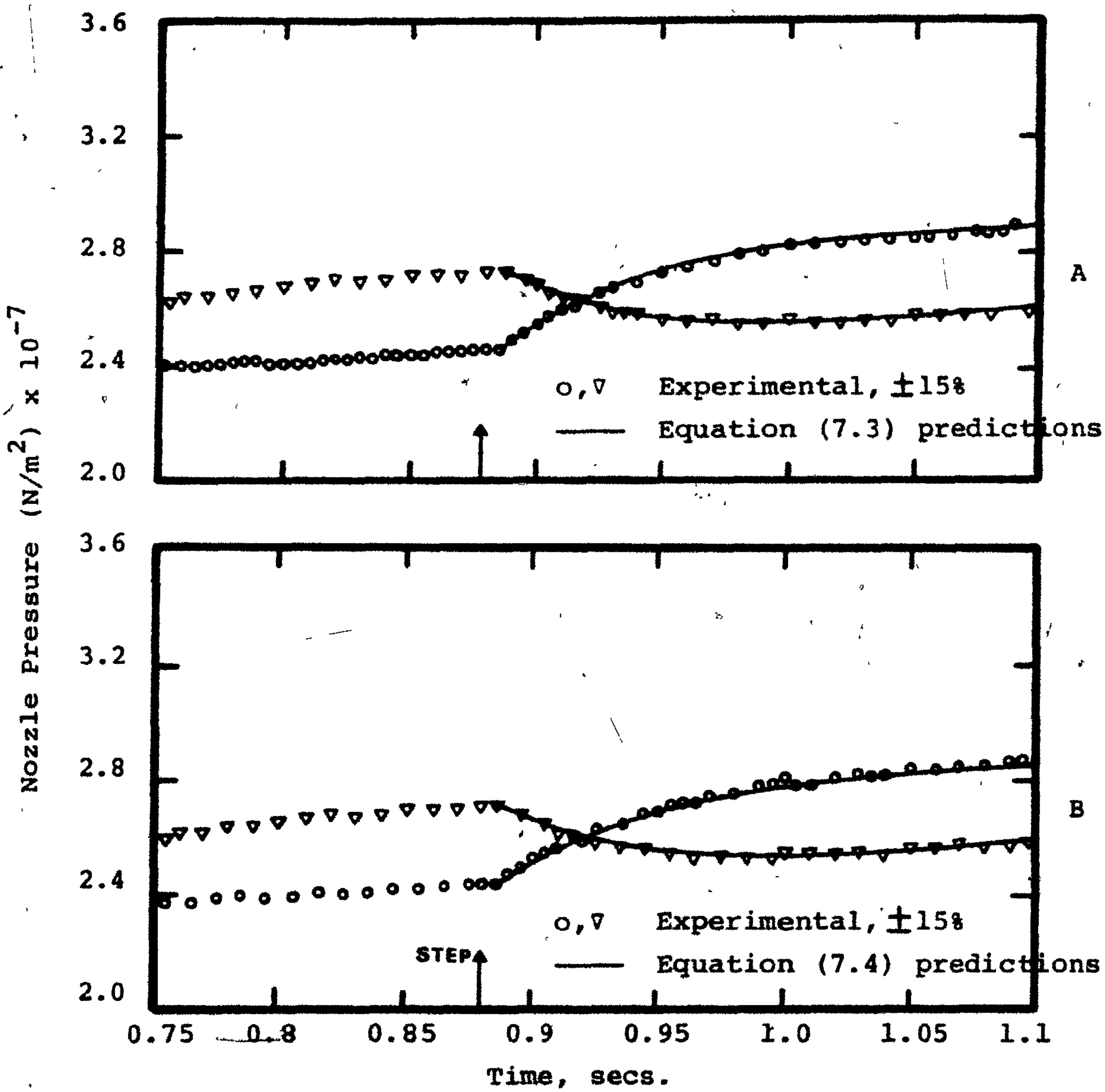

<u>Figure 7.5</u> Comparison of Experimental Nozzle Pressure Responses to Fitted Models (a) Equation (7.3 (b) Equation (7.4)

and the ram and polymer system can be considered as two first-order systems in series.

Figure 7.6 shows the nozzle pressure response linearity in the range of ±20% change in valve opening.

7.1.3 Linear Displacement

The ram displacements versus time for ±5, ±10 and ±15 percent changes in valve opening are shown in Figure 7.7. The change in valve opening is associated with a change in the slope of the displacement curve (ram velocity), which is very rapid. The displacement data are contaminated by considerable measurement noise. This is evident in Figure 7.8, which shows the ram velocity, obtained as the time derivative of the displacement data. The measurement noise precluded the possibility of obtaining a model for the ram velocity using these data. It seems probable that machine vibration was the source of the observed noise.

7.1.4 Ram Velocity

The difficulties encountered in modelling ram velocity by differentiating the linear displacement data led to the installation of a linear velocity transducer.

Figure 7.9 shows the response of ram velocity to ±10, ±15 and ±20 percent step changes in the valve opening. The velocity response is rapid, and it appears to be complete within one sampling interval. The data, once again, are

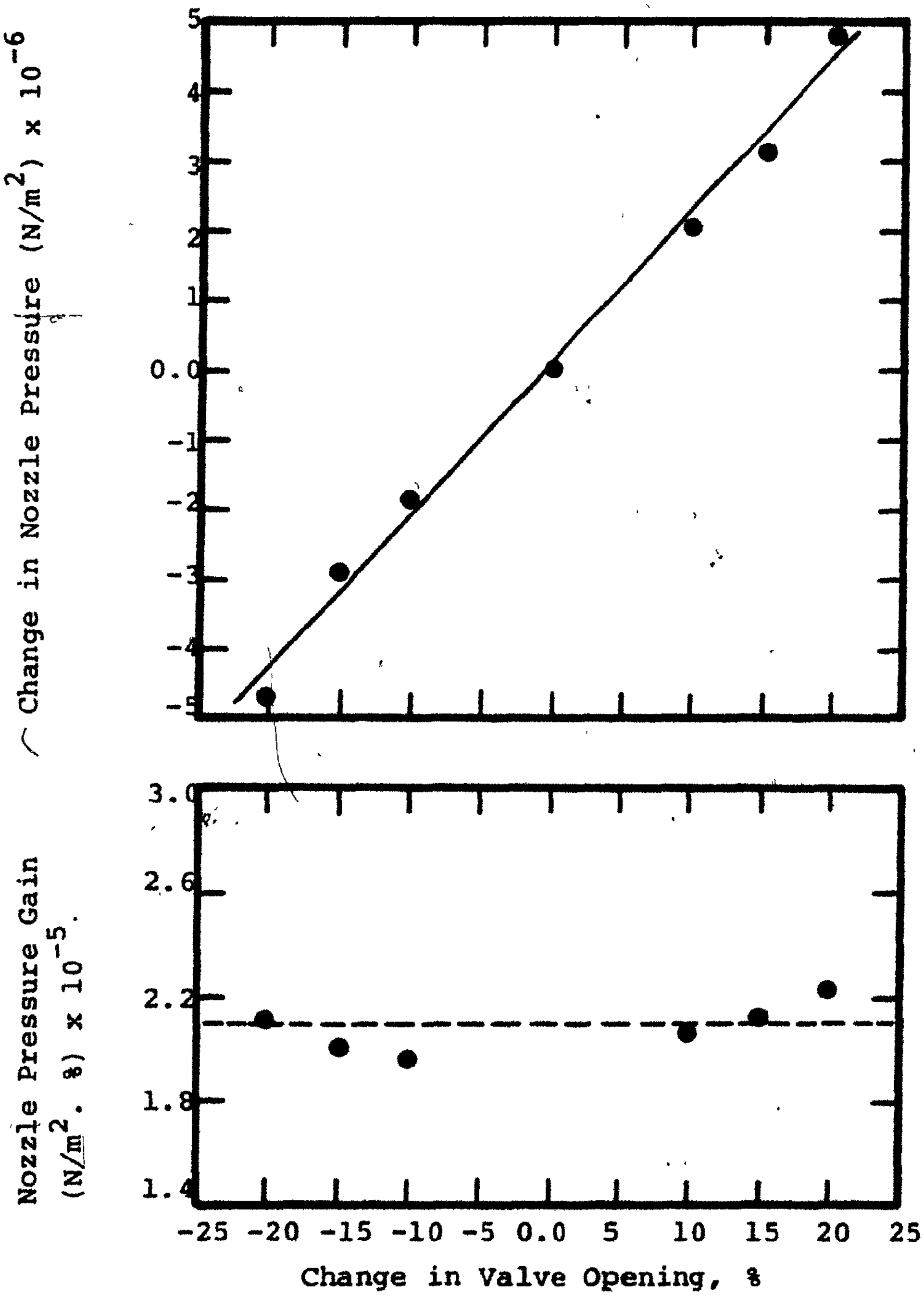

<u>Figure 7.6</u> Linearity of Nozzle Pressure Gain for Step Changes in Valve Opening

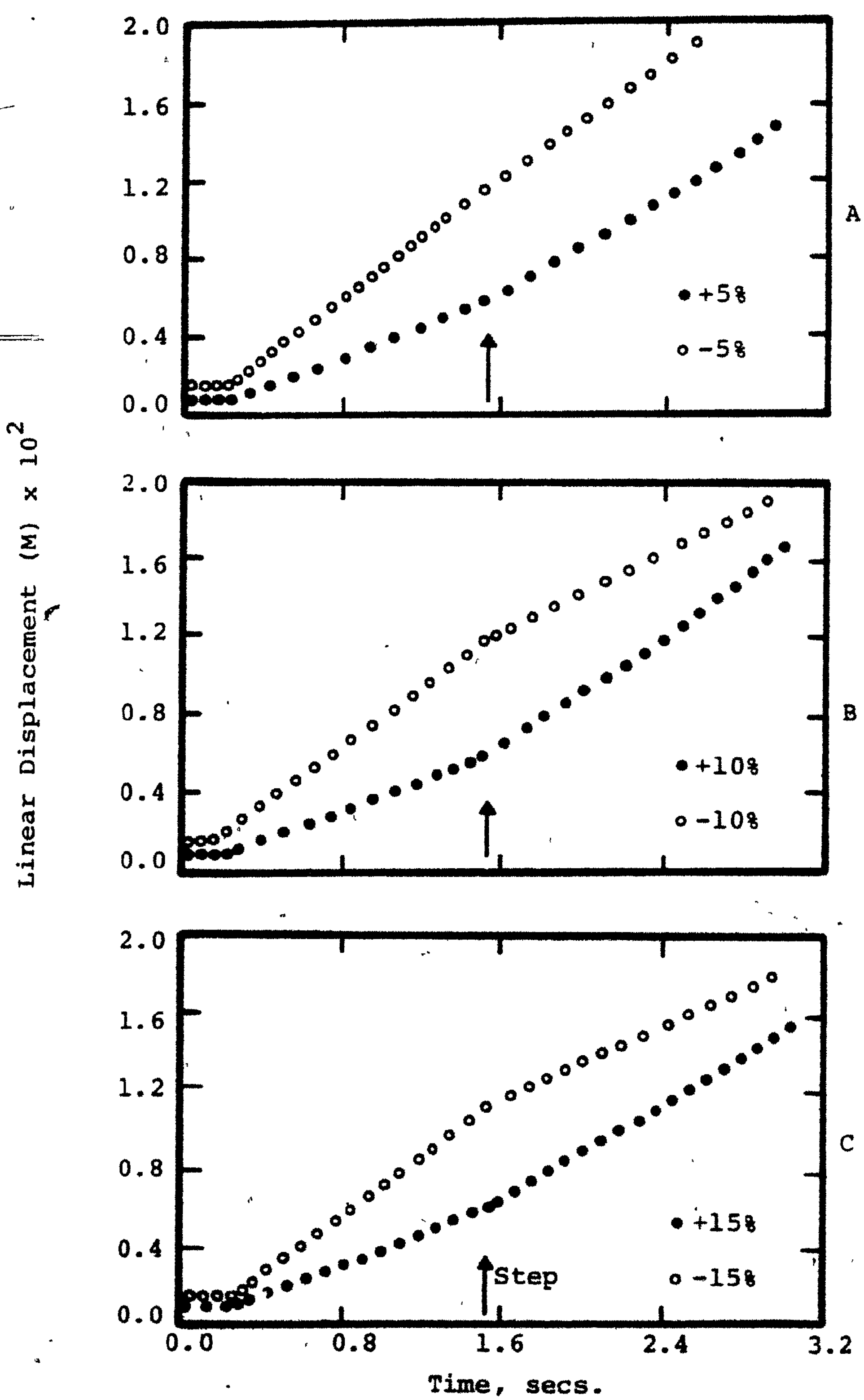

<u>Figure 7.7</u> Linear Displacement Response to (a) ±5, (b) ±10, (c) ±15% Step Changes in Valve Opening

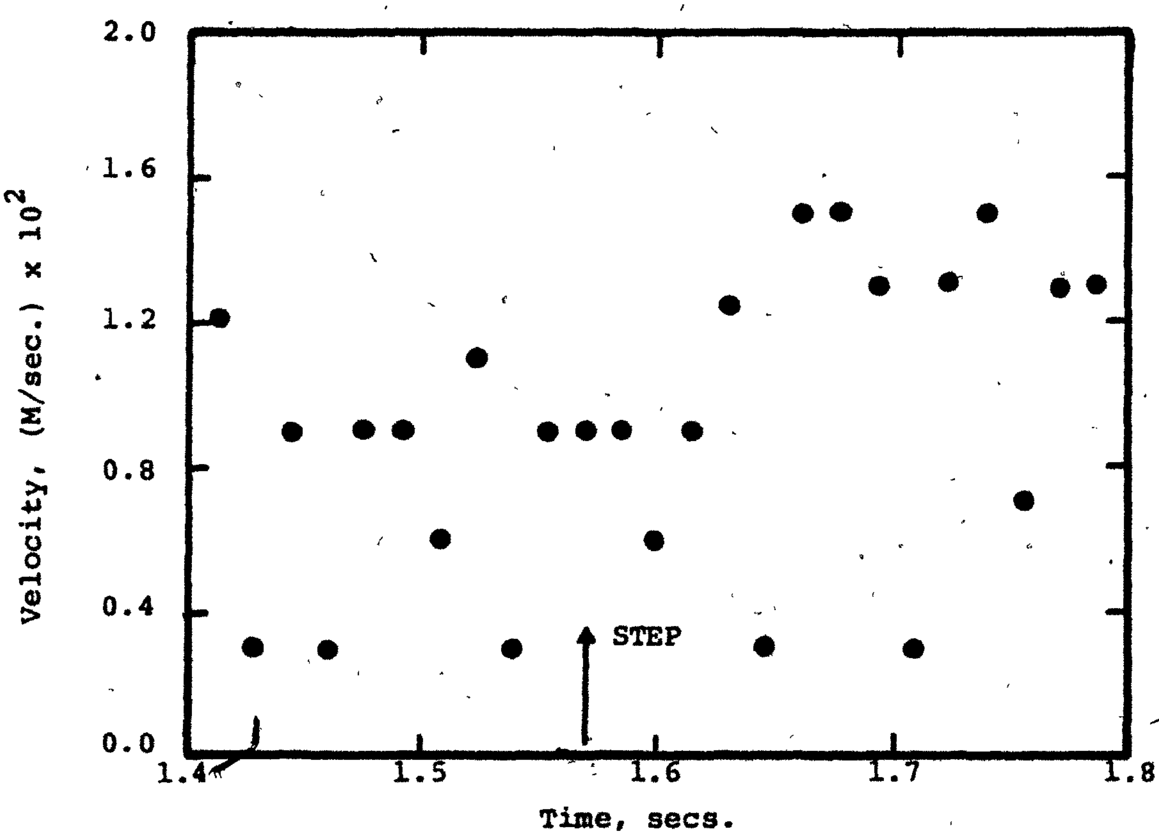

Figure 7.8 Velocity Derived from the Linear Displacement Data of Figure 7.7 for +10% Change in Valve Opening

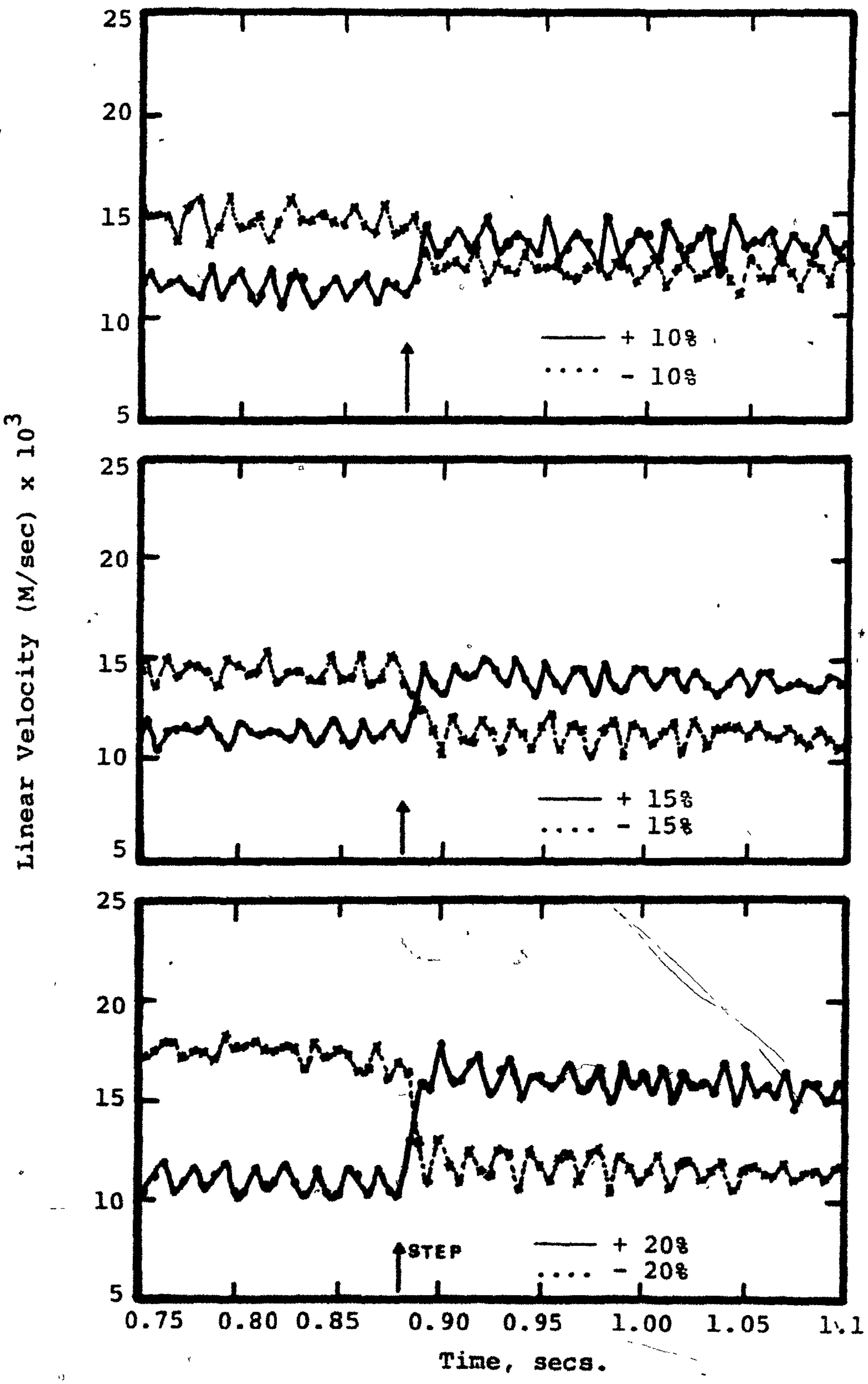

Figure 7.9 Linear Velocity Responses to Step Changes in Valve Opening; (a) ±10%, (b) ±15%, (c) ±20%

noisy, but the two steady states are distinguishable. The most reasonable model obtainable from these data comprises a simple gain term:

$$V_t = G \times U_t \tag{7.5}$$

where

V_t = ram velocity at sampling instant, t

U_t = percent change in valve opening

G = process gain

Table 7.4 gives the values of the gain of the velocity response to different step changes in valve opening. These values were obtained by averaging the velocities at steady state before and after the step.

Figure 7.10 shows the linearity of the velocity response to changes in the valve opening in the range of ±20%.

7.2 Time Series Modelling

Models for hydraulic pressure, nozzle pressure and ram linear velocity responses to changes in servovalve opening were presented in the previous section. However, Figures 7.1 and 7.9 show that the hydraulic pressure and velocity responses are confounded with an appreciable noise component,

TABLE 7.4

Values of the Gains for the

Ram Velocity Model, Equation (7.5)

Percent change in valve opening	Gain, G, (m/sec.%)X10^3
+10	0.216
-10	0.260
+15	0.20
-15	0.21
+20	0.25
-20	0.28

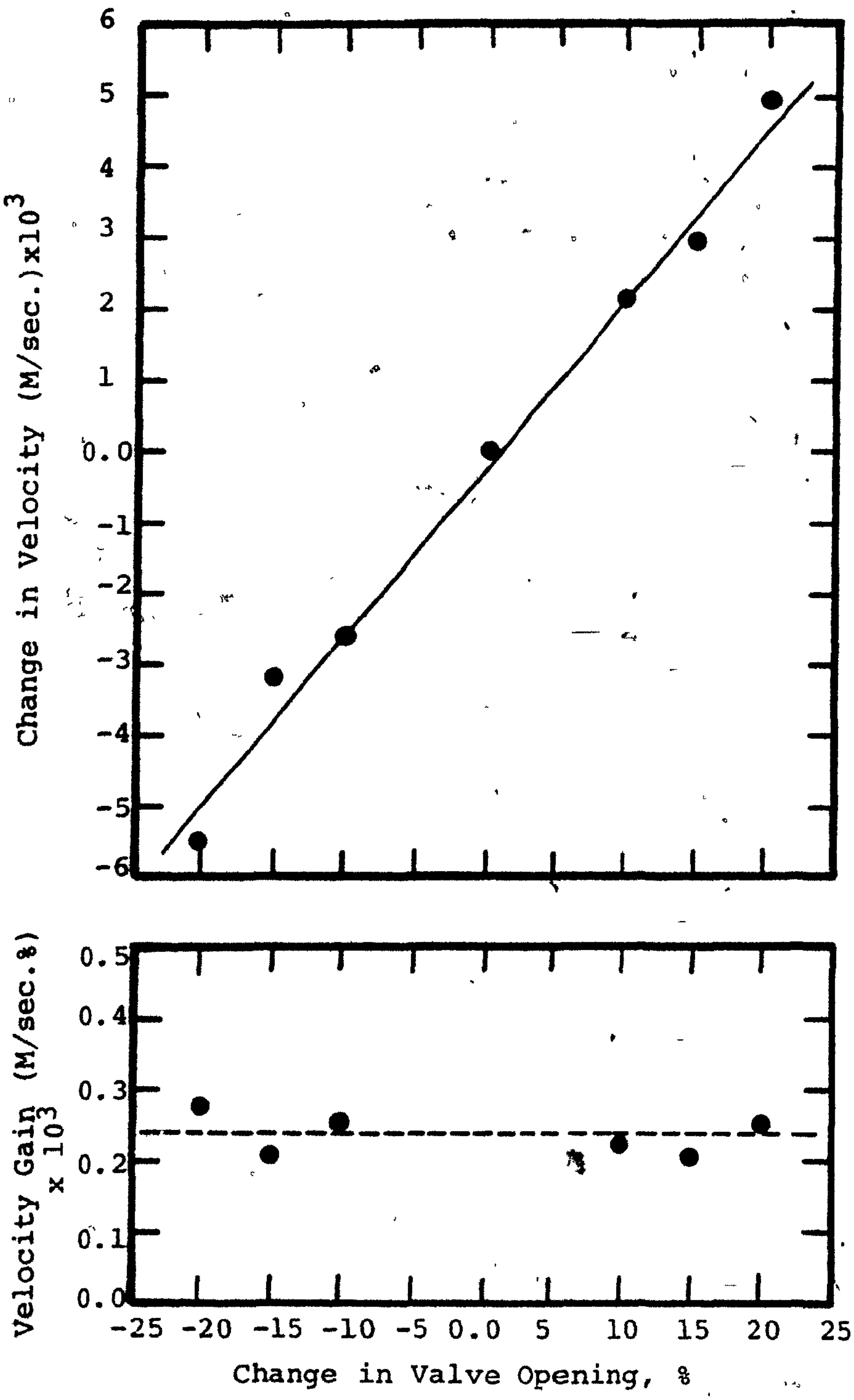

Figure 7.10 Linearity of Ram Velocity Gain for Step Changes in Valve Opening

which has to be identified so as to determine an effective control strategy. A serious defect of classical modelling techniques is that the process noise is neglected, because there are no procedures available to model it. The time series modelling approach, introduced in section 2.3, identifies both the process transfer function and a model of the associated noise. For this approach, as described in section 4.4.3, a PRBS was applied to the servovalve at 0.01 second intervals. The data were analyzed by the time series method described by Box and Jenkins (39).

7.2.1 Hydraulic Pressure

Figure 7.11 shows the hydraulic pressure response to a PRBS input. The oscillatory valve response superimposed on the hydraulic pressure response (see section 7.1.1) requires a seasonal type of time series model, as indicated by Figure 7.12, which shows the v-weights (Impulse Response Function) as a function of lag. However, this approach has not been pursued, since such a model cannot be justified physically.

7.2.2 Nozzle Pressure

The response of nozzle pressure to a PRBS input is shown in Figure 7.13. No differencing of the data was needed although a small degree of non-stationarity is evident. Figure 7.14 shows the v-weights for the nozzle pressure

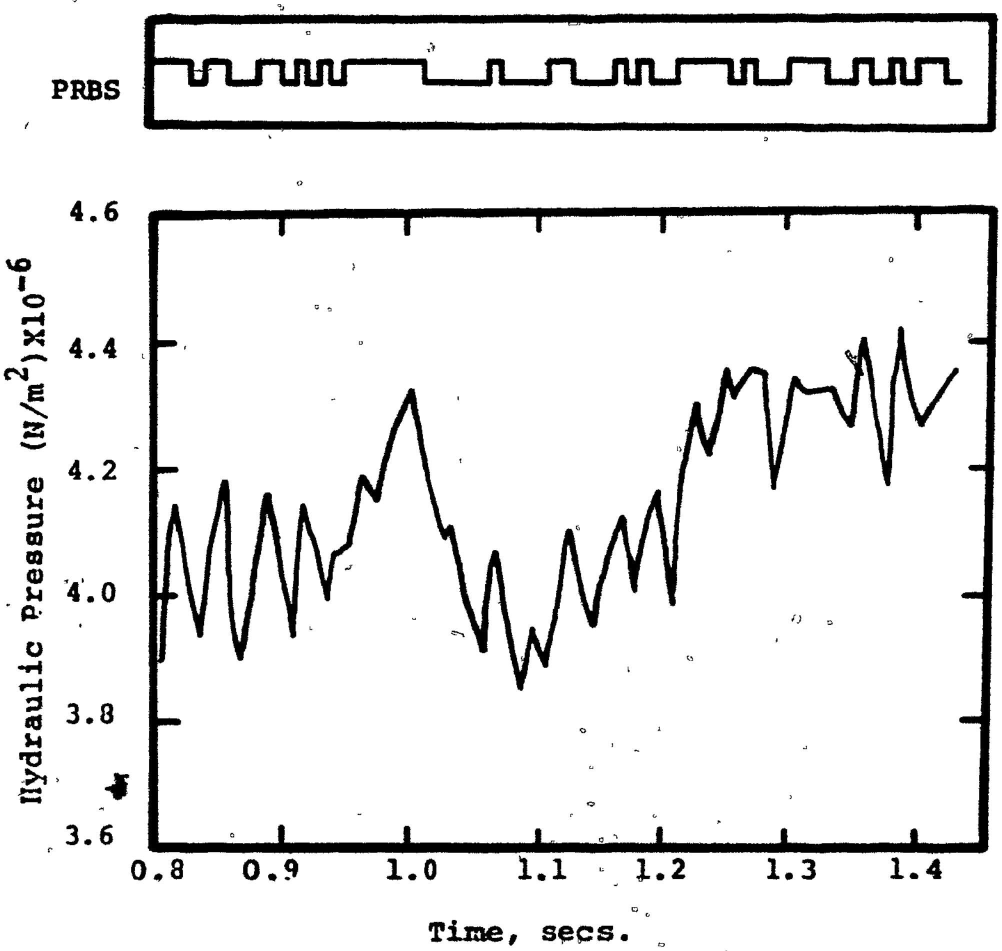

Figure 7.11 Hydraulic Pressure Response to PRBS Valve Signal (±10%)

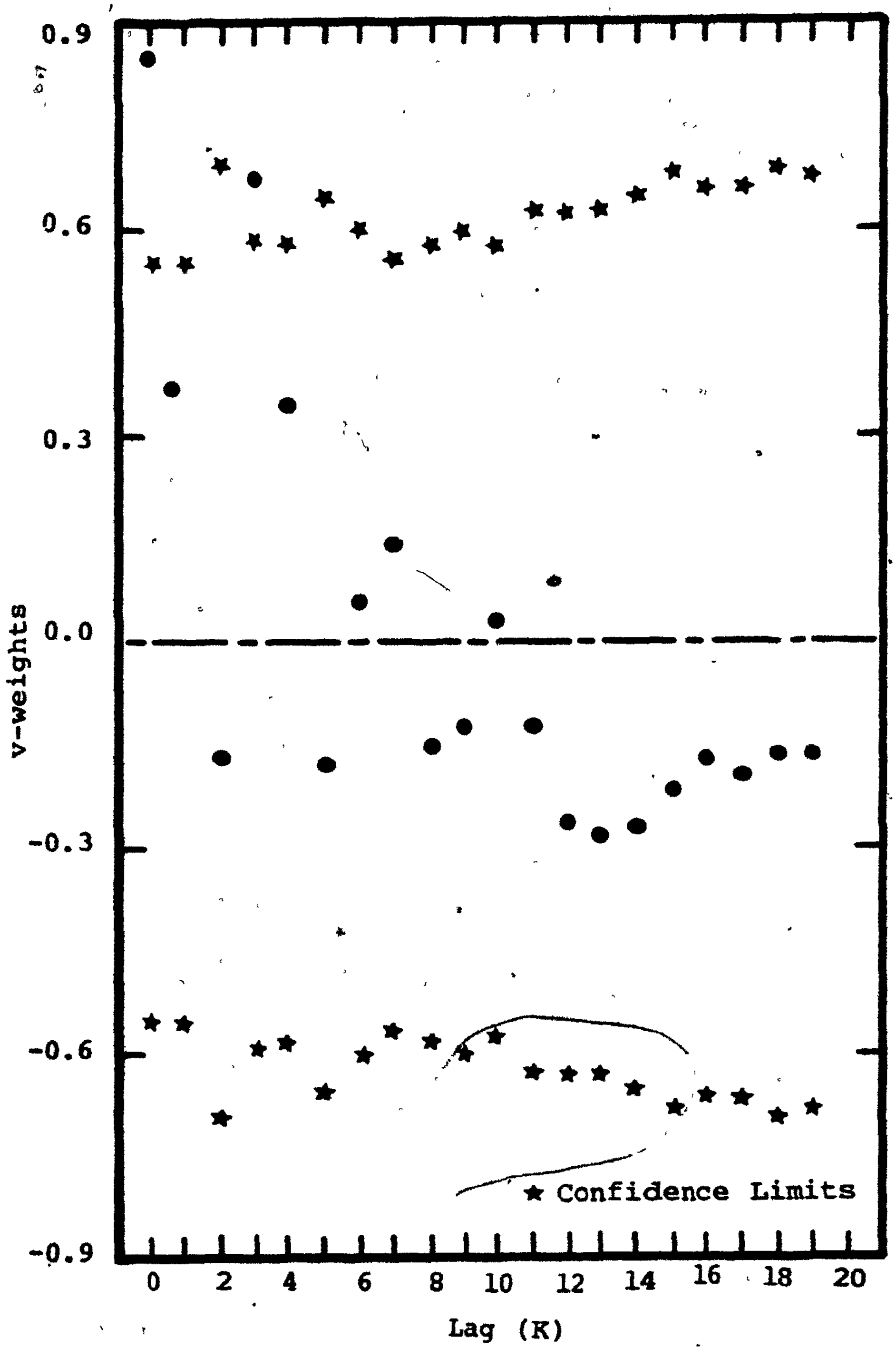

Figure 7.12 The v-weights for the Hydraulic Pressure Response to a PRBS Valve Signal (±10%)

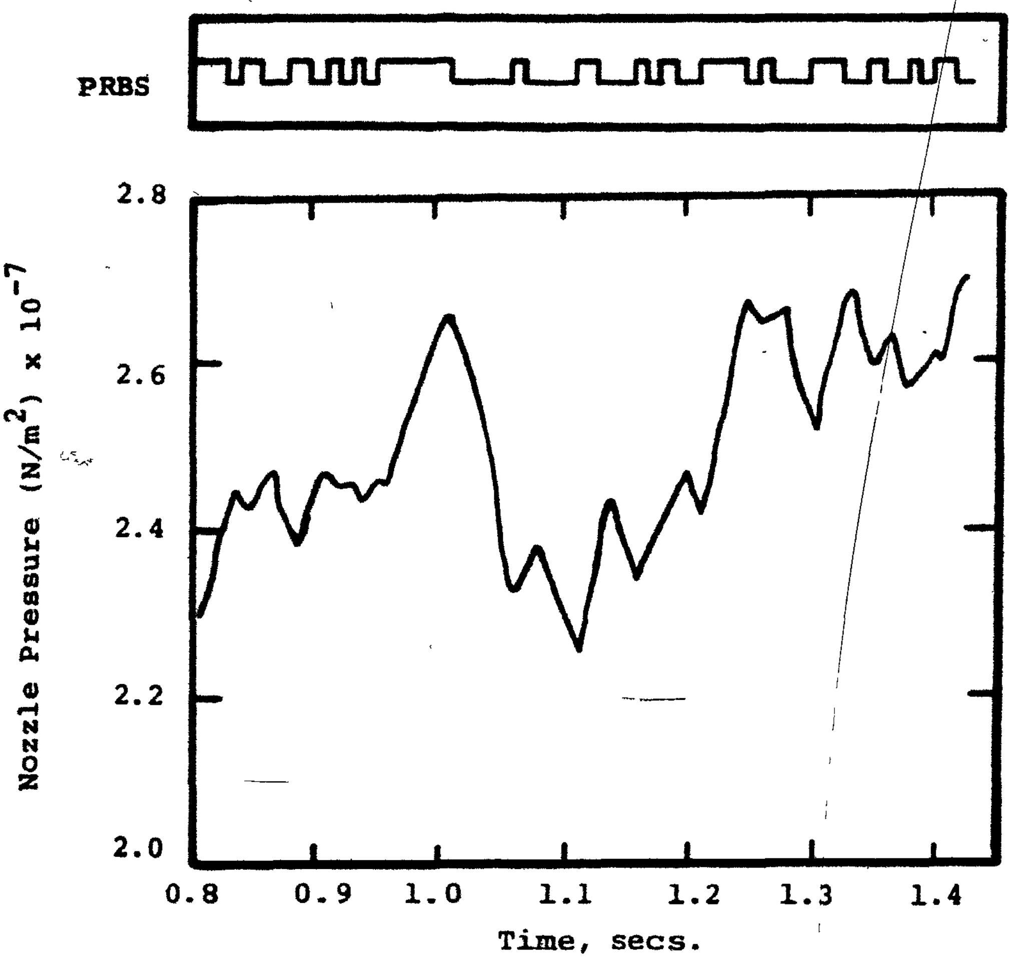

Figure 7.13 Nozzle Pressure Response to PRBS Valve Signal (±10%)

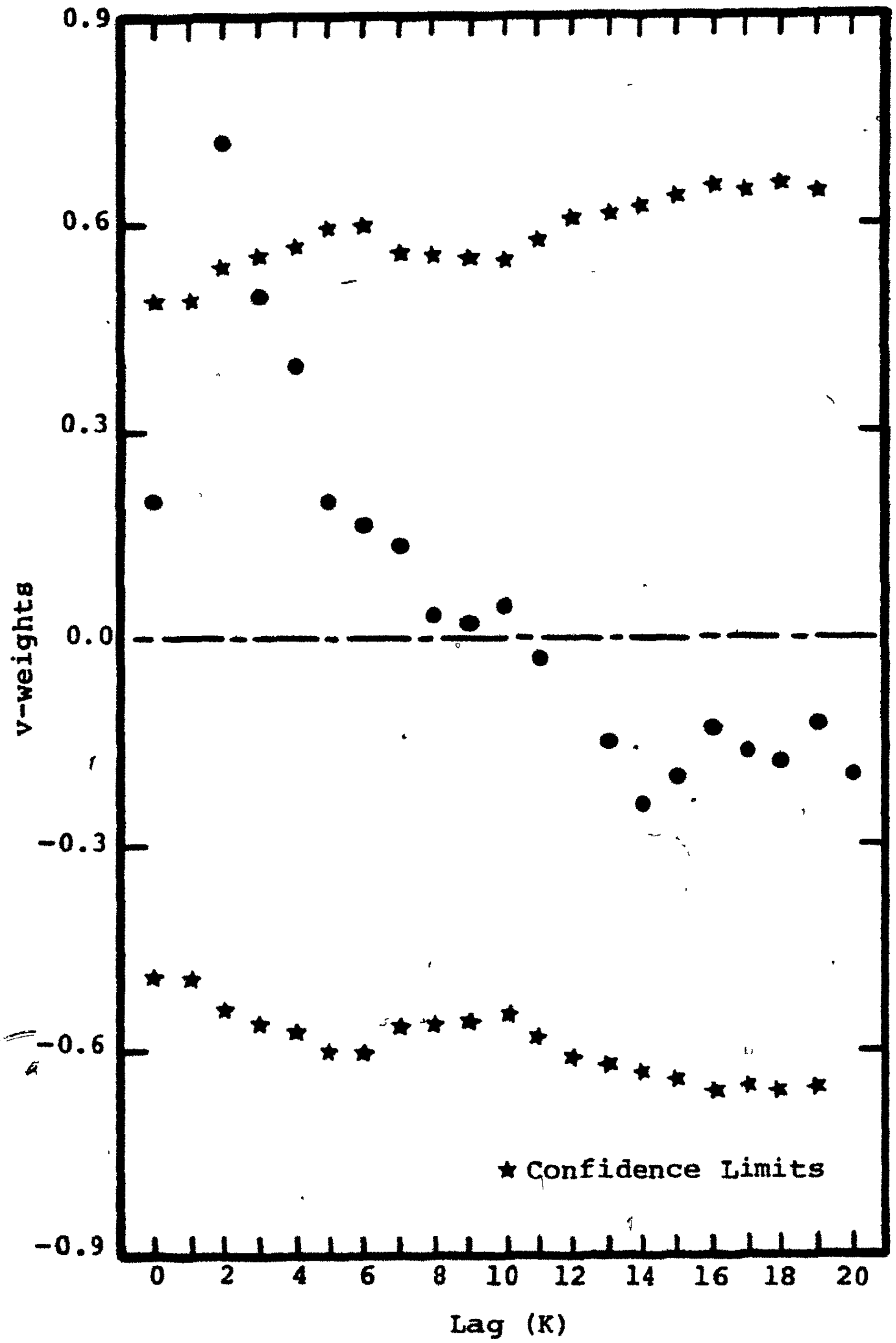

Figure 7.14 The v-weights for the Nozzle Pressure Response to a PRBS Valve Signal (±10%)

response. The comparison between these results and the standard responses indicates that the transfer function model for the nozzle pressure is of the form:

$$P_N(k) = \frac{\omega_0 - \omega_1 B}{1-\delta_1 B} U(k-2) \qquad (7.6)$$

where

$P_N(k)$ = nozzle pressure at discrete sampling instant, k

$U(k)$ = valve opening at discrete sampling instant, k

B = backwards difference operator defined as

$$U(k-1) = B\, U(k)$$

$\delta_1, \omega_0, \omega_1$ = the model parameters

Figure 7.15 shows the autocorrelation and partial autocorrelation functions of the residuals (noise). The autocorrelation function tails off exponentially, whereas the partial autocorrelation function cuts off after a lag of 1, indicating that the noise can be modelled as a first-order, autoregressive process:

$$N(k) = \frac{1}{1-\phi_1 B} a(k) \qquad (7.7)$$

where

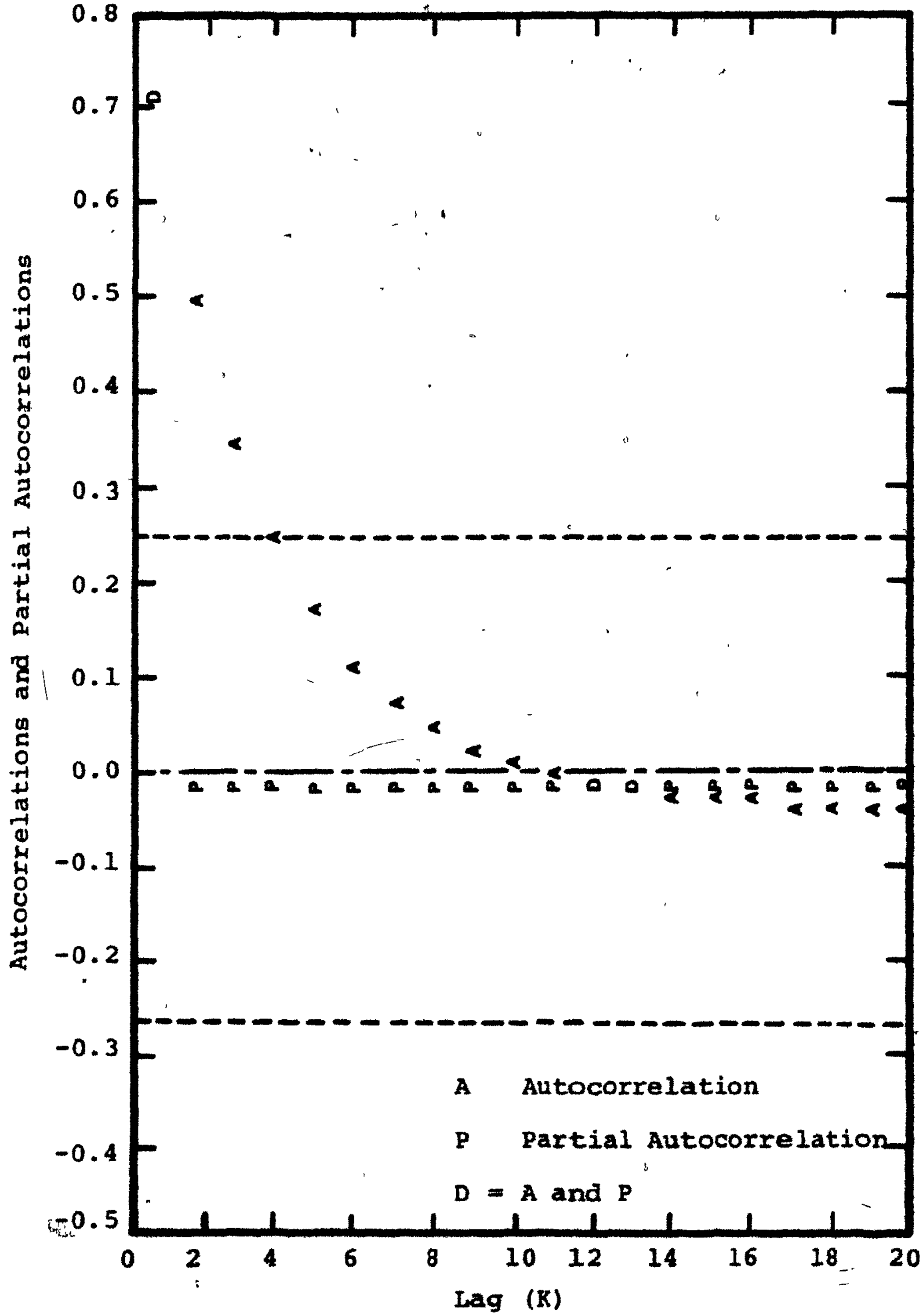

Figure 7.15 The Autocorrelation and Partial Autocorrelation Functions for the Noise of the Nozzle Pressure Response

$N(k)$ = noise at sampling instant, k

$a(k)$ = random noise value at sampling instant, k

ϕ_1 = noise model parameter

Thus the nozzle pressure was adequately modelled by:

$$P_N(k) = \frac{\omega_0 - \omega_1 B}{1-\delta_1 B} U(k-2) + \frac{1}{1-\phi_1 B} a(k) \tag{7.8}$$

with

$\omega_0 = 6.62$

$\omega_1 = -1.0$

$\delta_1 = 0.68$

$\phi_1 = 0.97$

Equation (7.8) distinguishes two components of the nozzle pressure response, the first term is the direct response defined in terms of previous values of P_N and U, while the second term describes the noise inherent in the variable.

7.2.3 Ram Velocity

The response of ram velocity to the PRBS input is shown in Figure 7.16. It is obvious that the response is very rapid, which is consistent with the response to the step change input (see Figure 7.9). The analysis of the

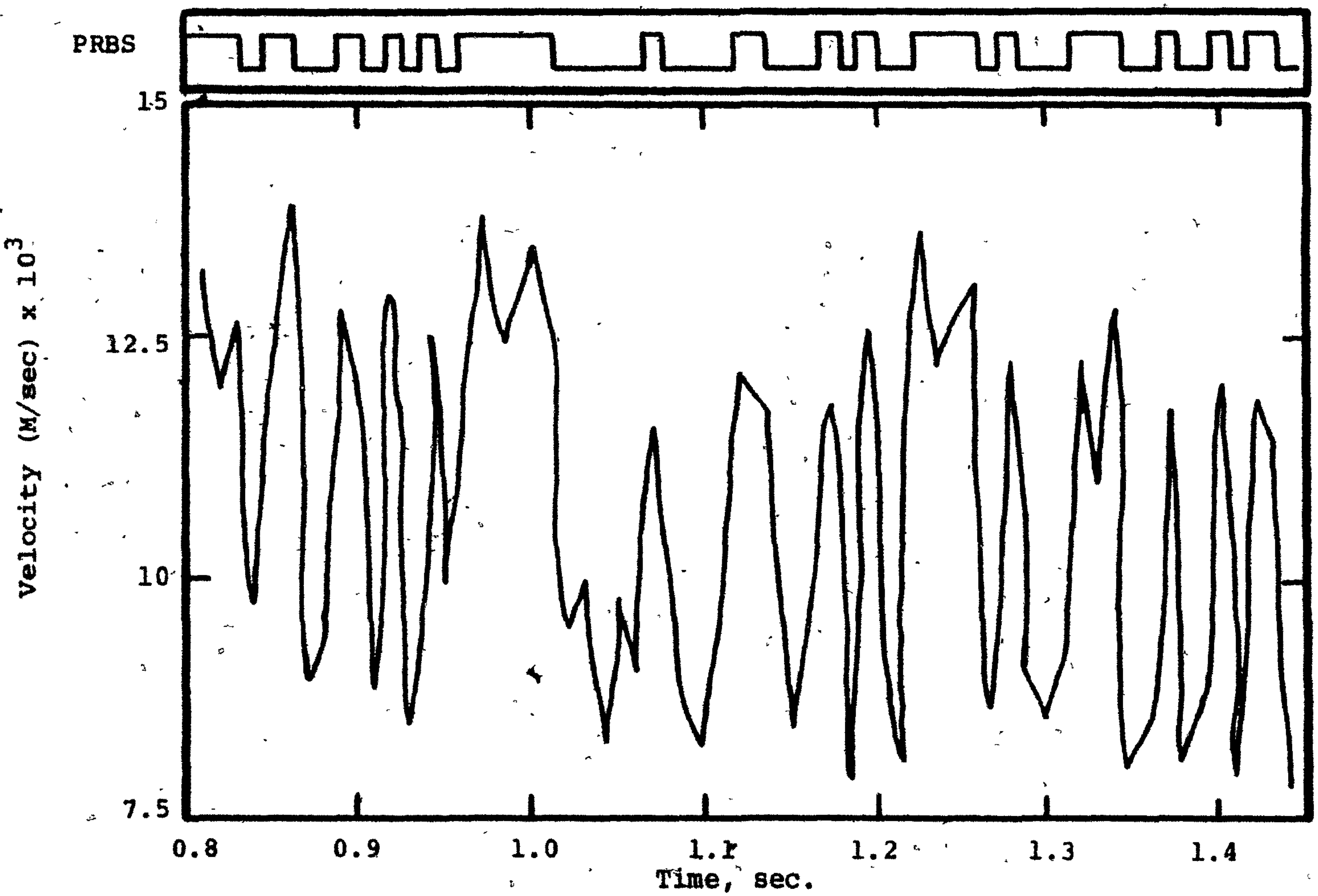

Figure 7.16 Ram Velocity Response to PRBS Valve Signal (±10%)

v-weights given in Figure 7.17 shows that the velocity response may be modelled by:

$$V(k) = \omega_0 U(k-1) \tag{7.9}$$

which contains only a gain term. The autocorrelation and partial autocorrelation functions for the noise, shown in Figure 7.18, indicate that it may be modelled by a first-order moving average process:

$$N(k) = (1-\theta B)a(k) \tag{7.10}$$

The ram velocity is thus modelled by:

$$V(k) = \omega_0 U(k-1) + (1-\theta B)a(k) \tag{7.11}$$

where

$\omega_0 = 0.3$

$\theta_1 = 0.4$

7.2.4 Comparison Between Deterministic and Stochastic Models

Box and Jenkins (39) have proposed relationships between the parameters obtained from discrete models and continuous model counterparts. In these relationships,

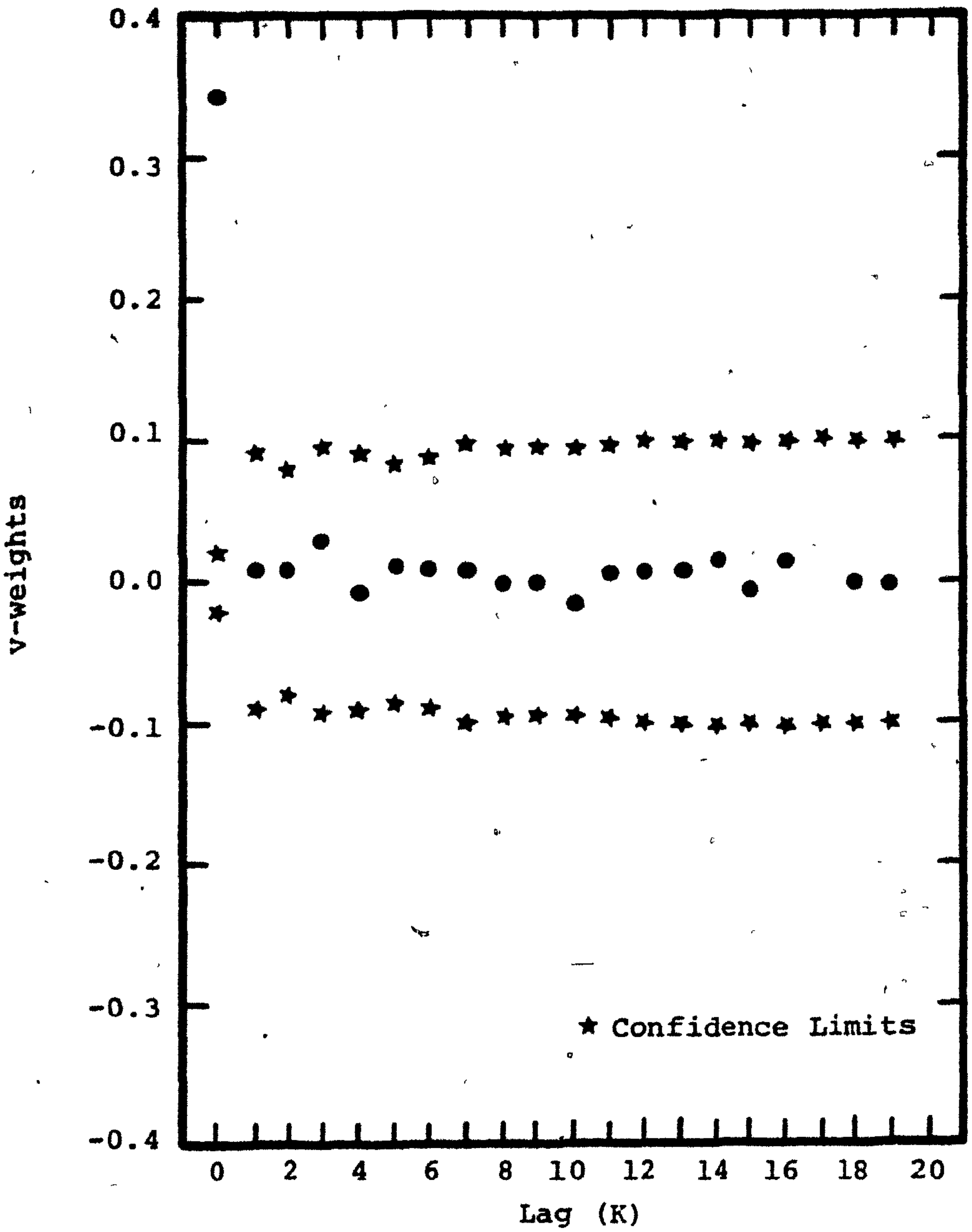

<u>Figure 7.17</u> The v-weights for the Ram Velocity Response to a PRBS Valve Signal (±5%)

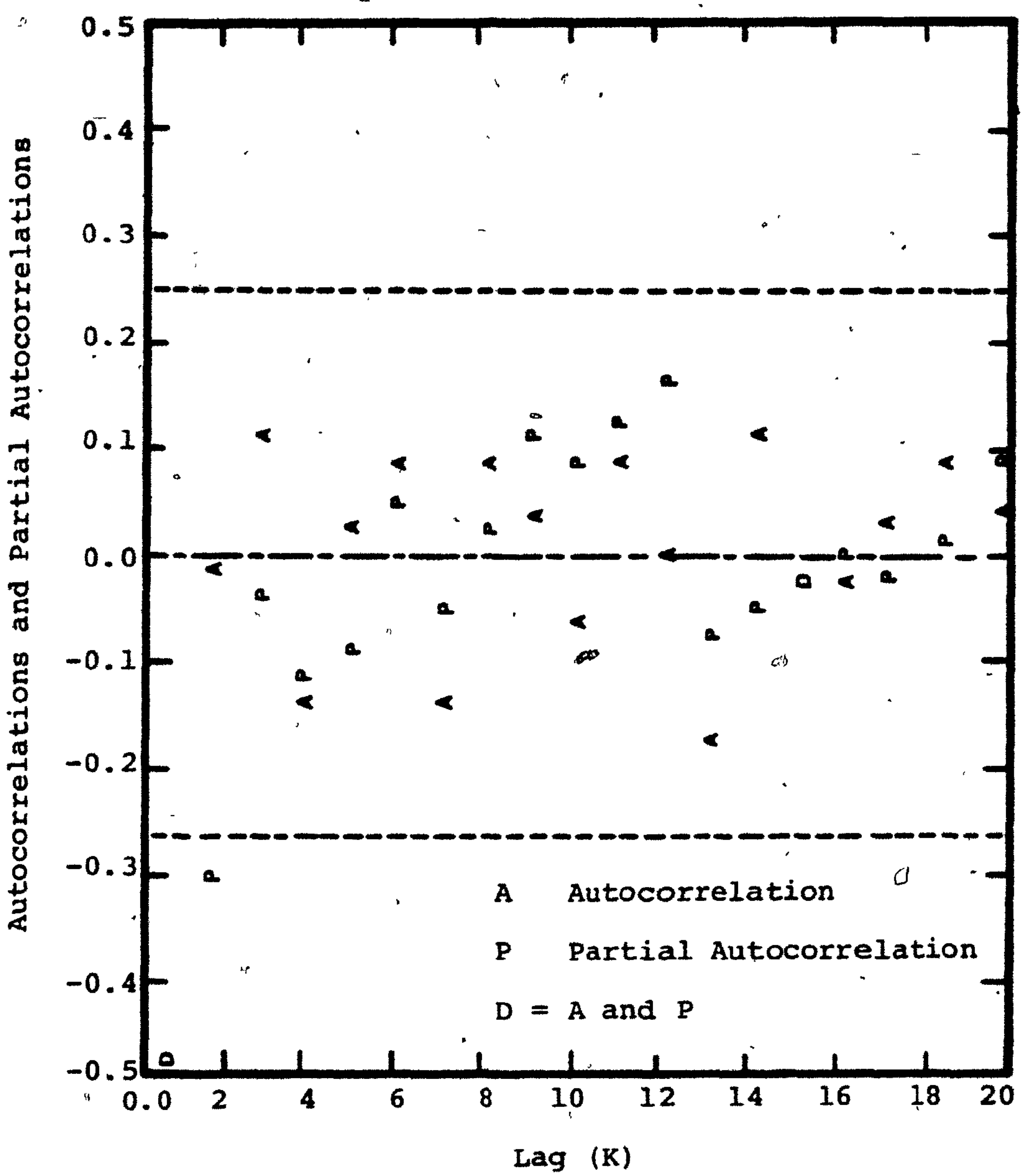

Figure 7.18 Autocorrelation and Partial Autocorrelation Functions for the Noise of the Velocity Response

the gain and time constants are given by:

$$g = \frac{\omega_0 - \omega_1 - \text{-----} - \omega_s}{1 - \delta_1 - \delta_2 \text{-----} - \delta_r} \qquad (7.12)$$

$$\tau = T_s / -\ln\delta$$

where T_s = sampling interval.

Models of the form of equations (7.8) and (7.11) were compared to the corresponding continuous models by calculating the gains and time constants. The results of the comparison are given in Table 7.5. These results show that the parameters obtained by deterministic and the stochastic models are in reasonably good agreement.

TABLE 7.5

Comparison of System Parameters Obtained by Deterministic and Stochastic Models for the Nozzle Pressure and Ram Velocity Models

Variable	Model	Gain	Time Constant, secs.
Nozzle Pressure	Deterministic	1.91×10^{5} N/m^{2}.%	0.035
	Stochastic	1.64×10^{5} N/m^{2}.%	0.030
Ram Velocity	Deterministic	0.26×10^{-3} m/sec.%	
	Stochastic	0.30×10^{-3} m/sec.%	

CHAPTER 8

CONCLUSIONS

Pseudo-static and dynamic experiments were performed to study the relations between different process variables during the injection stage of the injection molding process. A linear relationship between the hydraulic and nozzle pressures was derived from the empirical analysis of the pseudo-static data and substantiated by a simplified theoretical analysis of the injection phase. The dependence of nozzle pressure on hydraulic pressure, injection velocity, injection temperature, barrel and screw geometry and resin characteristic was examined.

Deterministic (step) and stochastic (PRBS) tests were performed to obtain dynamic models in the form of a transfer function relating the variation in servovalve opening to variations in hydraulic pressure, nozzle pressure, ram linear displacement and ram velocity. The hydraulic pressure response to step changes in the valve opening showed an oscillatory component superimposed on a delayed first-order response. The damped oscillations were attributed to the servovalve response. The nozzle pressure response was best modelled as a second-order overdamped process. The identification of a model for the ram velocity by differentiation of the displacement-time data was unsuccessful due to measurement noise. The model for ram velocity using direct measurements of the velocity was found to be a zero-order model which contains only a gain term.

Stochastic transfer function-noise models were obtained for the nozzle pressure and ram velocity. Both models were compared to the corresponding models determined from the step tests, and satisfactory agreement was obtained.

The responses of all variables were rapid (or the order of milliseconds) and are thus good candidates for controlling the injection process. It appears that, for pressure control of injection molding, it is preferable to use nozzle pressure rather than hydraulic pressure because of the oscillatory component superimposed on the hydraulic pressure response. The injection velocity seems to be the most favorable variable to be used in controlling the injection phase since it has a simultaneous response.

REFERENCES

1. D.H. Harry and R.G. Parrott, "Numerical Simulation of Injection Molding", Polym. Eng. Sci., 10, 209 (1970).

2. J.L. Berger and C.G. Gogos, Technical Papers, 29th ANTEC 17, 8 (1971).

3. J.L. Berger and C.G. Gogos, "A Numerical Simulation of the Cavity Filling Process", Polym. Eng. Sci., 13, 102 (1973).

4. P.C. Wu, C.F. Huang and C.G. Gogos, "Simulation of the Mold Filling Process", Polym. Eng. Sci., 14, 223 (1974).

5. M.R. Kamal and S. Kenig, "The Injection Molding of Thermoplastics. Part I: Theoretical Model", Polym. Eng. Sci., 12, 294 (1972).

6. S. Kenig, "Injection Molding of Thermoplastics", Ph.D. Thesis, McGill University, Montreal (1972).

7. M.R. Kamal and S. Kenig, "The Injection Molding of Thermoplastics. Part II: Experimental Test of the Model", Polym. Eng. Sci., 12, 302 (1972).

8. P.H. Doan, "Injection Molding of Thermoplastics in Rectangular Cavities", M.Eng. Thesis, McGill University, Montreal (1974).

9. M.R. Kamal, Y. Kuo and P.H. Doan, "The Injection Molding Behaviour of Thermoplastics in Thin Rectangular Cavities", Polym. Eng. Sci., 15, 863 (1975).

10. E. Broyer, C. Gutfinger and Z. Tadmor, "A Theoretical Model for the Cavity Filling Process in Injection Molding", Trans. of the Society of Rheology, 19, 423 (1975).

11. J.L. White, "Fluid Mechanical Analysis of Injection Mold Filling", Polym. Eng. Sci., 15, 44 (1975).

12. Y. Kuo and M.R. Kamal, "The Fluid Mechanics and Heat Transfer of Injection Mold Filling of Thermoplastics Materials", A.I.Ch.E. J., 22, 669 (1976).

13. Y. Kuo and M.R. Kamal, "Flows of Thermoplastics in the Filling and Packing Stages of Injection Molding", Science and Technology of Polymer Processing (1977).

14. M.R. Kamal and V. Tan, "Injection Molding: A Critical Profile", Science and Technology of Polymer Processing (1977).

15. H.A. Lord, "Flow of Polymers with Pressure-Dependent Viscosity in Injection Molding Dies", Polym. Eng. Sci., 19, 469 (1979).

16. W.L. Krueger and Z. Tadmor, "Injection Molding into a Rectangular Cavity with Inserts", Polym. Eng. Sci., 20, 426 (1980).

17. M.E. Ryan and T.S. Chung, "Conformal Mapping Analysis of Injection Mold Filling", Polym. Eng. Sci., 20, 642 (1980).

18. K.K. Wang, et al., Injection Molding Project, College of Engineering, Cornell University, Progress Report #6, September 1979.

19. P.G. Lafleur and M.R. Kamal, "Computer Simulation of Thermoplastic Injection Molding", Adv. Plast. Tech., 1, 4, 8 (1981).

20. G. Menges, S. Stitz and J. Vargel, "What Must Be Known About Injection Molding for Computer Control", Technical Papers, 30th ANTEC, 18, 843 (1972).

21. D.B. Hunkar, "The Interdependence of Part Parameters on Process Control Adjustable Functions in Injection Molding of Thermoplastics", Technical Papers, 33rd ANTEC, 21, 161 (1975).

22. John W. Mann, "Multi-Parameter Process Control for Injection Molding Machines", Technical Papers, 31st ANTEC, 19, 513 (1973).

23. D.C. Paulson, "Guide to Injection Machine Control", SPE Journal, 27, 37 (1971).

24. H.T. Plant and R.T. Maher, "A Preliminary Analysis of the Injection Molding Process and Factors Affecting Part Size Control", Technical Papers, 33rd ANTEC, 21, 74 (1975).

25. Carl Y. Ma, "A Design Approach to a Computer Controlled Injection Molding Machine", Polym. Eng. Sci., 14, 768 (1974).

26. J.W. Peter, "Injection Molding Investigation for Automatic Control", Technical Papers, 30th ANTEC, 18, 847 (1972).

27. J. Border and N.P. Suh, "Intelligent Injection Molding", Technical Papers, 40th ANTEC, 28, 323 (1982).

28. W. Ian Patterson and M.R. Kamal, "Injection Molding Control Strategies", SPE RETEC (1982).

29. M.A. Davis, "Servocontrolled Injection Molding", Technical Papers, 34th ANTEC, 22, 618 (1976).

30. M.A. Davis, "Process Control Applied to the Injection Molding of Thin Wall Parts", Technical Papers, 35th ANTEC, 23, 66 (1977).

31. W.J. Thayer and M.A. Davis, "Control for Injection Molding of Thermoplastics", Adv. Plast. Tech., 1, 3, 28 (1981).

32. M. Takizawa et al., "Programmed Injection Control in Injection Molding", Technical Papers, 32nd ANTEC, 20, 557 (1974).

33. W.L. Luyben, "Process Modeling, Simulation and Control for Chemical Engineers", McGraw Hill, N.Y. (1973).

34. D.R. Coughanowr and L.B. Koppel, "Process Systems Analysis and Control", McGraw-Hill, N.Y. (1965).

35. A.J. Young, "An Introduction to Process Control Systems Design", Longman Green, New York, 1955.

36. J.O. Hougen, "Experience and Experiments with Process Dynamics", Chemical Engineering Progress Monograph Series, 60, No. 4, 1964.

37. C. Daniel and F. Wood, "Fitting Equations to Data", John Wiley, N.Y. (1980).

38. E.A. Robison and M.T. Silvia, "Digital Signal Processing and Time Series Analysis", Holden-Day Inc., San Francisco (1978).

39. G.E. Box and G.M. Jenkins, "Time Series Analysis: Forecasting and Control", Holden-Day Inc., San Francisco (1976).

40. P.A.N. Briggs, P.H. Hammond, M.T.G. Hughes and G.O. Plumb, "Correlation Analysis of Process Dynamics Using Pseudo-Random Binary Test Perturbations", Inst. Mech. Eng., Advances in Automatic Control, Paper 7, Nottingham, U.K., April 1965.

41. W.D.T. Davis, "System Identification for Self-Adaptive Control", Wiley-Interscience (1970).

42. Z. Bakerdjian, "Experimental Study of Anisotropy in Injection Molded Thermoplastic Parts", M.Eng. Thesis, McGill University, Montreal (1978).

43. D. Kalyon, "An Experimental Study of Injection Molding", M.Eng. Thesis, McGill University, Montreal (1977).

44. F.H. Moy, "Microstructure and Distribution of Tensile Properties in Injection Molded Polyethylene", Ph.D. Thesis, McGill University, Montreal (1980).

45. A. Haber, "Microprocessor Control System for the Injection Molding Process", M.Eng. Thesis, McGill University, Montreal (1982).

46. R.B. Bird, W.E. Stewart and E.N. Lightfoot, "Transport Phenomena", John Wiley and Sons, N.Y. (1960).

47. Z. Tadmor and I. Klein, "Engineering Principles of Plasticating Extrusion", Robert E. Kreiger Publ. Co., Huntington, New York (1978).

48. Anon., "Moog A076 Servovalve Technical Manual", Moog Inc., Industrial Division, New York.

49. Danson Metalmec Injection Molding Machines, 60-SR Instruction Manual.

APPENDIX A

SERVOVALVE CHARACTERISTICS

The servovalve used in the system is a two-stage valve, MOOG A0-76-103 model. It has a rated flow of 10 gpm (U.S.) at 1000 psi valve pressure drop. Figure A.1.a shows the rated flows at other supply pressures. Figure A.1.b shows the step response of the valve and the frequency response characteristics are shown in Figures A.2.a and A.2.b (48).

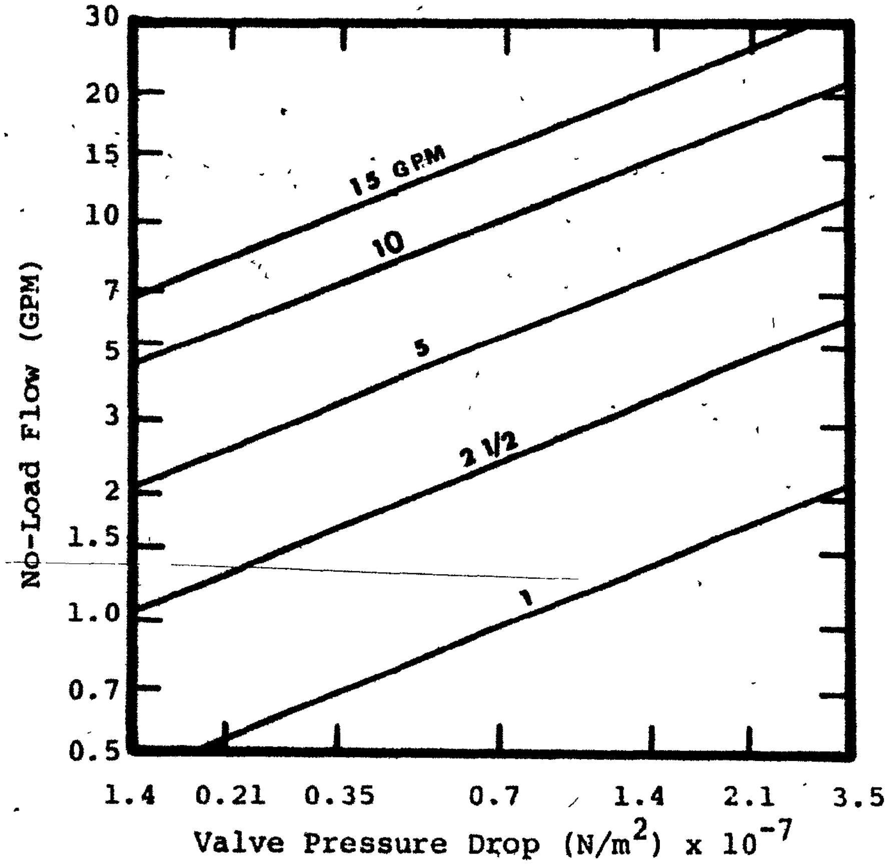

(a) Effect of Valve Pressure Drop on No-Load Flow Rate

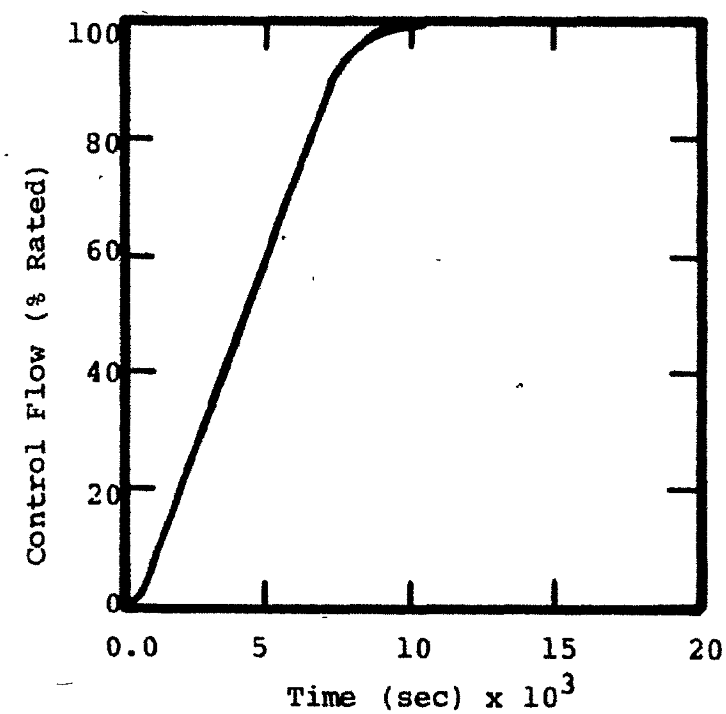

(b) Step Response of Servovalve

<u>Figure A.1</u> Flow Characteristics of the Servovalve (48)

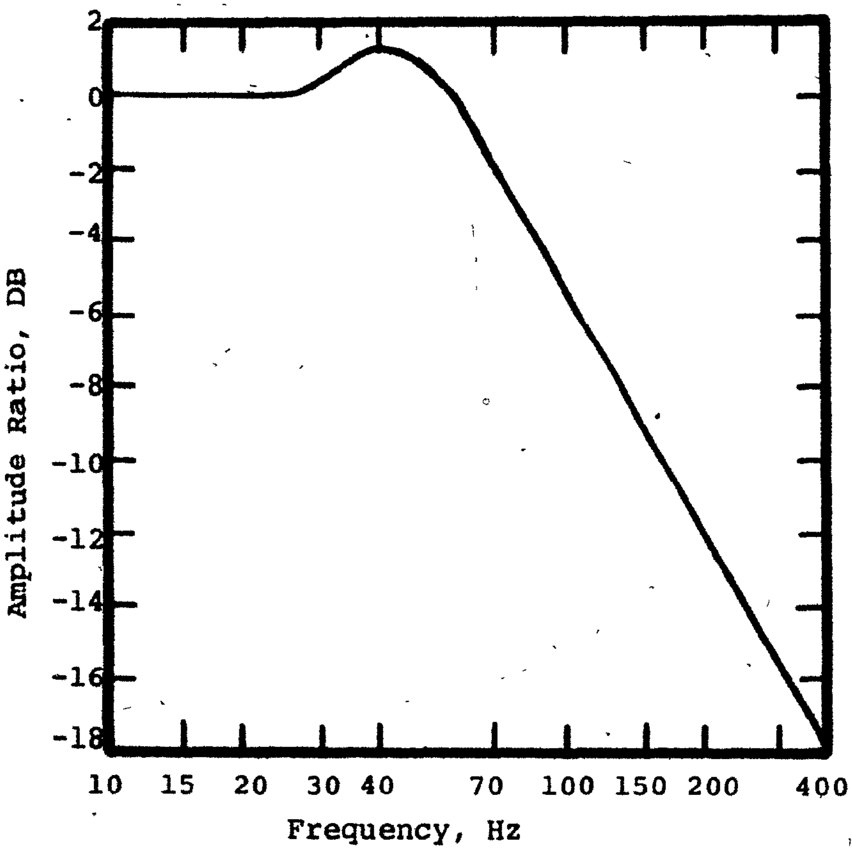

(a) Reduced Amplitude Frequency Response

(b) Full Amplitude Frequency Response

Figure A.2 Frequency Response of Servovalve (48)

APPENDIX B

TRANSDUCER CALIBRATION

B.1 Pressure Transducers

Calibration of the pressure transducers was performed with the aid of the specially-designed apparatus shown in Figure B.1. The transducer was mounted to the base of the cylindrical reservoir which was filled with Duckham's Hypoid 80 gear oil. The oil was compressed by a piston which was driven by the crosshead of the Instron Universal Testing Machine. The transducer output was recorded on a Hewlett-Packard strip chart recorder (Model 7100B). The force exerted by the crosshead was measured by the Instron load cell. A pressure gauge gave a direct indication of the pressure. The calibration data are given in Table B.1 and were correlated by linear regression to give the equations in Table 5.1.

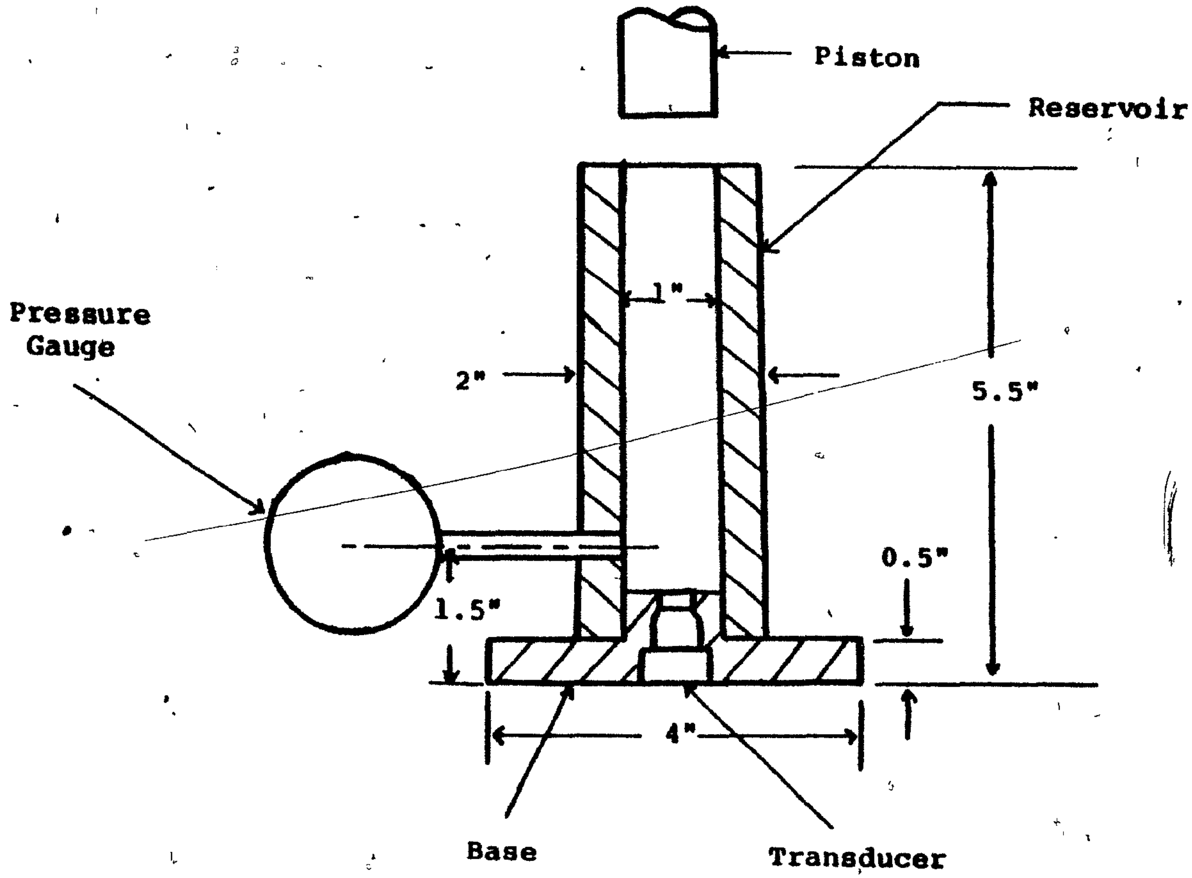

<u>Figure B.1</u> Pressure Calibration Apparatus

TABLE B.1

Pressure Transducer's Calibration Data

Hydraulic Pressure Transducer		Nozzle Pressure Transducer	
Pressure (psi)	Output (mV)	Pressure (psi)	Output (mV)
0.0	0.0	0.0	0.0
286.06	0.55	56.14	0.6
448.72	0.89	84.10	0.7
560.90	1.06	140.35	1.0
701.12	1.35	168.42	1.25
981.57	1.90	224.56	1.82
1402.27	2.80	277.89	2.50
1682.70	3.40	336.84	3.70
1963.14	4.00	392.98	5.60
2243.60	4.56	449.12	6.15
2804.50	5.73	499.64	7.0
3365.40	6.90	561.4	8.6
3926.30	8.10	617.54	9.9
4515.23	9.30		
5608.98	11.80		
7011.23	14.80		

Note: 1 psi = 6.895×10^3 N/m^2

B.2 Linear Displacement Transducer

The linear displacement transducer was calibrated by applying known displacement and determining the corresponding output in volts on a chart recorder. The experimental calibration data are given in Table B.2. The calibration curve is shown in Figure B.2. The regression equation obtained was as follows (correlation coefficient= 0.99):

$$L = 3.11 * V - 0.19$$

where L is the linear displacement in cm (10^{-2} m), and V is the output in volts.

TABLE B.2

Linear Displacement Transducer

Calibration Data

Displacement , M $X10^2$	Output , volts
3	1.05
4	1.35
5	1.65
6	2.00
7	2.40
8	2.70
9	2.95
10	3.30
11	3.52
12	3.90

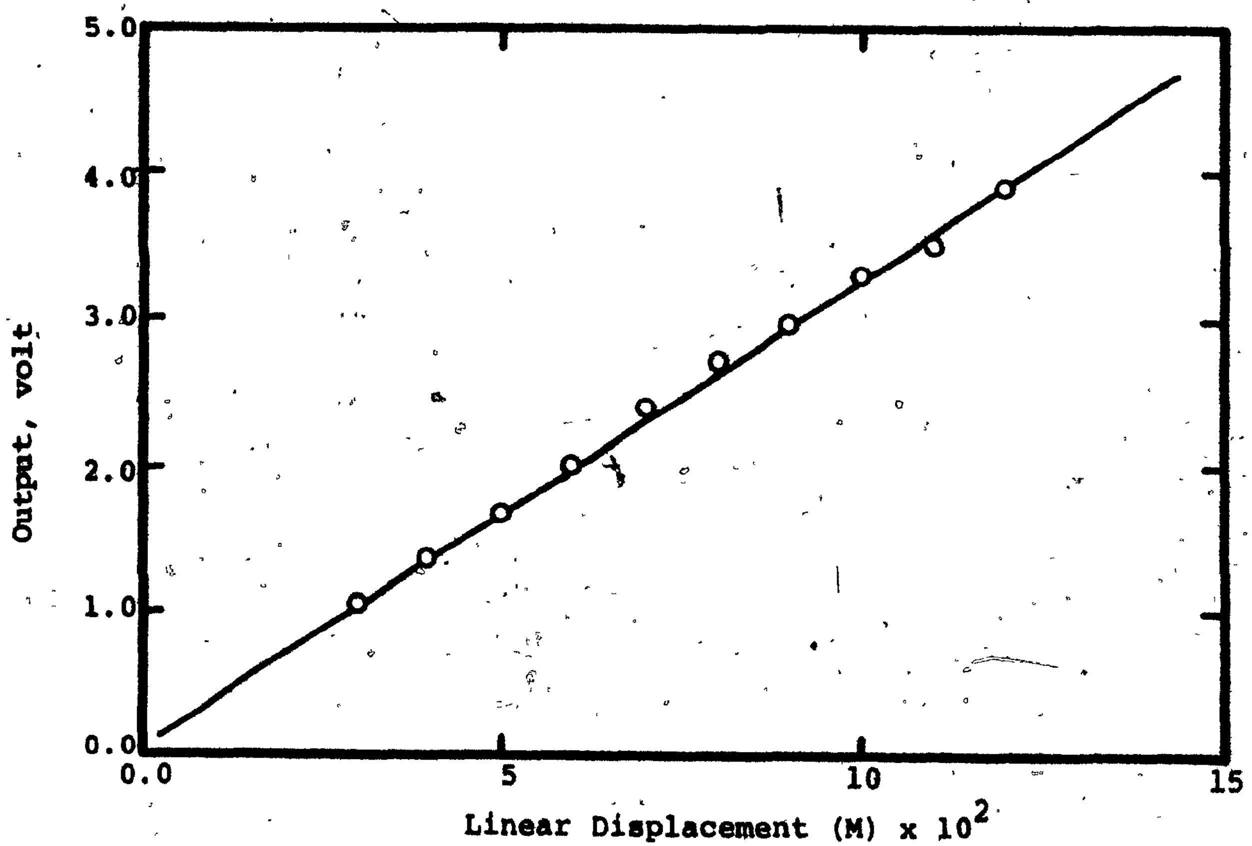

Figure B.2 Linear Displacement Transducer Calibration Curve

B.3 Velocity Transducer

The velocity transducer was calibrated using the Instron Universal Testing Machine in conjunction with known velocities, while the output was traced on a chart recorder. The calibration data are given in Table B.3, and the calibration curve is shown in Figure B.3. The calibration equation obtained by linear regression was as follows (correlation coefficient = 0.99):

$$V = 0.208 * Mv - 0.004$$

where V is the velocity in (mm/sec) and Mv is the output in Mv.

TABLE B.3

Velocity Transducer
Calibration Data

Velocity (mm/min)	Output (mV)
5	0.4
10	0.825
20	1.65
50	4.00
100	8.00
200	16.00

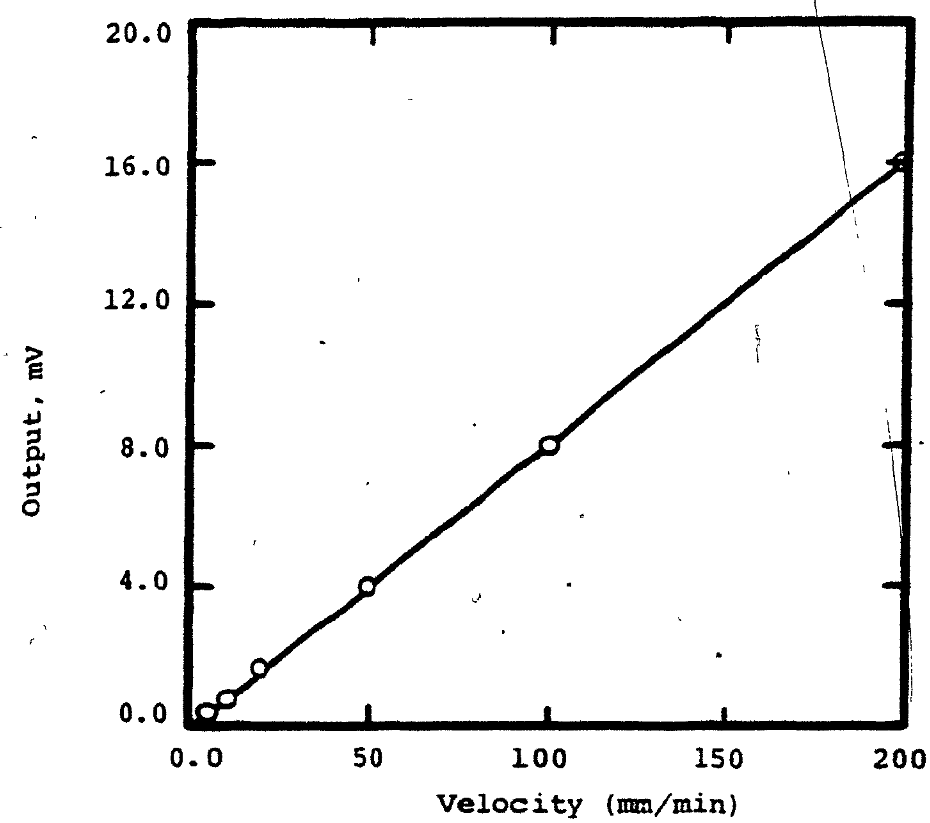

Figure B.3 Velocity Transducer Calibration Curve

APPENDIX C

GENERATION OF A PSEUDO-RANDOM BINARY SEQUENCE (PRBS)

One of the simplest ways of generating a PRBS uses basic shift register and one (or more) modulo-two gates in the feedback circuit, Figure C.1. The length of the sequence (N) is given by:

$$N = 2^n - 1$$

where n = number of stages (bits) in the shift register.

The following computer program was used to generate the PRBS :

PRBS Generator Program :

Nomenclatue of Variables

ILONG : Register (word) length

IWORD : Value of the register

IXOR : Second feed-back bit

IBIT1 : Value of the lowest significant bit, 0 or 1

IBIT2 : Value of IXOR bit, 0 or 1

IBIT3 : Result of exclusive OR between IBIT1 and IBIT2

IBUF1 : Buffer value to reduce calculation time

IBUF2 : Buffer value to reduce caculation time

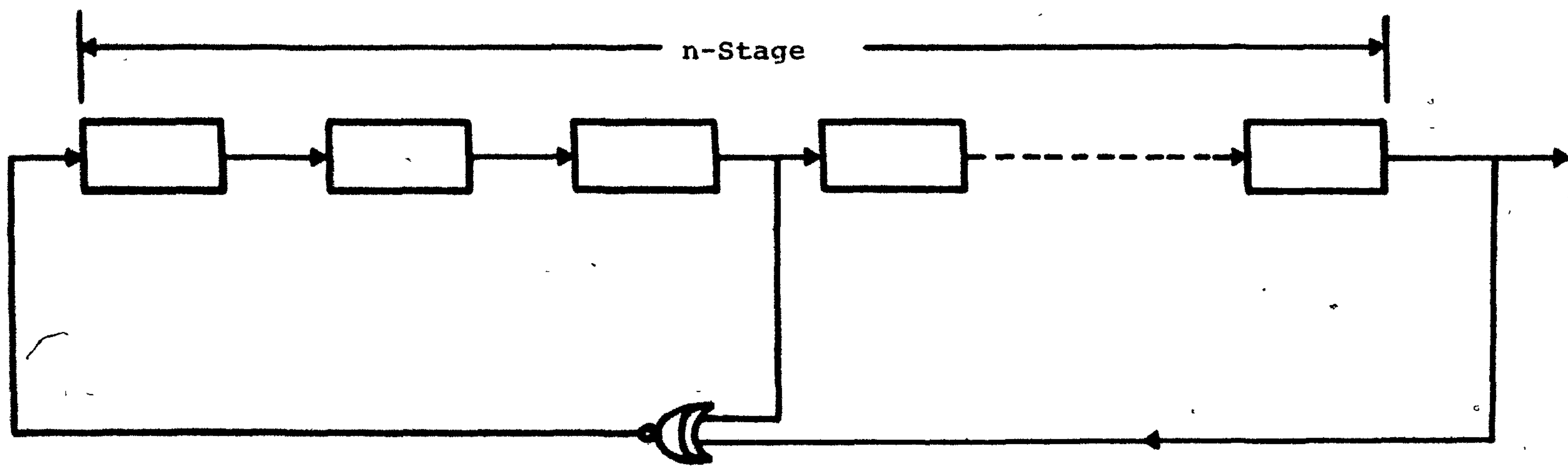

<u>Figure C.1</u>   n-Stage Shift Register Generator

PROGRAM

```
C   THE MAIN PROGRAM SPECIFIES THE REGESTER (WORD) LENGTH,
C   THE VALUE OF THE REGISTER AND THE SECOND FEED-BACK BIT.
C
C
          FUNCTION IPRBS(ILONG,IXOR,IWORD)
C
C   VALUE OF THE LOWEST SIGNIFICANT BIT
              IBUF1=IWORD/2
              IBIT1=IWORD-IBUF1*2
              IPRBS=IBIT1
C
C   VALUE OF THE IXOR-BIT
              IBUF2=IWORD/2**(IXOR-1)
              IBIT2=IBUF2-(IBUF2/2)*2
C
C   THE RESULT OF THE EXCLUSIVE OR BETWEEN IBIT1 AND IBIT2
              IBIT3=(IBIT1-IBIT2)*(IBIT1-IBIT2)
C
C   CREATION OF A NEW WORD BY SHIFTING THE PRECEEDING WORD TO
C   THE RIGHT AND PUTING THE VALUE OF IBIT3 IN THE MSB
              IWORD=IBUF1+IBIT3*2**(ILONG-1)
              RETURN
              END
```